THE TRIBOLOGY OF CARTILAGINOUS TISSUE: LUBRICATION IN HEALTH, DEGENERATION, AND TREATMENT

A Dissertation

Presented to the Faculty of the Graduate School

of Cornell University

In Partial Fulfillment of the Requirements for the Degree of

Doctor of Philosophy

by

Edward Daniel Bonnevie

August 2016

THE TRIBOLOGY OF CARTILAGINOUS TISSUE: LUBRICATION IN HEALTH, DEGENERATION, AND TREATMENT

Edward Daniel Bonnevie, Ph. D.

Cornell University 2016

Articular cartilage is one of the most remarkable materials found in nature. Its unique composition provides some of the lowest friction coefficients ever measured and allows nearly frictionless articulation of our bodies' joints. However, the breakdown and degeneration of cartilage in arthritis is one of the leading causes of severe disability in the industrialized world, and no effective disease-modifying treatments are currently available. With this in mind, fully understanding how the mechanisms of cartilage lubrication change between health and disease can provide insight to develop therapeutics targeted at restoring proper joint function.

In this dissertation, current theories on the natural mechanisms of synovial fluid will be explored (Chapter 1), and new theories on the lubricating mechanisms of synovial fluid will be developed based on new experimental evidence (Chapter 2). The role of cartilage damage and degradation will be explored to understand how the mechanisms of lubrication fail (Chapters 3-5). The detrimental effects of high friction will be studied to understand how cartilage deforms and what effect friction has on cells (Chapter 6). And, lubrication will be applied to tissue engineering to understand how to create engineered tissue that lubricates like native tissue (Chapters 7-8).

BIOGRAPHICAL SKETCH

Eddie grew up in the suburbs of Philadelphia (Lafayette Hill, PA), the youngest of three children. After finishing secondary education at LaSalle College High School, he enrolled in the mechanical engineering program at the University of Delaware. At Delaware, Eddie competed in NCAA D1 athletics for the Blue Hens, running both track and cross country. Ultimately, he was named team co-captain for cross country in the year he also gained Academic All-American honors. While also at Delaware, Eddie began researching cartilage lubrication under the guidance of Prof. Dave Burris. This opportunity for undergraduate research led him to pursue a doctorate focused on better understanding cartilage lubrication.

After graduating from Delaware, Eddie enrolled in the mechanical engineering PhD program at Cornell University. He joined the lab of Prof. Larry Bonassar to continue his research of cartilage lubrication, and was awarded the National Science Foundation Graduate Research Fellowship. Also while at Cornell, Eddie played club water polo for the Big Red and became an avid wind surfer – two hobbies he hopes to continue in the future.

Following graduation, Eddie has committed to a postdoctoral appointment at the University of Pennsylvania under the supervision of Prof. Rob Mauck.

Dedicated to my loving family and all of my friends.

ACKNOWLEDGMENTS

First, I would need to thank my advisor, Larry Bonassar, for investing a great deal of his time and knowledge into my education. I also need to thank my special committee members, Lisa Fortier and Itai Cohen, who served roles well above those expected from a special committee thanks to (almost) weekly meetings of the Cartilage Group.

The completion of this dissertation would have been impossible alone. My labmates in the Bonassar lab have been fantastic all throughout my 5 years at Cornell. Firstly, "Team Lube" has been a fantastic group of researchers to work with. With Kirk Samaroo and Natalie Galley showing me the ropes, I've been able to teach the next group of lubrication researchers in Liz Feeney and Jill Middendorf. Being an honorary member or "Team Meniscus" there are two chapters in this dissertation that would not have been possible without collaborations with Jenny Puetzer and Mary Clare McCorry. Also, all of the other members of the Bonassar lab, past and present., have been fantastic colleagues and friends throughout my time here. Nizeet Aguilar, Dravin Griffen, Brandon Borde, Katie Hudson, Jorge Mojica Santiago, Ben Cohen, Chris Didomenico, Nicole Diamentides, Stephen Sloan, and Becka Irwin have all become great friends.

Outside of the Bonassar lab, the student members of Cartilage Group have brought both new ideas and unique perspectives to my research. Members of both Lisa Fortier's lab and Itai Cohen's lab have been great resources over the years. Specifically, Lena Bartell, Michelle Delco, Derek Holyoak, Kira Novakofski, and Jesse Silverberg all have been helpful along the way. Also, our industrial collaborators at Fidia, Devis Galesso and Cynthia Secchieri, have provided a unique perspective to our research and its broader implications.

These past five years would not have flown by without the fantastic friends I've made along the way. In addition to both mechanical engineering and biomedical engineering friends, members of both the Cornell Water Polo team and Cayuga Windsurfing Club have made my stay in Ithaca a time I'll never forget.

This dissertation would also not be possible without all of the people working hard to make sure our paths to degrees are not riddled with administrative and bureaucratic obstacles. Marcia Sawyer and Judy Thoroughman have done fantastic jobs to help me make sure I have fulfilled my degree requirements.

Most importantly, I need to thank my wonderful family and girlfriend. My parents and my siblings, Beth and Paul, have been supportive every step along the way, and I will always be indebted to them.

Finally, the work contained in this dissertation was supported by the National Science Foundation Graduate Research Fellowship Program.

TABLE OF CONTENTS

CHAPTER 1

Cartilage Lubrication: Evolution of Theories and Treatments

Abstract

Articular cartilage is one of the most lubricious materials found in nature. Its role in promoting lubrication within the body's joints is pivotal to mammalian locomotion, but its breakdown and degeneration is the leading cause of severe disability in the industrialized world. In this chapter, introductions to both cartilage and lubrication will be presented. A brief history of the progress of cartilage lubrication theory will be presented, as will the progress on lubrication's role in cartilage therapy. These historical perspectives will highlight the open questions in cartilage lubrication research and provide a basis for the studies to follow later in this dissertation.

Introductions to Cartilage and to Lubrication

Articular cartilage, a soft tissue that surrounds the ends of the body's long bones, is the most robust bearing material found in nature. This aneural, avascular tissue can withstand over 100 million loading cycles over a lifetime [1] due to its unique lubricating and load bearing properties [2], [3]. Consequently, decades of research have focused on discovering the mechanisms through which cartilage exhibits friction coefficients lower than almost everything found in nature, including ice sliding on ice [4]. Over the last decade, progress has been made to better understand distinct mechanisms that work synergistically to promote cartilage's very low friction. The key factors in these mechanisms are pressurization of interstitial fluid and viscous boundary lubrication by synovial fluid [3], [5], [6].

Over a century of engineering research has been dedicated to understanding how friction scales with operating parameters. Factors such as how fast surfaces are moving past each other, how hard they are being pressed together, how viscous the lubricating fluid is, and the geometry of the contact all affect a measured friction coefficient [7]. For an engineered system, such as a journal bearing, the Stribeck curve (Figure 1.1) describes how changes in these parameters can lead to different modes of lubrication: boundary, mixed, elastohydrodynamic, and hydrodynamic. In boundary lubrication, contact and friction is dictated by surface chemistry, hardness, and roughness [8]. The friction is due primarily to the contact of opposing solid asperities, and the boundary friction coefficient is relatively insensitive to changes in sliding speed, and contact pressure. As contact pressure drops, or relative surface speeds increase, the system begins to experience viscous effects due to the lubricating fluid.

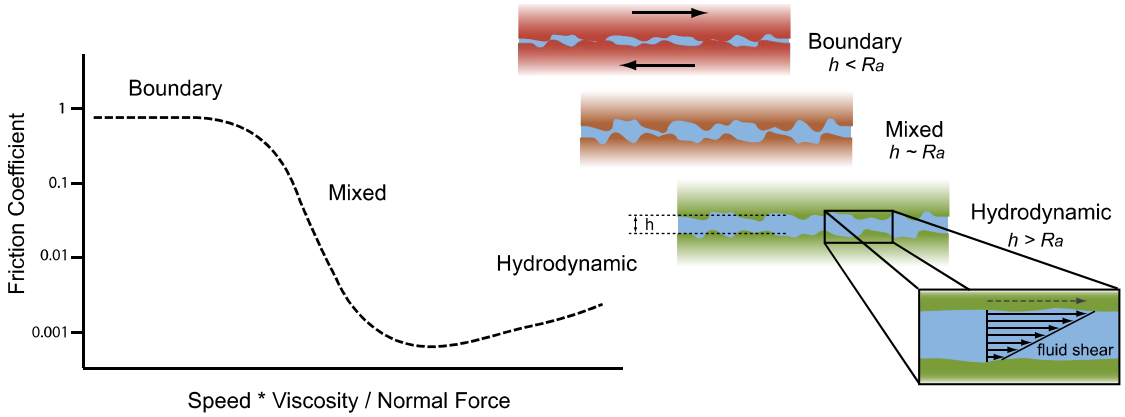

Figure 1.1 The classical Stribeck curve describes lubrication modes. In the boundary regime, asperity contact dominates the load, and consequently friction is high and insensitive to changes in the operating conditions. In mixed lubrication, interfacial fluid begins to pressurize and the load is supported by a balance of both fluid pressurization and asperity contact. As the system transitions to hydrodynamic lubrication, the load is fully supported by a viscous film that is thicker than the surface roughness and friction results from fluid shear.

In this mixed mode of lubrication, friction is dictated by both the boundary friction coefficient and viscous effects as the contact is supported both by solid asperities and pressurized viscous fluid. At the minimum friction coefficient of the Stribeck curve, the system experiences elastohydrodynamic lubrication where the surfaces are fully separated by a thin viscous lubricant film across the interface. As this film thickens and relative surface speed increase, the resulting stresses from shearing the interfacial film dominate the friction coefficient and cause friction increases in hydrodynamic lubrication.

Unlike the classical framework for understanding the lubrication of hard, impermeable materials, there is no consensus on a framework to study the lubrication modes and mechanisms of soft and permeable materials like hydrogels and most biological tissues. It is hypothesized that there is distinct and considerable deviations from the classical Stribeck curve [9]. In classical boundary mode lubrication, friction is dictated by surface roughness, chemistry, and any lubricant additives, with minimal effects due to interfacial fluid. However, for soft hydrogel materials, surface roughness alone does not play a dominant role in boundary lubrication [10], but friction is instead predicted to be dependent on factors such as mesh size or porosity [9]. Effectively, under hydrated conditions, the contact does not experience true dry friction as the contact will contain confined fluid due to the porous nature of the materials. This friction regime has been called mesh-confined lubrication [9]. However, throughout this dissertation, this regime of lubrication will still be denoted by boundary lubrication for the sake of simplicity and connection to previous studies.

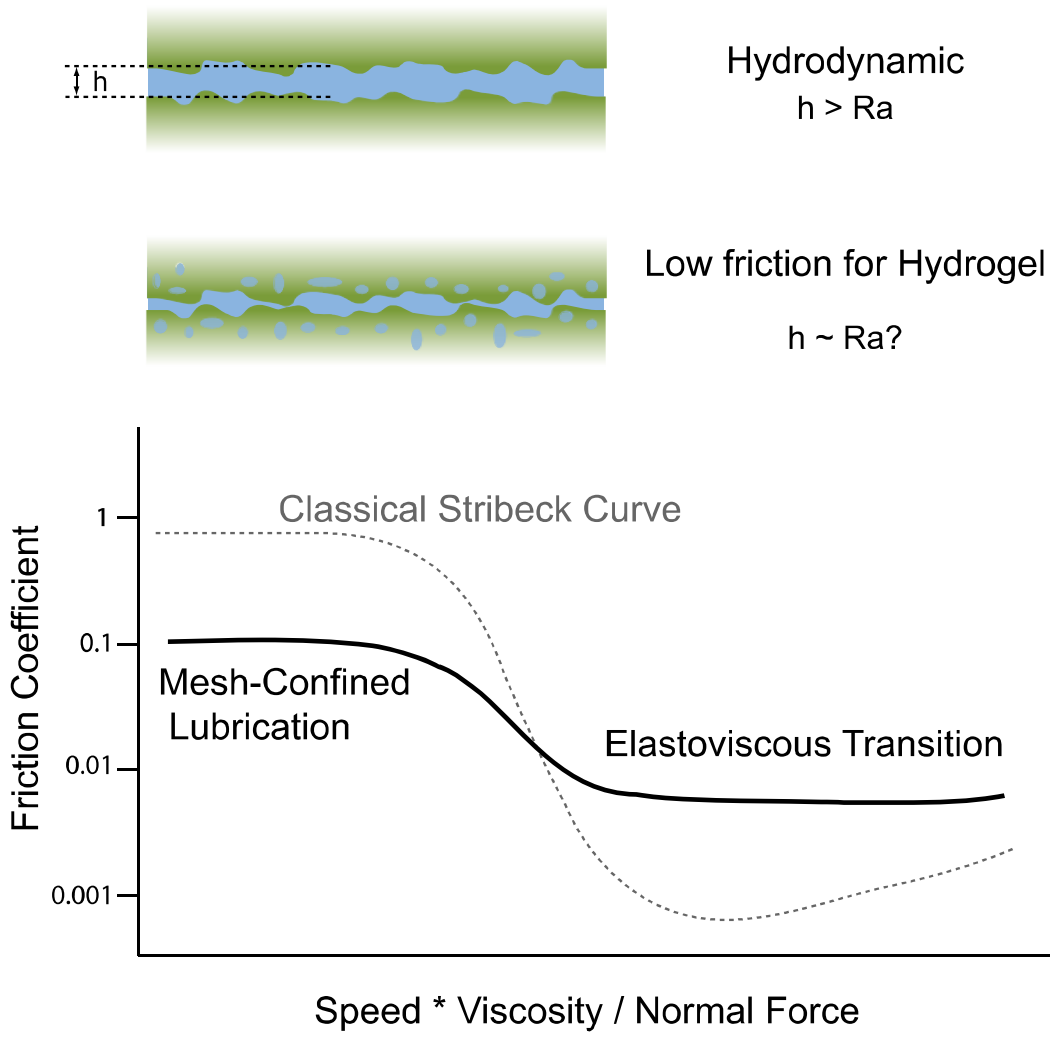

Figure 1.2 Stribeck-like behavior of a hydrogel contact. Due to a hydrogel's hydrated and permeable structure, lubrication does not scale in the same manner as a traditional Stribeck Curve [9].

Despite their porosity, hydrogels can still diverge from the high friction in boundary mode lubrication as parameters such as viscosity and sliding speed increase or normal load decreases. However, it is hypothesized that hydrogels transition to lower friction in a manner distinct from the transition to EHL in the classical Stribeck curve [9], [10]. This transition to low friction has recently been called the elastoviscous transition [9].

Cartilage Structure and Function

Articular cartilage, the soft tissue that surrounds the ends of the body's long bones, is up to 85% water by weight [11]. The main structural components of cartilage are type II collagen and proteoglycans [12]. The collagen within the extracellular matrix of cartilage is attributed to giving cartilage its tensile properties. In contrast, the compressive properties of cartilage are often attributed to the proteoglycan content on the tissue [13]. The proteoglycan component, which is mostly aggrecan, provides cartilage with a significant fixed charge density [13], [14]. Consequently, under physiologic conditions, cartilage experiences an osmotic swelling due to an abundance of fixed negative charges [15]. This biochemical attribute of cartilage is the key factor in maintaining the highly hydrated nature of the tissue. The combination of a high tensile strength, low permeability, and highly hydrated nature of cartilage provide it with very unique load bearing capabilities [16].

As stated, the structure of cartilage provides it with unique load bearing capabilities that have been known for decades to be both time- and load-dependent. While cartilage could classically be thought of as a viscoelastic material, cartilage has

more appropriately been described as a biphasic (or triphasic) and poroelastic (or poro-visco-elastic) material [15], [17]–[19]. In compression, cartilage can be orders of magnitude stiffer under instantaneous conditions compared to static, steady-state loading. The aggregate modulus of cartilage typically is on the order of 1 MPa, with instantaneous moduli of cartilage that can well exceed 10 MPa depending on the loading conditions and configuration [17]. This effect is typically attributed to the biphasic/poroelastic nature of cartilage in which interstitial fluid is pressurized under volumetric changes and the low permeability serves to increase the time constant of fluid pressure relaxation. Further, the high tensile modulus of cartilage also plays a role in the load bearing properties of cartilage [20]. With a high tensile modulus, lateral expansion (i.e., Poisson effect) can be restricted allowing higher interstitial fluid pressure than would be predicted by linear biphasic theory. These properties of cartilage not only have effects on load bearing, but also the lubrication of cartilage to be addressed later.

The structure and function of cartilage is dependent on distinct heterogeneity from the articular surface deep to the subchondral bone [21]–[23]. The depth-dependent heterogeneity of cartilage is typically classified into 3 zones of tissue: superficial, middle, and deep. These zones are distinct due to water content, collagen organization and density, proteoglycan content and fixed charge density, and cellular density and shape [24]–[26]. The superficial zone, which extends from the articular surface to ~200 μm into the tissue, is characterized by collagen fibrils aligned parallel to the articular surface and cells with an elongated morphology. This zone of tissue is mechanically more compliant in both shear and compression than the deeper cartilage

tissue [21], [22]. This more compliant and dissipative behavior of the tissue has been connected to the collagen orientation, but is more strongly correlated with locally lower collagen and proteoglycan content and, consequently, fixed charge density [23]. In the middle zone of cartilage, collagen fibril orientations are more random with no distinct orientation direction, and in the deep zone collagen fibrils have an orientation that is perpendicular to the subchondral bone and tide mark. These depth dependent properties of cartilage have been hypothesized to be protective of the middle and deep tissue as the surface absorbs and dissipates a significant portion of the applied energy [21], [22], [27].

A Brief History of Cartilage Lubrication

Classical Theories of Cartilage Lubrication (1930-1950)

Cartilage tribology emerged as a field in the 1930's pioneered by engineers applying fundamentals of journal bearing tribology to the body's joints. Early theories claimed the mechanism of low friction for cartilage was fluid film lubrication [28], [29]. Calling on fundamentals of tribology such as the Stribeck curve, it was purported that the mechanism of lubrication was due to entrainment of the viscous synovial fluid into the areas of joint contact and the formation of a fluid film was responsible for the measured low friction coefficients ($\mu < 0.01$). In the 1950's analysis of synovial fluid explicitly revealed the role of hyaluronic acid in providing the viscoelastic properties of synovial fluid [30], [31].

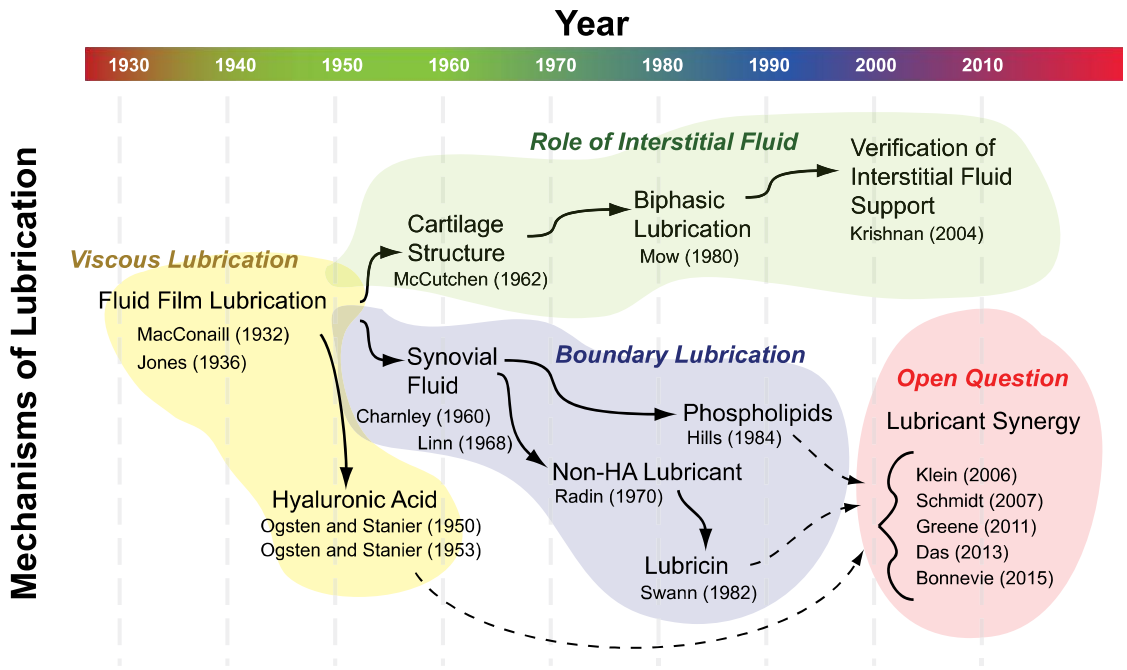

Figure 1.3 Seminal works on cartilage lubrication are highlighted by mechanism of lubrication (viscous, boundary, interstitial fluid pressure, and lubricant synergy) and date of publication to display the evolution of lubrication theories.

The Role of the Biphasic Structure of Cartilage in Lubrication (1960-Present)

In the 1960's, McCutchen showed experimentally that cartilage excised from a joint can provide low friction when slid against glass [2]. He revealed however, that this friction was time-dependent and lubricant-dependent (i.e., synovial fluid provided lower friction than PBS). This time dependent friction phenomenon, which would not be indicative of sustained fluid film lubrication, was theorized to be a function of pressurized interstitial fluid weeping into the contacting region providing a hydrated contact. In the 1980's, Mow developed a rigorous theoretical framework to understand interstitial fluid pressurization in cartilage and this theory supported experimental evidence [17]. Decades later in the 2000's, Krishnan *et al.* experimentally verified the role of interstitial fluid pressurization in low friction measurements by simultaneously recording interstitial fluid pressure and friction coefficient as a function of time for cartilage friction [32]. The correlation between fluid pressure and friction was linear, supporting the theory that interstitial fluid pressurization supports a substantial portion of the contact stress and shields the contacting asperities. Further research has since explained the mechanical phenomena that lead to enhanced interstitial fluid pressurization in articular cartilage. Factors such as cartilage's high tensile modulus, and active deformation of the cartilage matrix where convective fluid flow surpasses diffusive fluid flow (i.e., Peclet number > 1) lead to high interstitial fluid pressurization and consequently low measured friction coefficients [20], [33].

The Role of Synovial Fluid in Cartilage Lubrication (1960 – 2000)

Similarly to McCutchen, in the 1960's Charnley also found fault with the idea of sustained hydrodynamic lubrication as the lubricating mechanism in mammalian

joints [34]. Instead, it was postulated that boundary lubrication from synovial fluid was the mechanism by which cartilage could achieve low friction coefficients (i.e., $\mu <$ 0.1 with synovial fluid). Shortly thereafter, Linn and Radin (1968) experimentally demonstrated the boundary lubricating ability of synovial fluid and relative independence of friction on synovial fluid viscosity [35]. In fact, hyaluronidase digestion of synovial fluid left its lubricating ability relatively intact; however, trypsin digestion, which degraded proteins but left hyaluronic acid and viscosity unaffected, significantly altered the lubricating ability of synovial fluid. Consequently, a non-HA mechanism was theorized to be the avenue for boundary lubrication by synovial fluid.

In 1981 and 1984, Swann and Hills, respectively, described their theories on synovial fluid boundary lubrication [36], [37]. Swann described a boundary lubricating glycoprotein purified from synovial fluid, which would come to be known as lubricin, superficial zone protein, and also proteoglycan 4 (PRG4). Hills described the boundary lubricating phospholipid fraction of synovial fluid which was predominantly phosphatidyl choline. Both molecules have been shown to be effective boundary lubricants, but it was unclear which, was the dominant factor in the lubrication of synovial fluid. However in 1999, Jay and Cha showed that both phosphatidyl choline and intact synovial fluid were both exceptional boundary lubricants[38], but phospholipase treatment of synovial fluid was not as effective as trypsin digestion in removing the boundary lubricating ability of synovial fluid. This experiment revealed that although synovial fluid boundary lubrication is enhanced by phospholipids, the main boundary lubricating action comes from another molecule such as lubricin.

Molecular Mechanisms of Synovial Fluid Lubrication (2000 – Present)

With increasing sophistication in both tribometer design and analysis techniques, recent research has aimed to elucidate the molecular mechanisms by which synovial fluid lubricates cartilage. While research on the boundary lubrication of cartilage has largely concluded that hyaluronic acid does not provide synovial fluid with its boundary lubricating ability [35], there is recent evidence outside the realm of fluid film lubrication that hyaluronic acid contributes to lower friction. Research into the molecular mechanisms of synovial fluid lubrication have largely focused on the synergy between lubricin, HA, and phospholipids [5], [39]–[42]. Through these recent studies, a common theme has emerged that lubricin, HA, or phospholipids alone do not describe the lubricating ability of synovial fluid. It is hypothesized that molecular interactions of some currently unknown nature are what provide synovial fluid with its robust ability to minimize cartilage friction.

Open Questions in Cartilage Lubrication Mechanisms

There are currently several important questions open in cartilage lubrication. One major question is how the molecules in synovial fluid lubricate in concert with each other more effectively than they do on their own. That is, what is the mechanism of synergy between synovial fluid macromolecules at the articular surface? Chapter 2 of this dissertation will be dedicated to that phenomenon. A second major question is, how does lubrication of a cartilage surface in either injury or degeneration change? Chapter 3 of this dissertation will focus on the role of inflammatory degradation by Interleukin-1β, and chapters 4 and 5 will focus on applying a traumatic impact to cartilage and analyzing changes in lubrication, respectively.

The Role of Lubrication in Cartilage Homeostasis

Being an avascular, aneural tissue, articular cartilage relies heavily on mechanical cues for healthy function. The chondrocytes within the cartilage matrix are sparse compared to other tissue, comprising ~1% of the total weight of the tissue, and direct cell-cell communication is virtually nonexistent. Consequently, chondrocyte homeostasis is dictated by mechanotransduction and soluble factors. Both shear and compressive loadings on articular cartilage can stimulate anabolic genes and enhance the transport of signaling molecules such as IGF-1 [43]. However, in cases of overloading, such as a traumatic injury adverse effects may occur [44]. With traumatic compressive strains, cell death, mitochondrial depolarization, and chondrocyte apoptosis can occur in addition to upregulating inflammatory signals [27], [45]–[49].

However, unlike traumatic compressive loading, there is less known about the adverse effects of excess shear on articular cartilage. Aspects such as disease, aging, and cartilage degeneration can all have adverse effects on the lubricating mechanisms described above [50]–[52]. For example after a traumatic ACL tear, lubricin levels can fall 90% below pre-injury levels and take an entire year to normalize [51]. Additionally, aging alone can affect both lubricin content, HA concentration, and HA molecular weight [50], [52]. All of these factors can diminish the lubricating advantage of synovial fluid and increase the friction coefficient experienced at the cartilage surface. Recent experimental work has shown that increased friction can lead to chondrocyte apoptosis [53], revealing an adverse biological phenomenon as a function of inferior lubrication. Further, increased friction also increases the depth-dependent shear strains in articular cartilage [54]. However, the link between

increased shear strain and apoptosis has not been explored. Chapter 6 of this dissertation will explore the link between inferior lubrication, increased depth-dependent shear strains, and chondrocyte responses including acute cell death, mitochondrial depolarization, and caspase activation to better understand the coupling between mechanical and biological factors that are likely important in the progression of diseases such as osteoarthritis. The main groups of therapies are viscosupplements, boundary lubricants, cartilage implants and synthetic lubricants with substantial overlap in some cases.

Lubrication in Cartilage Therapy

Because of the adverse mechanical and biological consequences that can arise from inferior cartilage lubrication, many researchers have focused on restoring healthy lubricating function to diseased and injured joints. Over the last several decades, tribosupplementation [55] and tissue engineering [56] have both emerged as therapeutic strategies in this field to reduce pain and slow cartilage degeneration. Briefly, tribosupplementation is the concept of utilizing intraarticular injection of a lubricant to minimize friction and protect contacting cartilage layers. Additionally, replacing degenerated cartilage with tissue engineered implants has also emerged as an option to inhibit the progression of arthritis. In most cases, the scientific understanding of lubrication mechanisms have predated their utilization in the treatments described below by around two decades (see Figures 1.3 and 1.4).

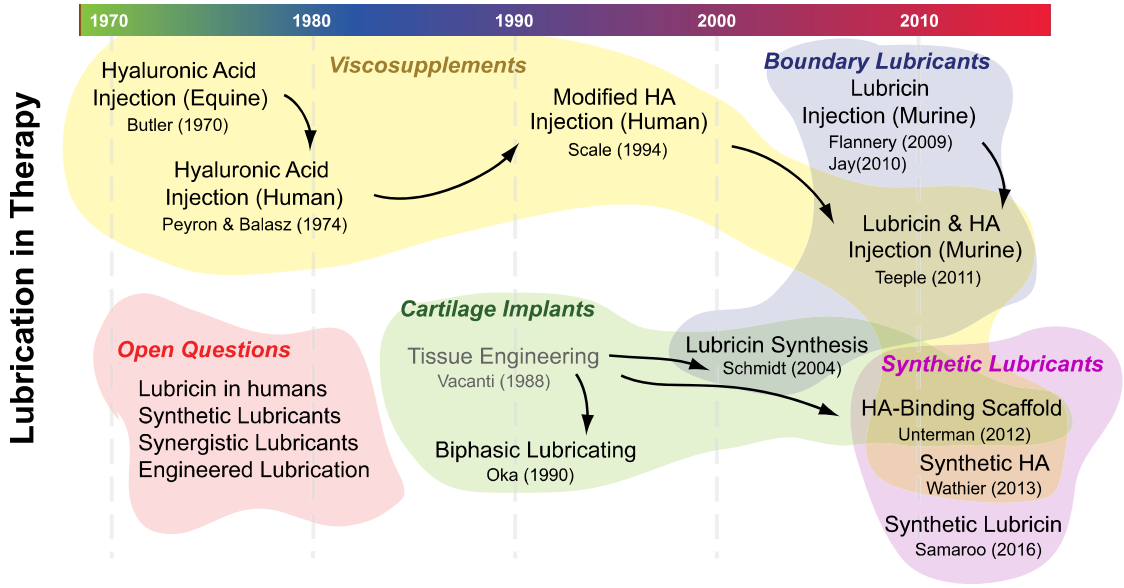

Figure 1.4 Lubrication therapies have typically lagged behind their research disclosures by around two decades (see Figure 1.4). Lubrication therapies can be grouped into either tribosupplements (i.e., lubricant injections) or lubricating implants.

Viscosupplementation

Viscosupplementation emerged as the first lubrication-based therapeutic to slow progression of cartilage degeneration or alleviate the pain associated with cartilage degeneration. In the 1970's Balasz introduced the concept of intraarticular injection of hyaluronic acid, which at the time was thought to be the key lubricant within synovial fluid. First tested in race horses, viscosupplementation had beneficial effects on the arthritis symptoms [57]. Similarly, the first trials in humans also revealed promising effects in reducing joint pain [58]. Drawing on the theory that the viscosity of both synovial fluid and HA are important factors in cartilage lubrication, more viscous HA derivatives were developed through either cross-linking [59] or chemical modification [60]. In the mid 1990's these products were proven effective at reducing pain [59], [61]; however, their relative effectiveness over placebo (i.e., saline injection) and their ability to halt the progression of cartilage damage is still a topic of concern.

Boundary Lubrication Tribosupplementation

Drawing upon the experimental support that the lubricating action of synovial fluid is due mostly to boundary lubrication as a function of lubricin, tribosupplementation with boundary lubricants emerged as a treatment option in 2009 [62]. In rodent models of arthritis, lubricin injections have proven effective in slowing the progression of cartilage damage compared to both saline injection and HA injection [62]–[64]. However, this treatment has not been investigated in either large animal models or humans yet.

Synthetic and Biomimetic Lubricants

The major drawback in lubricin tribosupplementation is the costs associated with either production or purification of the protein. Consequently, synthetic and biomimetic cartilage lubricants have emerged as possible alternatives. A synthetic viscous lubricant was developed as an alternative to HA injection and *in vitro* was able to lubricate cartilage at a similar level to that of synovial fluid [65]. More recently, lubricin biomimetics have emerged as alternative treatment options [66]. These bottle-brush-like polymers have the ability to bind to the articular surface and lubricate cartilage, and have shown promise in preventing cartilage damage in a rodent model [67]. Like lubricin however, they are yet to be tested in either large animal or human trials.

Lubrication in Tissue Engineering

In parallel to progress on tribosupplementation, tissue engineering has emerged as a strategy to return normal function to damaged or degenerated joints, and lubrication is theorized to play a large role in the successful replacement of cartilage tissue [68]. In the late 1980's tissue engineering emerged as a field [56], and in the mid-1990's the first human trials of cartilage tissue engineering in the form of autologous chondrocyte implantation showed promise [69]. However, there has been minimal research focused on evaluating the lubricating properties of tissue engineered cartilage implants [70]. Since lubrication has emerged as an important aspect of cartilage homeostasis, the role of lubrication in cartilage tissue engineering can take on two forms: creating tissue with the mechanical properties that can sustain interstitial fluid lubrication [71], [72], or surface modification to localize lubricants [73]–[77].

These aspects are important not only to ensure a tissue engineered construct can withstand the repeated cycles of friction within a joint, but they are also important to ensure there is not elevated friction applied to the contacting cartilage that a tissue engineered implant may articulate against [68].

Open Questions about Lubrication in Cartilage Therapy

Several questions remain unanswered in the role of lubrication in cartilage therapy. One major question remains to the effectiveness of boundary lubricant tribosupplementation in humans. Whether lubricin, or a synthetic boundary lubricant, can effectively inhibit cartilage damage propagation in a large weight bearing joint is a question that will hopefully be answered within the coming years. Another major question surrounds the methods to facilitate proper lubrication in tissue engineering. In Chapters 7 and 8 of this dissertation, the role of lubricin localization at tissue engineered surfaces will be evaluated for boundary lubrication. These chapters will study the effects of chemical stimulation with insulin-like growth factor I and the role of stem cells versus primary cells in promoting effective lubrication, respectively.

REFERENCES

[1] M. Silva, E. F. Shepherd, W. O. Jackson, F. J. Dorey, and T. P. Schmalzried, "Average patient walking activity approaches 2 million cycles per year: Pedometers under-record walking activity," *J. Arthroplasty*, vol. 17, no. 6, pp. 693–697, 2002.

[2] C. W. McCutchen, "The frictional properties of animal joints," *Wear*, vol. 5, no. 1, pp. 1–17, Jan. 1962.

[3] G. A. Ateshian, "The role of interstitial fluid pressurization in articular cartilage lubrication.," *J. Biomech.*, vol. 42, no. 9, pp. 1163–76, Jun. 2009.

[4] M. Miller, S. Thompson, and J. Hart, *Review of orthopaedics*. 2012.

[5] T. A. Schmidt, N. S. Gastelum, Q. T. Nguyen, B. L. Schumacher, and R. L. Sah, "Boundary lubrication of articular cartilage: role of synovial fluid constituents.," *Arthritis Rheum.*, vol. 56, no. 3, pp. 882–91, Mar. 2007.

[6] E. D. Bonnevie, D. Galesso, C. Secchieri, I. Cohen, and L. J. Bonassar, "Elastoviscous Transitions of Articular Cartilage Reveal a Mechanism of Synergy between Lubricin and Hyaluronic Acid.," *PLoS One*, vol. 10, no. 11, p. e0143415, Jan. 2015.

[7] M. D. Hersey, "The laws of lubrication of horizontal journal bearings," *J. Washingt. Acad. Sci.*, vol. 4, no. August, pp. 542–552, 1914.

[8] F. P. Bowden and D. Tabor, *The Friction and Lubrication of Solids*. Oxford:

Clarendon Press, 1950.

[9] A. C. Dunn, W. G. Sawyer, and T. E. Angelini, “Gemini Interfaces in Aqueous Lubrication with Hydrogels,” *Tribol. Lett.*, vol. 54, no. 1, pp. 59–66, Mar. 2014.

[10] S. Yashima, N. Takase, T. Kurokawa, and J. P. Gong, “Friction of hydrogels with controlled surface roughness on solid flat substrates.,” *Soft Matter*, vol. 10, no. 18, pp. 3192–9, May 2014.

[11] N. P. Cohen, R. J. Foster, and V. C. Mow, “Composition and Dynamics of Articular Cartilage: Structure, Function, and Maintaining Healthy State,” *http://dx.doi.org/10.2519/jospt.1998.28.4.203*, 1998.

[12] Y. Fung, *Biomechanics: mechanical properties of living tissues.* SPringer Science & Business Media, 2013.

[13] P. J. Roughley, “The structure and function of cartilage proteoglycans.,” *Eur. Cell. Mater.*, vol. 12, pp. 92–101, 2006.

[14] A. Maroudas, H. Muir, and J. Wingham, “The correlation of fixed negative charge with glycosaminoglycan content of human articular cartilage,” *Biochim. Biophys. Acta - Gen. Subj.*, vol. 177, no. 3, pp. 492–500, May 1969.

[15] W. M. Lai, J. S. Hou, and V. C. Mow, “A Triphasic Theory for the Swelling and Deformation Behaviors of Articular Cartilage,” *J. Biomech. Eng.*, vol. 113, no. 3, p. 245, 1991.

[16] G. A. Ateshian, M. A. Soltz, R. L. Mauck, I. M. Basalo, C. T. Hung, and W.

Michael Lai, “The Role of Osmotic Pressure and Tension-Compression Nonlinearity in the Frictional Response of Articular Cartilage,” *Transp. Porous Media*, vol. 50, no. 1/2, pp. 5–33, 2003.

[17] V. C. Mow, S. C. Kuei, W. M. Lai, and C. G. Armstrong, “Biphasic Creep and Stress Relaxation of Articular Cartilage in Compression: Theory and Experiments,” *J. Biomech. Eng.*, vol. 102, no. 1, p. 73, Feb. 1980.

[18] L. A. Setton, W. Zhu, and V. C. Mow, “The biphasic poroviscoelastic behavior of articular cartilage: Role of the surface zone in governing the compressive behavior,” *J. Biomech.*, vol. 26, no. 4–5, pp. 581–592, Apr. 1993.

[19] L. . Li, J. Soulhat, M. . Buschmann, and A. Shirazi-Adl, “Nonlinear analysis of cartilage in unconfined ramp compression using a fibril reinforced poroelastic model,” *Clin. Biomech.*, vol. 14, no. 9, pp. 673–682, 1999.

[20] C.-Y. Huang, M. A. Soltz, M. Kopacz, V. C. Mow, and G. A. Ateshian, “Experimental Verification of the Roles of Intrinsic Matrix Viscoelasticity and Tension-Compression Nonlinearity in the Biphasic Response of Cartilage,” *J. Biomech. Eng.*, vol. 125, no. 1, p. 84, 2003.

[21] R. M. Schinagl, D. Gurskis, A. C. Chen, and R. L. Sah, “Depth-dependent confined compression modulus of full-thickness bovine articular cartilage,” *J. Orthop. Res.*, vol. 15, no. 4, pp. 499–506, Jul. 1997.

[22] M. R. Buckley, A. J. Bergou, J. Fouchard, L. J. Bonassar, and I. Cohen, “High-resolution spatial mapping of shear properties in cartilage,” 2010.

[23] J. L. Silverberg, A. R. Barrett, M. Das, P. B. Petersen, L. J. Bonassar, and I. Cohen, "Structure-Function Relations and Rigidity Percolation in the Shear Properties of Articular Cartilage," *Biophys. J.*, vol. 107, no. 7, pp. 1721–1730, 2014.

[24] N. P. Camacho, P. West, P. A. Torzilli, and R. Mendelsohn, "FTIR microscopic imaging of collagen and proteoglycan in bovine cartilage," *Biopolymers*, vol. 62, no. 1, pp. 1–8, 2001.

[25] M. B. Aydelotte and K. E. Kuettner, "Differences between sub-populations of cultured bovine articular chondrocytes. I. Morphology and cartilage matrix production," *http://dx.doi.org/10.3109/03008208809016808*, 2009.

[26] S. S. Chen, Y. H. Falcovitz, R. Schneiderman, A. Maroudas, and R. L. Sah, "Depth-dependent compressive properties of normal aged human femoral head articular cartilage: relationship to fixed charge density," *Osteoarthr. Cartil.*, vol. 9, no. 6, pp. 561–569, Aug. 2001.

[27] L. R. Bartell, L. A. Fortier, L. J. Bonassar, and I. Cohen, "Measuring microscale strain fields in articular cartilage during rapid impact reveals thresholds for chondrocyte death and a protective role for the superficial layer," *J. Biomech.*, vol. 48, no. 12, pp. 3440–3446, Sep. 2015.

[28] M. A. Macconaill, "The Function of Intra-Articular Fibrocartilages, with Special Reference to the Knee and Inferior Radio-Ulnar Joints.," *J. Anat.*, vol. 66, no. Pt 2, pp. 210–27, Jan. 1932.

[29] E. S. Jones, “Joint lubrication,” *Lancet*, vol. 227, no. 5879, pp. 1043–1045, 1936.

[30] A. G. OGSTON and J. E. STANIER, “The physiological function of hyaluronic acid in synovial fluid; viscous, elastic and lubricant properties.,” *J. Physiol.*, vol. 119, no. 2–3, pp. 244–52, Feb. 1953.

[31] A. G. Ogston and J. E. Stanier, “On the state of hyaluronic acid in synovial fluid.,” *Biochem. J.*, vol. 46, no. 3, pp. 364–76, Mar. 1950.

[32] R. Krishnan, M. Kopacz, and G. A. Ateshian, “Experimental verification of the role of interstitial fluid pressurization in cartilage lubrication.,” *J. Orthop. Res.*, vol. 22, no. 3, pp. 565–70, May 2004.

[33] M. Caligaris and G. A. Ateshian, “Effects of sustained interstitial fluid pressurization under migrating contact area, and boundary lubrication by synovial fluid, on cartilage friction.,” *Osteoarthritis Cartilage*, vol. 16, no. 10, pp. 1220–7, Oct. 2008.

[34] J. CHARNLEY, “The lubrication of animal joints in relation to surgical reconstruction by arthroplasty.,” *Ann. Rheum. Dis.*, vol. 19, no. 1, pp. 10–9, Mar. 1960.

[35] F. C. Linn and E. L. Radin, “Lubrication of animal joints. iii. the effect of certain chemical alterations of the cartilage and lubricant,” *Arthritis Rheum.*, vol. 11, no. 5, pp. 674–682, Oct. 1968.

[36] D. A. Swann, R. B. Hendren, E. L. Radin, and S. L. Sotman, “The lubricating activity of synovial fluid glycoproteins,” *Arthritis Rheum.*, vol. 24, no. 1, pp. 22–30, Jan. 1981.

[37] B. A. Hills and B. D. Butler, “Surfactants identified in synovial fluid and their ability to act as boundary lubricants.,” *Ann. Rheum. Dis.*, vol. 43, no. 4, pp. 641–648, Aug. 1984.

[38] G. D. Jay and C. J. Cha, “The effect of phospholipase digestion upon the boundary lubricating ability of synovial fluid.,” *J. Rheumatol.*, vol. 26, no. 11, pp. 2454–7, Nov. 1999.

[39] S. Das, X. Banquy, B. Zappone, G. W. Greene, G. D. Jay, and J. N. Israelachvili, “Synergistic interactions between grafted hyaluronic acid and lubricin provide enhanced wear protection and lubrication.,” *Biomacromolecules*, vol. 14, no. 5, pp. 1669–77, May 2013.

[40] G. W. Greene, X. Banquy, D. W. Lee, D. D. Lowrey, J. Yu, and J. N. Israelachvili, “Adaptive mechanically controlled lubrication mechanism found in articular joints.,” *Proc. Natl. Acad. Sci. U. S. A.*, vol. 108, no. 13, pp. 5255–9, Mar. 2011.

[41] S. E. Majd, R. Kuijer, A. Köwitsch, T. Groth, T. A. Schmidt, and P. K. Sharma, “Both hyaluronan and collagen type II keep proteoglycan 4 (lubricin) at the cartilage surface in a condition that provides low friction during boundary lubrication.,” *Langmuir*, vol. 30, no. 48, pp. 14566–72, Dec. 2014.

[42] J. Seror, L. Zhu, R. Goldberg, A. J. Day, and J. Klein, “Supramolecular synergy in the boundary lubrication of synovial joints,” *Nat. Commun.*, vol. 6, p. 6497, Mar. 2015.

[43] J. B. Fitzgerald, M. Jin, and A. J. Grodzinsky, “Shear and Compression Differentially Regulate Clusters of Functionally Related Temporal Transcription Patterns in Cartilage Tissue,” *J. Biol. Chem.*, vol. 281, no. 34, pp. 24095–24103, Aug. 2006.

[44] D. D. Anderson, S. Chubinskaya, F. Guilak, J. A. Martin, T. R. Oegema, S. A. Olson, and J. A. Buckwalter, “Post-traumatic osteoarthritis: improved understanding and opportunities for early intervention.,” *J. Orthop. Res.*, vol. 29, no. 6, pp. 802–9, Jun. 2011.

[45] C.-T. Chen, N. Burton-Wurster, C. Borden, K. Hueffer, S. E. Bloom, and G. Lust, “Chondrocyte necrosis and apoptosis in impact damaged articular cartilage,” *J. Orthop. Res.*, vol. 19, no. 4, pp. 703–711, Jul. 2001.

[46] T. M. Quinn, R. G. Allen, B. J. Schalet, P. Perumbuli, and E. B. Hunziker, “Matrix and cell injury due to sub-impact loading of adult bovine articular cartilage explants: effects of strain rate and peak stress.,” *J. Orthop. Res.*, vol. 19, no. 2, pp. 242–9, Mar. 2001.

[47] T. M. Quinn, A. J. Grodzinsky, E. B. Hunziker, and J. D. Sandy, “Effects of injurious compression on matrix turnover around individual cells in calf articular cartilage explants.,” *J. Orthop. Res.*, vol. 16, no. 4, pp. 490–9, Jul.

1998.

[48] V. Morel and T. M. Quinn, “Cartilage injury by ramp compression near the gel diffusion rate.,” *J. Orthop. Res.*, vol. 22, no. 1, pp. 145–51, Jan. 2004.

[49] M. L. Delco, “Acute mitochondrial dysfunction in cartilage following mechanical injury,” *Osteoarthr. Cartil.*, vol. 23, pp. A288–A289, Apr. 2015.

[50] M. M. Temple-Wong, S. Ren, P. Quach, B. C. Hansen, A. C. Chen, A. Hasegawa, D. D. D’Lima, J. Koziol, K. Masuda, M. K. Lotz, and R. L. Sah, “Hyaluronan concentration and size distribution in human knee synovial fluid: variations with age and cartilage degeneration,” *Arthritis Res. Ther.*, vol. 18, no. 1, p. 18, Dec. 2016.

[51] K. A. Elsaid, B. C. Fleming, H. L. Oksendahl, J. T. Machan, P. D. Fadale, M. J. Hulstyn, R. Shalvoy, and G. D. Jay, “Decreased lubricin concentrations and markers of joint inflammation in the synovial fluid of patients with anterior cruciate ligament injury.,” *Arthritis Rheum.*, vol. 58, no. 6, pp. 1707–15, Jun. 2008.

[52] M. K. Kosinska, T. E. Ludwig, G. Liebisch, R. Zhang, H.-C. Siebert, J. Wilhelm, U. Kaesser, R. B. Dettmeyer, H. Klein, B. Ishaque, M. Rickert, G. Schmitz, T. A. Schmidt, and J. Steinmeyer, “Articular Joint Lubricants during Osteoarthritis and Rheumatoid Arthritis Display Altered Levels and Molecular Species,” *PLoS One*, vol. 10, no. 5, p. e0125192, May 2015.

[53] K. A. Waller, L. X. Zhang, K. A. Elsaid, B. C. Fleming, M. L. Warman, and G.

D. Jay, “Role of lubricin and boundary lubrication in the prevention of chondrocyte apoptosis.,” *Proc. Natl. Acad. Sci. U. S. A.*, vol. 110, no. 15, pp. 5852–7, Apr. 2013.

[54] B. L. Wong, W. C. Bae, J. Chun, K. R. Gratz, M. Lotz, and R. L. Robert L. Sah, “Biomechanics of cartilage articulation: Effects of lubrication and degeneration on shear deformation,” *Arthritis Rheum.*, vol. 58, no. 7, pp. 2065–2074, Jul. 2008.

[55] E. A. Balazs and J. L. Denlinger, “Viscosupplementation: a new concept in the treatment of osteoarthritis.,” *J. Rheumatol. Suppl.*, vol. 39, pp. 3–9, Aug. 1993.

[56] J. P. Vacanti and R. Langer, “Tissue engineering: the design and fabrication of living replacement devices for surgical reconstruction and transplantation,” *Lancet*, vol. 354, pp. S32–S34, Jul. 1999.

[57] N. W. Rydell, J. Butler, and E. A. Balazs, “Hyaluronic acid in synovial fluid. VI. Effect of intra-articular injection of hyaluronic acid on the clinical symptoms of arthritis in track horses.,” *Acta vet.*, vol. 11, pp. 139–155, 1970.

[58] J. G. Peyron and E. A. Balazs, “Preliminary clinical assessment of Na-hyaluronate injection into human arthritic joints.,” *Pathol. Biol. (Paris).*, vol. 22, no. 8, pp. 731–6, Oct. 1974.

[59] M. E. Adams, M. H. Atkinson, A. J. Lussier, J. I. Schulz, K. A. Siminovitch, J. P. Wade, and M. Zummer, “The role of viscosupplementation with hylan G-F 20 (Synvisc) in the treatment of osteoarthritis of the knee: a Canadian

multicenter trial comparing hylan G-F 20 alone, hylan G-F 20 with non-steroidal anti-inflammatory drugs (NSAIDs) and NSAIDs alone.," *Osteoarthritis Cartilage*, vol. 3, no. 4, pp. 213–25, Dec. 1995.

[60] I. Finelli, E. Chiessi, D. Galesso, D. Renier, and G. Paradossi, "Gel-like structure of a hexadecyl derivative of hyaluronic acid for the treatment of osteoarthritis.," *Macromol. Biosci.*, vol. 9, no. 7, pp. 646–53, Jul. 2009.

[61] D. Scale, M. Wobig, and W. Wolpert, "Viscosupplementation of osteoarthritic knees with hylan: A treatment schedule study," *Curr. Ther. Res.*, vol. 55, no. 3, pp. 220–232, Mar. 1994.

[62] C. R. Flannery, R. Zollner, C. Corcoran, A. R. Jones, A. Root, M. A. Rivera-Bermúdez, T. Blanchet, J. P. Gleghorn, L. J. Bonassar, A. M. Bendele, E. A. Morris, and S. S. Glasson, "Prevention of cartilage degeneration in a rat model of osteoarthritis by intraarticular treatment with recombinant lubricin.," *Arthritis Rheum.*, vol. 60, no. 3, pp. 840–7, Mar. 2009.

[63] E. Teeple, K. A. Elsaid, G. D. Jay, L. Zhang, G. J. Badger, M. Akelman, T. F. Bliss, and B. C. Fleming, "Effects of supplemental intra-articular lubricin and hyaluronic acid on the progression of posttraumatic arthritis in the anterior cruciate ligament-deficient rat knee.," *Am. J. Sports Med.*, vol. 39, no. 1, pp. 164–72, Jan. 2011.

[64] G. D. Jay, B. C. Fleming, B. A. Watkins, K. A. McHugh, S. C. Anderson, L. X. Zhang, E. Teeple, K. A. Waller, and K. A. Elsaid, "Prevention of cartilage

degeneration and restoration of chondroprotection by lubricin tribosupplementation in the rat following anterior cruciate ligament transection.," *Arthritis Rheum.*, vol. 62, no. 8, pp. 2382–91, Aug. 2010.

[65] M. Wathier, B. A. Lakin, P. N. Bansal, S. S. Stoddart, B. D. Snyder, and M. W. Grinstaff, "A Large-Molecular-Weight Polyanion, Synthesized via Ring-Opening Metathesis Polymerization, as a Lubricant for Human Articular Cartilage," 2013.

[66] K. J. Samaroo, M. Tan, D. Putnam, and L. J. Bonassar, "Binding and lubrication of biomimetic boundary lubricants on articular cartilage," *J. Orthop. Res.*, Jul. 2016.

[67] K. Samaroo, "Biomimetic Boundary Lubricants Of Articular Cartilage," 2015.

[68] S. M. McNary, K. A. Athanasiou, and A. H. Reddi, "Engineering lubrication in articular cartilage.," *Tissue Eng. Part B. Rev.*, vol. 18, no. 2, pp. 88–100, Apr. 2012.

[69] M. Brittberg, A. Lindahl, A. Nilsson, C. Ohlsson, O. Isaksson, and L. Peterson, "Treatment of deep cartilage defects in the knee with autologous chondrocyte transplantation.," *N. Engl. J. Med.*, vol. 331, no. 14, pp. 889–95, Oct. 1994.

[70] D. J. Griffin, E. D. Bonnevie, D. J. Lachowsky, J. C. A. Hart, H. D. Sparks, N. Moran, G. Matthews, A. J. Nixon, I. Cohen, and L. J. Bonassar, "Mechanical characterization of matrix-induced autologous chondrocyte implantation (MACI®) grafts in an equine model at 53 weeks," *J. Biomech.*, vol. 48, no. 10,

pp. 1944–1949, 2015.

[71] M. Oka, T. Noguchi, P. Kumar, K. Ikeuchi, T. Yamamuro, S. H. Hyon, and Y. Ikada, “Development of an artificial articular cartilage.,” *Clin. Mater.*, vol. 6, no. 4, pp. 361–81, 1990.

[72] M. A. Accardi, S. D. McCullen, A. Callanan, S. Chung, P. M. Cann, M. M. Stevens, and D. Dini, “Effects of fiber orientation on the frictional properties and damage of regenerative articular cartilage surfaces.,” *Tissue Eng. Part A*, vol. 19, no. 19–20, pp. 2300–10, Oct. 2013.

[73] S. Grad, M. Loparic, R. Peter, M. Stolz, U. Aebi, and M. Alini, “Sliding motion modulates stiffness and friction coefficient at the surface of tissue engineered cartilage.,” *Osteoarthritis Cartilage*, vol. 20, no. 4, pp. 288–95, Apr. 2012.

[74] S. Grad, C. R. Lee, K. Gorna, S. Gogolewski, M. A. Wimmer, and M. Alini, “Surface motion upregulates superficial zone protein and hyaluronan production in chondrocyte-seeded three-dimensional scaffolds.,” *Tissue Eng.*, vol. 11, no. 1–2, pp. 249–56, Jan. 2005.

[75] S. A. Unterman, M. Gibson, J. H. Lee, J. Crist, T. Chansakul, E. C. Yang, and J. H. Elisseeff, “Hyaluronic acid-binding scaffold for articular cartilage repair.,” *Tissue Eng. Part A*, vol. 18, no. 23–24, pp. 2497–506, Dec. 2012.

[76] A. Singh, M. Corvelli, S. A. Unterman, K. A. Wepasnick, P. McDonnell, and J. H. Elisseeff, “Enhanced lubrication on tissue and biomaterial surfaces through peptide-mediated binding of hyaluronic acid.,” *Nat. Mater.*, vol. 13, no. 10, pp.

988–95, Oct. 2014.

[77] T. J. Klein, B. L. Schumacher, T. A. Schmidt, K. W. Li, M. S. Voegtline, K. Masuda, E. J.-M. A. Thonar, and R. L. Sah, “Tissue engineering of stratified articular cartilage from chondrocyte subpopulations,” *Osteoarthr. Cartil.*, vol. 11, no. 8, pp. 595–602, Aug. 2003.

CHAPTER 2

Elastoviscous Transitions of Articular Cartilage Reveal a Mechanism of Synergy between Lubricin and Hyaluronic Acid[1]

Abstract

When lubricated by synovial fluid, articular cartilage provides some of the lowest friction coefficients found in nature. While it is known that macromolecular constituents of synovial fluid provide it with its lubricating ability, it is not fully understood how two of the main molecules, lubricin and hyaluronic acid, lubricate and interact with one another. Here, we develop a novel framework for cartilage lubrication based on the elastoviscous transition to show that lubricin and hyaluronic acid lubricate by distinct mechanisms. Such analysis revealed nonspecific interactions between these molecules in which lubricin acts to concentrate hyaluronic acid near the tissue surface and promotes a transition to a low friction regime consistent with the theory of viscous boundary lubrication. Understanding the mechanics of synovial fluid not only provides insight into the progression of diseases such as arthritis, but also may be applicable to the development of new biomimetic lubricants.

[1] This chapter is published: Bonnevie, ED, Galesso, D, Secchieri, C, Cohen, I, Bonassar, LJ. Elastoviscous Transitions of Articular Cartilage Reveal a Mechanism of Synergy between Lubricin and Hyaluronic Acid. *PLoS ONE,* 2015

Introduction

The healthy function of the body's articular joints has long been considered a remarkable tribological phenomenon. The main bearing surface, articular cartilage, provides low friction ($\mu < 0.01$) and low wear over decades of constant use [1], [2]. This superior function of cartilage has been tied to several mechanical factors including, most notably, lubrication by molecules in synovial fluid and interstitial fluid pressurization within the cartilage matrix [2]–[5]. In a healthy joint, pressurization of the interstitial fluid supports a substantial portion of the normal load, reducing the stresses experienced by solid-solid contact of apposing asperities. This load sharing between fluid and solid states is the main contributor in the very low friction coefficients previously measured [1], [6], [7]. However, macromolecules in synovial fluid reduce the shear stresses at the asperity contacts [3]–[5], and associated tissue damage [8] and cell death [9].

The main macromolecules attributed to synovial fluid lubrication are lubricin (also known as Proteoglycan-4 and superficial zone protein) and hyaluronic acid (HA) [4], [10]. Lubricin is considered to be the principal boundary lubricant in synovial fluid [5], [11]. Found in relatively low concentrations (~200 μg/mL), the molecule's carboxy-terminus, a hemopexin-like domain, anchors the molecule to the articular surface, and a hydrophilic oligosaccharide brush domain attracts water to the surface, lowering the boundary friction coefficient [12], [13]. Further, intra-articular injection of lubricin in animal models of osteoarthritis inhibited degeneration of articular cartilage [14]–[16], but this therapy has not yet been tested in humans.

Previous studies using HA have been less clear regarding its lubricating ability.

There is evidence that this larger molecule, often over 1 MDa (compared to ~220 kDa for lubricin) can reduce the friction coefficient of cartilage. However, the mechanisms by which this molecule lubricates are not fully understood [5], [11], [17]–[19]. In fact, some studies suggest that HA has little lubrication benefit at all [3], [11]. Despite this confusion, the use of HA in intra-articular injections, commonly referred to as viscosupplementation, is widespread [20], [21]. The lack of consensus regarding the lubricating mechanisms of HA can be attributed to the lack of a suitable analysis framework to account to for its viscosity, which is on the order of 100 times more viscous than water for concentrations found in synovial fluid [10], [11]. Although synovial fluid can retain its boundary lubricating ability in the absence of HA [22], recently it has been hypothesized that lubricin and HA may work synergistically to promote more effective lubrication [18], [19], [23], [24]. It has however, been challenging to determine the mechanism for this synergistic interaction.

To unambiguously decouple the contributions from viscous lubricants (i.e., HA) and boundary lubricants (i.e., lubricin), it is necessary to map out lubrication modes. Classically, the Stribeck curve revealed distinct modes of lubrication for hard, impermeable materials when friction was presented as a function of sliding speed, lubricant viscosity, and normal load (Fig 2.1 dashed line) [25]. At low speeds and viscosities, and high loads, contacting asperities support the normal stress, and consequently friction and wear are high – called boundary mode lubrication. As speed and viscosity increase or load decreases, a film of interfacial fluid pressurizes reducing the stress on asperities. In the classical analysis with hard, impermeable materials with

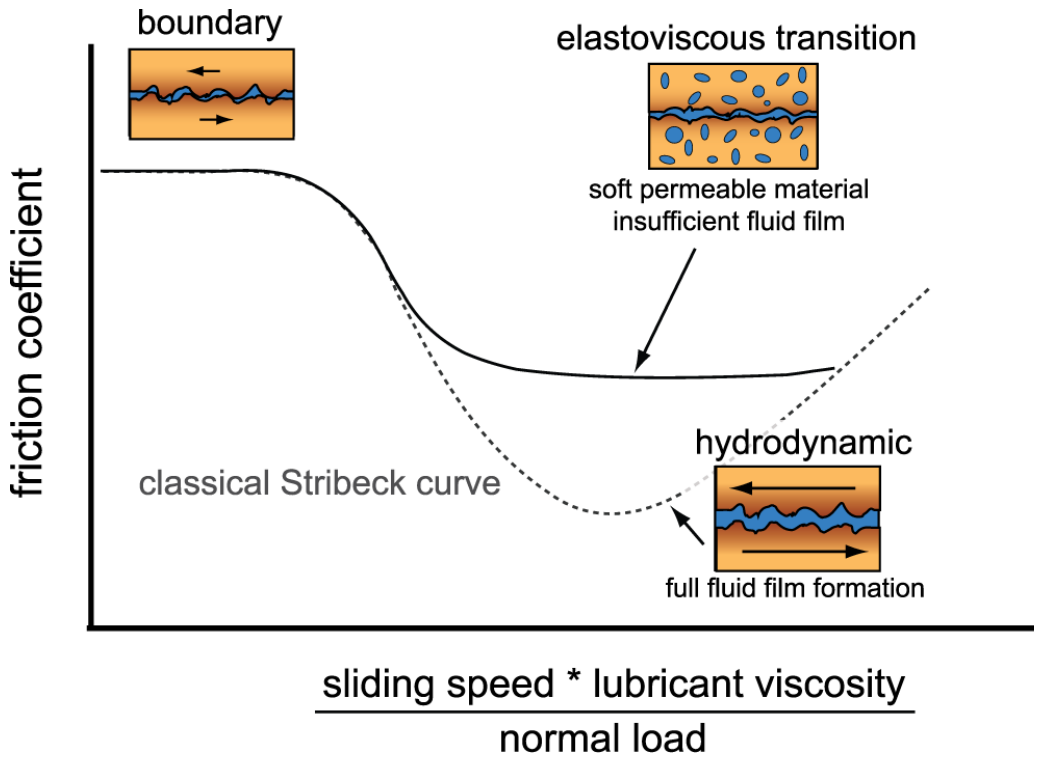

Figure 2.1 A classical Stribeck curve (dotted line) maps the transition of friction from high (boundary) friction to low (hydrodynamic) friction. For soft, permeable contacts like articular cartilage, a divergence from the classical curve is described by an elastoviscous transition [26] where contact compliance and permeability hinder the transition to hydrodynamic lubrication.

specific geometries, the curve mapped out a friction transition as interfacial fluid pressurized until the surfaces were fully separated – called hydrodynamic lubrication. Recently, it was shown that soft, permeable materials undergo similar transitions in lubrication behavior, but do not appear to achieve full hydrodynamic lubrication [26]. It was hypothesized that these transitions resulted from fluid pressurization, and that these deviations from the classical Stribeck behavior were due to fluid flow into and out of the contacting surfaces. This transition away from the classical curve was coined the elastoviscous transition (Fig 2.1 solid line) [26].

In this study, we apply this framework of lubrication to articular cartilage by mapping its elastoviscous transition. To accomplish this, we performed experiments with Sommerfeld number ranging 7 orders of magnitude by changing both sliding speed and viscosity. This framework enabled calculation of maximum and minimum friction, and a key parameter describing the transition between them. Carrying out these tests in combinations of lubricin and HA enabled assessment of their independent contributions to the elastoviscous transition curve. In addition, our studies revealed a synergistic mechanism in which HA is localized to the articular surface by lubricin that drives the system towards a low friction regime. Importantly, this synergy was not specific to HA, but was replicated by another viscous polymer dextran, albeit at much higher concentrations. As such, our studies suggest a new strategy for designing lubricating systems.

Results

Elastoviscous Transitions of Cartilage

In order to measure lubrication mode transitions of articular cartilage, friction coefficients of cartilage on glass were collected over speeds ranging 2 orders of magnitude while bathed in lubricants with viscosities varying 5 orders of magnitude (Fig. 2.2A). The lubricants used were phosphate buffered saline (PBS, 1 mPa·s dynamic viscosity), 700 kDa HA at 10 mg/mL (150 mPa·s), and a hydrophobic HA derivative (HYADD4; 72,000 mPa·s) [27]. The lubricants with elevated viscosities provided lower friction coefficients for unaltered cartilage surfaces (i.e., surfaces containing endogenously bound lubricin) (Fig 2.2A). Notably, HA reduced friction coefficients at elevated sliding speeds. This same data, was then presented as a function of the dimensionless Sommerfeld number [26], [28], *S*:

$$S = {}^{V\eta a}/_{F_n} \qquad \text{(equation 1)}$$

where V is sliding speed, η is lubricant viscosity, a is contact width (6 mm), and F_n is normal load (2.6 ± 0.11 N, corresponding to a 92 ± 4 kPa normal stress). Such analysis revealed μ to be a continuous function of S for all studies, which included changes in lubricant composition and concentration, sliding speed, and normal load (Figure 2.2BC). Reduced friction as a function of S was classically described by the formation of a pressurized fluid film between hard bodies in contact [25], but notably, for soft, permeable contacts, even though asperities may not fully separate, μ can still be described as a continuous function of S [26]. In such systems, it has been observed that these friction reductions can result from the formation of a viscous film [29], and we

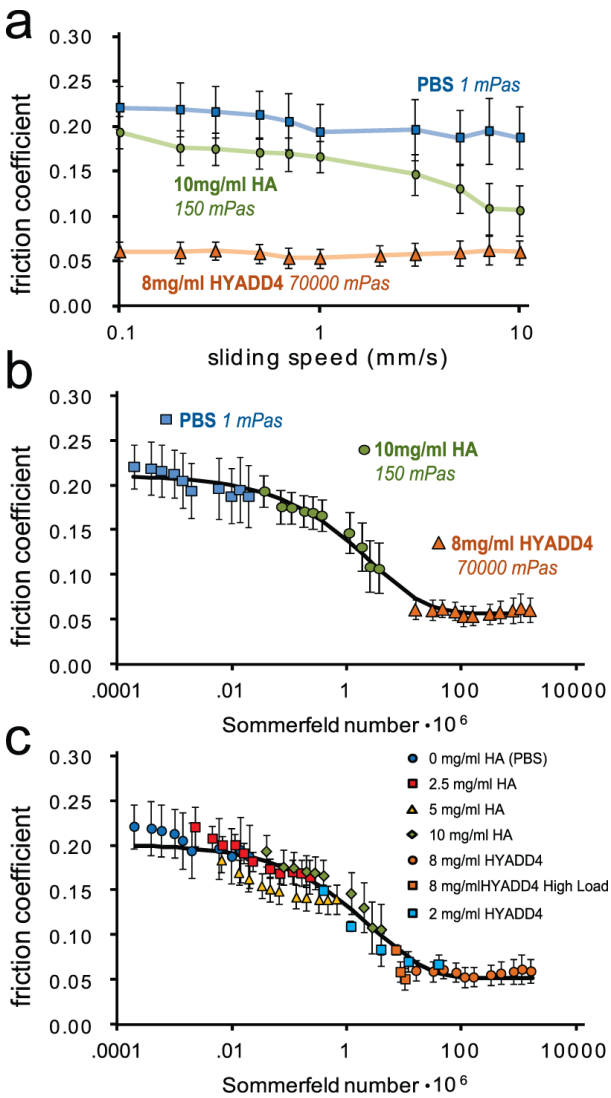

Figure 2.2 Presentation of friction coefficient as a function of the Sommerfeld number reveals viscous lubrication by HA. (Top) Friction coefficient as a function of sliding speed for three different lubricants with a wide range of viscosities provided a range of friction coefficients that span almost an order of magnitude (n=5). (Middle) When the friction coefficients from the top panel are presented as a function of the Sommerfeld number (equation 1) instead of sliding speed, the mechanisms of lubrication become apparent and are fit to a model curve (equation 2) to determine alterations of the elastoviscous transition. (Bottom) Serial dilutions of the HA solution provided overlapping data sets confirming HA had no influence on the boundary friction coefficient, and increased load (4.2, 5.2, and 6.2 N; all at 0.1 mm/s) and decreased concentration (2 mg/ml) tests with HYADD4 revealed convergence of HA and HYADD4 in the transition region (HYADD4 2 mg/ml and high load, n=4, all others n=5) (data points represent mean±SEM).

have previously reported on similar friction decreases in this system at increased speed or decreased load for cartilage bathed in PBS [30]. Further, we examined dilutions of HA at 5 and 2.5 mg/mL to examine the convergence of the HA solutions towards the boundary mode plateau and found no differences at low *S* between PBS and HA. This finding confirmed previous reports that HA has no effect on the boundary mode friction coefficient of healthy cartilage (Fig 2.2C) [3], [11], [22]. We also noted that HA and HYADD4 data converged near the transition to minimum friction and dilution of HYADD4 to 2 mg/mL confirmed viscous lubrication by HYADD4. The data were fit to a curve [31] where friction coefficient, μ, transitioned from a boundary friction coefficient, μ_B (the value of μ at *S=0)*, to a minimum friction coefficient, μ_{min} (the value of μ at $S=\infty$), and allowed the determination of a transition number, S_t, that is representative of the Sommerfeld number at the midpoint of the transition. This equation was given by:

$$\mu(S) = \mu_{min} + (\mu_B - \mu_{min})e^{-(S/S_t)^d} \qquad \text{(equation 2)}$$

where *d* is a fitting parameter controlling the slope of the transition zone. The data (both Fig 2.1B and 2.1C) fit the curve well with a coefficient of variation of the RMS error below 0.08 and curve fit coefficients that differed by less than 7% between the two data sets. Collectively, these data revealed that cartilage transitioned smoothly from high to low friction modes as a function of the Sommerfeld number, consistent with an elastoviscous transition previously described for soft, permeable materials [26].

Synergy Between Lubricin and HA

Friction transitions were mapped for two other lubricin conditions in addition to the unaltered cartilage surfaces (Fig 2.3A). Samples with lubricin removed from the articular surface [13], [32], [33] produced a similarly shaped transition curve, but the boundary friction coefficient (μ_B) increased 27% from 0.22 to 0.28 ($p < 0.05$; Fig 2.3B). The transition number (S_t) increased from $3.7 \cdot 10^{-6}$ to $7.6 \cdot 10^{-6}$ ($p = 0.10$; Fig 2.3D) and there was no noticeable increase in the minimum friction coefficient (μ_{min}) (Fig 2.3C), indicating that minimum friction may be dependent on other factors such as counterface roughness or permeability. Interestingly, in the absence of lubricin, cartilage lubricated by HYADD4 achieved μ_{min} only at elevated speeds.

Addition of 20 μg/mL full-length recombinant lubricin [13], [32] lowered the boundary friction coefficient more than a factor of 2 ($\mu_B = 0.12$, $p < 0.05$) (Fig 2.3B), a result previously reported for this concentration of lubricin [32]. More interestingly, the transition number decreased 2 orders of magnitude ($S_t = 0.06 \cdot 10^{-6}$) ($p < 0.05$; Fig 2.3D). Consequently, HA solutions also yielded μ_{min} at relatively low sliding speeds ($V > 0.3$ mm/s). While the mechanism of viscous boundary lubrication has been used to explain similar observations in salivary mucins [29], our studies indicate this theory of lubrication is also applicable to articular cartilage. In essence, lubricin may act to localize HA near the articular surface, locally increase the viscosity, and drive the surfaces away from boundary mode lubrication. This idea of increasing local viscosity would not be expected from bulk rheology measurements where lubricin decreases viscosity by a factor of ~3 when added to HA solutions [34], but may be indicative of

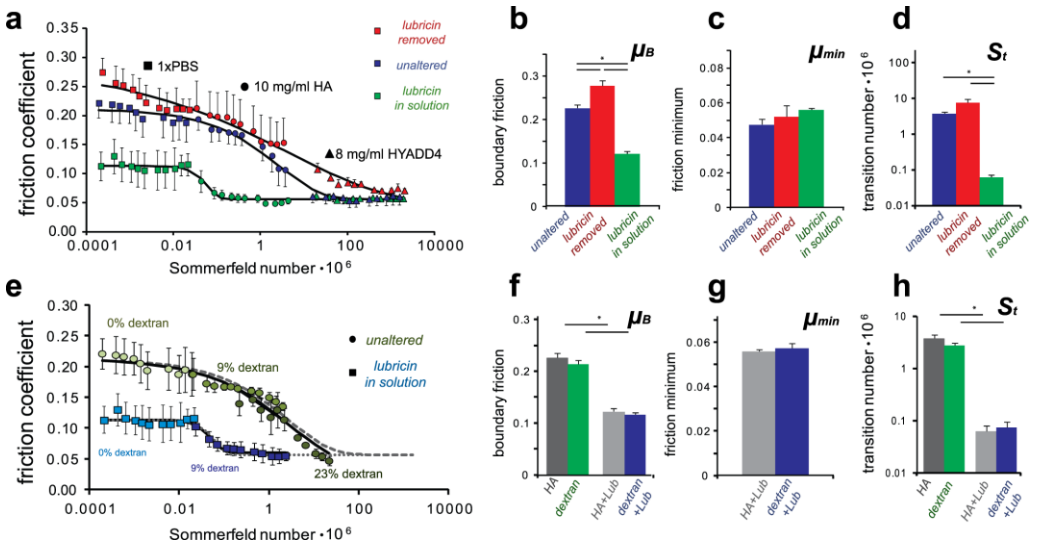

Figure 2.3 (A) Altering the presence of lubricin at the articular surface and in the lubricant solution revealed distinct elastoviscous transition curves. (B-D) The curve fit parameters revealed the importance of lubricin in boundary lubrication and also its importance in facilitating the transition away from boundary mode lubrication when present with HA. (E-H) Replication of the HA curves by dextran revealed that both the viscous lubrication by HA and the synergy with lubricin are not specific to the chemistry of HA. (n = 5 for unaltered, n = 3 for lubricin removed and lubricin in solution; data points represent mean±SEM)

a mechanism of confined fluid which has been shown to increase measured viscosities of synovial fluid by orders of magnitude [35].

Lubricin-HA Synergy is not Specific to HA Chemistry

Lubricin and HA together facilitated the transition away from boundary mode lubrication, but the question remains whether this interaction is specific to these molecules. To answer this question, the above experiments were repeated, replacing HA with another viscous polymer, 2 MDa dextran (Fig 2.3E-H). For the unaltered cartilage surfaces, the friction transition curves were similar for both dextran and HA. Notably, even 23% dextran (w/v) was not able to induce minimum friction even at the highest testing speeds. In the presence of exogenous lubricin, dextran again produced similar lubrication curves to HA. Collectively, these data show that HA and dextran produce similar elastoviscous transitions with μ_B, μ_{min}, and S_t coefficients that differ by less than 25%. As such, these data indicate that the viscous lubrication by HA and interaction with lubricin at the cartilage surface is not specific to the chemistry of HA. Due to the similarities between the HA and dextran curves, it is likely this phenomenon is mechanically motivated and could arise from entanglement, or hydrophobicity/hydrophilicity. While it is possible that similarities between HA and dextran as viscous polysaccharides are important to this interaction, it is noteworthy that this interaction with lubricin can occur with other molecules than HA.

Lubricin Facilitates the Aggregation of HA at the Articular Surface

To further test the hypothesis that lubricin enhances lubrication through localizing HA near the surface, we imaged articular cartilage with and without lubricin after exposure to HA. Specifically, unaltered cartilage samples were incubated in a

fluorescein-tagged HA solution, tapped dry and viewed on a confocal microscope. Simultaneous imaging of both the extracellular matrix through confocal reflectance and the labeled HA, revealed that HA aggregated at the articular surface (Figure 2.4A), but this aggregation was absent when lubricin was removed from the surface (Figure 2.4B). We also found that the aggregation of HA at the surface was weak, as the presence of HA at the lubricin-containing surfaces disappeared after a short rinse with physiologic saline. The weak nature of this interaction can explain why HA appears to have no effect on the boundary friction coefficient and why its results are replicable by another biopolymer.

Lubricin-HA Synergy Replicates Lubrication by Synovial Fluid

There are a multitude of other proposed molecular lubricants in synovial fluid (e.g., phospholipids, gamma globulin, etc.) [5], [36]. Consequently, to determine whether this interaction between lubricin and HA replicates the full lubricating effect of synovial fluid, subsequent tests were performed using intact equine synovial fluid, as well as synovial fluid depleted of HA by hyaluronidase [22] and depleted of lubricin by trypsin [34] (Fig 2.4C). For synovial fluid incubated with hyaluronidase (20 mPa·s viscosity), friction coefficients approached the boundary mode plateau at slow sliding speed and transitioned toward the minimum friction at elevated speed, with little indication that the results diverged from the previously found curve for lubricin in solution (Fig 2.4C). In contrast, trypsin treatment had little effect on viscosity (146 mPa·s) but yielded data consistent with curves for cartilage in the absence of lubricin. Thus, in agreement with the above studies using recombinant molecules (Fig 2.3), we find that in synovial fluid HA provides elevated viscosity to

transition away from boundary mode, lubricin alters boundary mode friction, and the synergistic mechanism between them reduces the viscosity necessary to transition away from boundary mode.

Discussion

Lubricin-Mediated Synergy

In this paper, we identified an interaction between lubricin and HA that synergistically enhances lubrication of articular cartilage. This synergy between HA and lubricin is dependent on the binding of lubricin to surfaces and is not specific to the chemistry of HA. Other theories of lubricin-HA synergy at the articular surface exist [18], [19], [24], [37], but we have shown here that together, lubricin and HA are effective by forcing the transition away from the relatively higher friction associated with the boundary mode of lubrication. Recently, Das *et al* showed that adsorbed HA on mica surfaces interacted with lubricin and prevented wear, likely by forming a viscous gel layer at the surface [19]. This gel layer was estimated to be four orders of magnitude more viscous than the free solution. Similarly, Greene *et al* theorized that the chondroprotective basis of synovial fluid lubrication was mechanically driven [18] by trapping of HA near the surface and subsequent aggregation and cross-linking with lubricin. In this study we build upon these mechanically motivated gel-layer theories, and provide evidence that lubricin binding to articular surfaces initiates this mechanism with HA.

This theory of surface protection and lubrication by formation of a gel layer is not specific to HA and lubricin, and it has been previously referred to as “viscous boundary lubrication” [29]. This mechanism of lubrication was observed for the

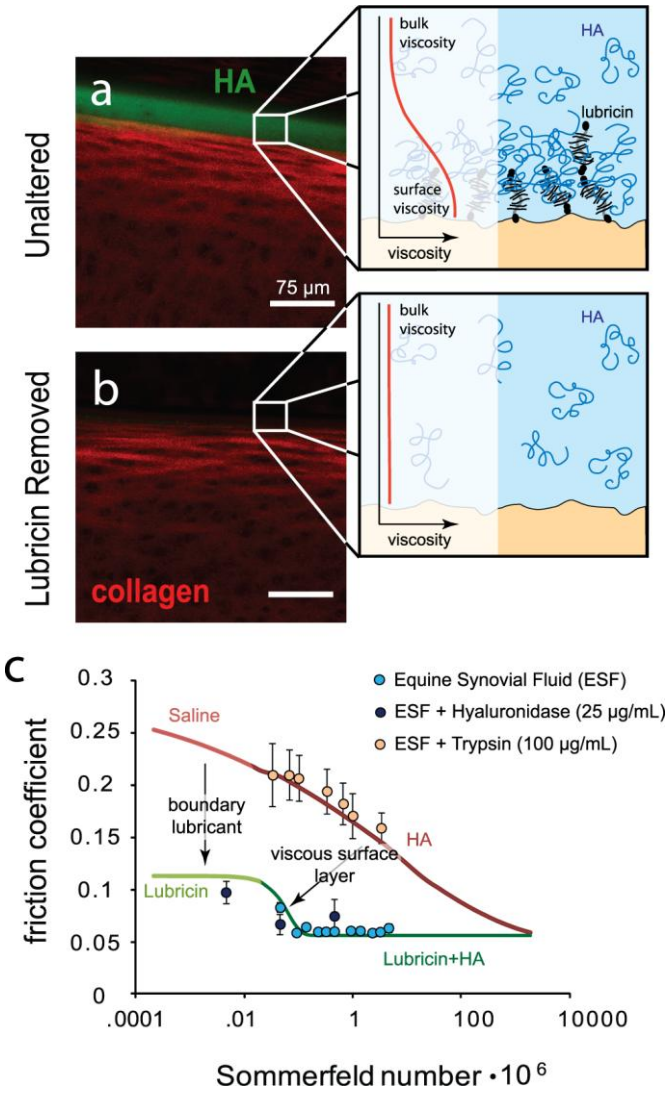

Figure 4: In native cartilage, lubricin bound to the surface facilitates HA aggregation near the surface (A). Lubricin likely entraps HA through entanglements, causing a local increase in viscosity near the tissue surface (A, inset). When lubricin is removed from the surface, HA does not aggregate (B) and surface viscosity is likely similar to the bulk (B, inset). Boundary lubrication by lubricin shifts the boundary regime down and increased viscosity near the surface shifts the elastoviscous transition such that the low friction regime occurs at lower sliding speeds consistent with viscous boundary lubrication (C). These phenomena of lubricin and HA replicate the lubrication by synovial fluid which transition to low friction at low speeds. By treating synovial fluid with hyaluronidase, friction is shifted back towards the boundary mode plateau as the fluid viscosity decreases, and trypsin treatment disrupts the synergy between lubricin and HA by digesting lubricin (n=4; data points represent mean±SEM).

aggregation of salivary mucins. With viscous, protein-adsorbed layers at sliding interfaces, the transition away from boundary mode lubrication may not scale with bulk solution rheology, but instead scale with the viscosity of the adsorbed layers [29]. In a similar manner to salivary mucins, we note that a surface gel layer of lubricin and HA could be a factor of 100 times more viscous than the bulk solution (Figure 2.4A inset; based on the alterations of S_t) which serves to reduce the operating time of a joint in boundary mode lubrication.

Lubrication by a gel layer in synovial fluid is distinct from the mechanism for salivary mucins, which appears to be mediated by protein aggregation. The present study indicates that sufficient lubrication of mammalian joints is dependent on the interaction of two molecules with different structures. Lubricin can be thought of simply as an amphiphillic tethered polymer brush that interacts in a non-specific manner with HA, which can be thought of as a linear viscous polymer. Whether this interaction is purely a mechanical entanglement, or it is dictated by the hydrophobic and hydrophilic nature of these molecules remains a subject of further exploration. The results presented here indicate that this interaction facilitates the formation of a gel-like layer at the articular surface where optimal lubrication is achieved by the cooperation of two molecules, lubricin and HA.

The Role of HA Viscosity in Cartilage Lubrication

In a classical analysis of rheology, HA solutions have exhibited significant shear thinning when tested using model shear configurations (e.g., metal plates or couettes) [38], [39]. This rheological behavior led previous researchers to note that friction reduction through increased normal stresses would be overshadowed by shear

thinning. Similarly, shear thinning behavior has been observed for synovial fluid as well [34], [40]. Recently; however, it was shown that microstructurally, synovial fluid may behave very differently when confined [35]. Banquy *et al.* showed orders of magnitude increases in viscosity of synovial fluid when confined between mica surfaces. Similarly in this study, the friction trends appeared to scale with the viscosities at low shear rates, which would not be expected if significant shear thinning occurred at the tissue surface. However, the affinity of HA to the articular surface may prove to be a crucial mechanism in restricting shear thinning or possibly in facilitating increased viscosity in a surface gel layer, as the molecules may behave similarly to the confined synovial fluid [35].

Divergence from the Classical Stribeck Curve

The Stribeck curve has been used for more than a century to describe lubrication modes of both engineering machines and the natural mechanisms at play in mammalian joints. However, recent experiments and theories of hydrogel lubrication proposed a divergence from the classical curve, which assumes full separation of solid asperities at high values of a lubricant parameter (e.g. the Sommerfeld number) [26]. Due to the compliance of soft materials like cartilage, it is possible that localized pools of pressurized fluid may form and reduce friction but not fully separate the surfaces in cases where pressurized fluid may flow into and out of the contact, a phenomenon that may be dictated by pore size or permeability [26]. In this study, we observed a transition away from the relatively higher boundary mode lubrication consistent with mixed-mode lubrication, but friction coefficients reached minimum values ($\mu > 0.04$) above what would be expected for true hydrodynamic friction ($\mu << 0.01$).

Nevertheless, these data demonstrate cartilage lubrication over 7 orders of magnitude in *S* that is consistent with an elastoviscous transition. Further studies may reveal what role the mechanics of the articular cartilage play in the transitions outlined above and what implications degradation of the extracellular matrix may have on lubrication mechanisms.

Limitations

While this study establishes the framework for studying the elastoviscous transition in cartilage lubrication, there are several limitations to be discussed. Although the concentration of lubricin used in this study was sub-physiologic, the level of lubrication observed, although not identical, was largely comparable to that of saturating levels of lubricin ($\mu = 0.12 \pm 0.01$ at 20 mcg/ml in the current study vs $\mu = 0.10 \pm 0.01$ at 300 mcg/ml reported previously [32]). Nevertheless, further studies should be aimed at elucidating the role of lubricin concentration on the lubrication mechanisms found in this study." Further, this study utilized a stationary contact area configuration [41] where polished glass was used as the counterface. Notably, boundary friction coefficients for PBS, lubricin, and synovial fluid are similar in this system to a cartilage-cartilage bearing [42], but further studies may be aimed at analyzing the synergistic mechanism found in this study for configurations of cartilage on cartilage or cartilage on meniscus. Lastly, the Sommerfeld number is a function of normal load in addition to sliding speed and viscosity (equation 1), and while increases in friction coefficient were observed at higher loads (Figure 2.2C), load was not studied extensively for all lubricant formulations. Consequently, a systematic evaluation of the contributions of load to the elastoviscous transition can solidify this

system as a robust tool to study the lubrication mechanisms of cartilage and other soft material bearings.

Implications for Joint Injury, Disease, and Therapy

This study shows that articular cartilage lubrication can be described as a smooth continuous function of the Sommerfeld number, and cartilage likely experiences lubrication throughout a wide range of Sommerfeld numbers. High *S* can occur during the unloaded swing phase of gait (high relative velocity and low load), and low *S* may can occur during foot strike (low relative velocity and high load). Additionally, changes in viscosity affect *S*, and this is particularly important in joint injury and disease, where the composition of synovial fluid changes significantly [10], [12], [43]. Notably, HA concentration and size, as well as lubricin concentration, are altered for extensive periods of time after the initiation of trauma or disease. As such, both of these molecules have been targets for joint therapy, with HA injections being used clinically for decades [20] and multiple recent studies demonstrating disease-modifying capabilities of lubricin injections in animal models of joint injury [14], [44]. The experimental and analytical framework used in this study gives unique insights into the mechanisms of action of these therapies. First, mapping the elastoviscous transition makes it clear that HA is an exceptional viscous lubricant, with modified forms (HYADD4) producing superior lubrication to dextrans that are more than double in size and are present in over 30 fold higher concentrations. Secondly, it is clear that localization of HA by lubricin synergistically enhances lubrication, suggesting that lubricin delivery to joints may be an important therapy, both alone or in combination with HA. Collectively, these data point to the importance

of studying the regulation of both of these molecules in acute and chronic diseases to more fully understand the pathogenesis of arthritis.

More broadly, the identification of this lubrication mechanism that relies on the cooperation of two different lubricating molecules to protect soft surfaces from high friction and wear is applicable outside of the realm of biology. Through creation of biomimetic systems that exploit this naturally occurring mechanism, scientists can create more efficient bearing systems of soft material interfaces.

Methods

Tribological Testing

Friction coefficients were measured on our previously described, custom-built tribometer [30], [32], [33]. Cartilage samples were obtained from the patellofemoral groove of neonatal (1-3 day old) bovine stifles. Cylindrical cartilage samples (6 mm in diameter by 2 mm high) were mated against a polished glass flat counterface while bathed in a lubricant bath in a configuration consistent with a tilt pad bearing (See: Gleghorn *et al.* 2008). Samples were tested in a stationary contact area configuration that mitigates the effects of interstitial fluid pressurization on friction coefficient measurements [33], [41]. Before friction testing, samples were compressed to 25% strain and allowed to depressurize over the course of 1 hour resulting in average normal loads of 2.6 N. After fluid pressure dropped to the ambient pressure, the glass counterface was reciprocated at predetermined speeds ranging from 0.1 to 10 mm/s. Friction coefficients were recorded as the ratio of shear load to normal load measured by a biaxial load cell. Coefficients were calculated at the end of sliding when friction

had reached an equilibrium value and averaged for both the forward and reverse sliding directions [45].

Lubricant Formulations and Cartilage Surfaces

The role of hyaluronic acid and viscosity were analyzed using three different HA conditions within the lubricant bath. A HA-free control bath was phosphate buffered saline (PBS; Corning, Manassas VA). Sodium hyaluronate (Fidia Farmaceutici, Padua Italy) with 500-730 kDa molecular weight obtained from *Streptococcus Equi* fermentation and formulated to a final solution of 10 mg/mL in PBS was used as the HA solution . HYADD4 (Fidia Farmaceutici, Padua Italy) which is a partially hydrophobic hexadecyl derivative of HA with a 3% mol/mol repeating unit substitution provided a lubricant bath with increased viscosity at a concentration of 8 mg/mL in PBS [27], [46]. These three lubricant baths were also tested with and without rhLubricin added into solution at a concentration of 20 μg/mL (a gift from Dr. Carl Flannery, Pfizer). The 20 μg/mL concentration was chosen as we have previously shown a saturation of boundary lubrication in this system for this concentration [32]. For the baths without lubricin, two cartilage surface conditions were tested. First cartilage samples were tested unaltered after dissection containing their endogenously bound lubricin, and samples were also tested after lubricin was removed from the articular surface via a hypertonic (1.5M) saline incubation for 25 minutes followed by a 1 hr re-equilibration in PBS [13]. The efficacy of lubricin extraction was analyzed via immunohistochemical staining (see supplemental material). For the lubricant baths containing lubricin, only unaltered cartilage surfaces were tested.

Subsequent tests using 2 MDa dextran (Sigma Aldrich, St Louis MO) in place

of HA were carried out using cartilage with unaltered surfaces using 9% (w/v) and 23% solutions and also 9% solution with 20 μg/mL rhLubricin added. Finally, tests using equine synovial fluid from the carpus joints of skeletally mature horses provided a comparison of the solutions to the native synovial fluid. To determine the role of synovial fluid viscosity, equine synovial fluid (ESF) was also tested after two hour incubation with 25 μg/mL bovine testes hyaluronidase (Sigma Aldrich, St Louis MO) added into the solution [22]. To determine the role of lubricin, ESF was also digested with TPCK trypsin (Sigma Aldrich, St Louis MO) from bovine pancreas as previously reported [34]. Briefly, 100 μL of 2 mg/mL trypsin was added to ESF for 2 hours at 37 °C under constant stirring conditions.

Rheological Testing

To determine the role of viscosity, a commercial rheometer (TA Instruments DHR3 Rheometer, New Castle DE) was used to measure the low shear rate viscosity of the lubricant baths. For most lubricants, a 40 mm diameter cone-plate set up with a 2° angle was used at a shear rate of $\dot{\gamma} = 1\ s^{-1}$. For HYADD4 a custom sandblasted 25 mm plate-plate set up was used to mitigate wall slip due to elevated viscosity. Viscosities were measured of 156 mPas for 10 mg/mL HA, 72,000 mPas for 8 mg/mL HYADD4, 200 mPas for equine synovial fluid, 20 mPas for ESF incubated with hyaluronidase, 146 mPas for ESF incubated with trypsin, 108 mPas for 9% dextran, and 884 mPas for 23% dextran. Subsequent serial dilutions of the HA solutions provided viscosities of 30 mPas and 11 mPas for 5 mg/mL and 2.5 mg/mL solutions, respectively, and dilution of HYADD4 to 2 mg/mL provided a viscosity of 1400 mPas.

Confocal Imaging

Articular cartilage explants both containing the endogenously bound lubricin and with endogenous lubricin removed were incubated in 1 mg/mL 750 kDa fluorescein-tagged HA (Creative PEG Works, Winston Salem NC) that was dialyzed overnight to remove any unbound label for 5 minutes. After incubation, samples were cut into hemicylinders, tapped dry on a glass slide and a cross-sectional view was imaged on a Zeiss LSM710 confocal microscope. Both the fluorecein signal and reflectance from the collagen extracellular matrix were merged in images to view whether affinity of HA to the articular surface is dictated by localized lubricin.

Statistical Analysis

To determine the uncertainty in the curve fit parameters of importance (i.e., boundary friction, minimum friction, and the Sommerfeld number at the mid-point along the transition), a Monte Carlo simulation was conducted on a point-by-point basis based on the standard deviation of measurements and a random normal distribution with a mean of 0 and a standard deviation of 1 [45], [47]. To determine differences in curve fit parameters between groups, a one way ANOVA was conducted and significance was set at $p < 0.05$. Data and error bars represent mean ± SEM.

REFERENCES

[1] C. W. McCutchen, “The frictional properties of animal joints,” *Wear*, vol. 5, no. 1, pp. 1–17, Jan. 1962.

[2] G. A. Ateshian, “The role of interstitial fluid pressurization in articular cartilage lubrication.,” *J. Biomech.*, vol. 42, no. 9, pp. 1163–76, Jun. 2009.

[3] D. A. Swann, F. H. Silver, H. S. Slayter, W. Stafford, and E. Shore, “The molecular structure and lubricating activity of lubricin isolated from bovine and human synovial fluids.,” *Biochem. J.*, vol. 225, no. 1, pp. 195–201, Jan. 1985.

[4] G. D. Jay, “Characterization of a bovine synovial fluid lubricating factor. I. Chemical, Surface activity and lubricating properties,” Jul. 2009.

[5] T. A. Schmidt, N. S. Gastelum, Q. T. Nguyen, B. L. Schumacher, and R. L. Sah, “Boundary lubrication of articular cartilage: role of synovial fluid constituents.,” *Arthritis Rheum.*, vol. 56, no. 3, pp. 882–91, Mar. 2007.

[6] R. Krishnan, M. Kopacz, and G. A. Ateshian, “Experimental verification of the role of interstitial fluid pressurization in cartilage lubrication.,” *J. Orthop. Res.*, vol. 22, no. 3, pp. 565–70, May 2004.

[7] E. D. Bonnevie, V. Baro, L. Wang, and D. L. Burris, “In-situ studies of cartilage microtribology: roles of speed and contact area.,” *Tribol. Lett.*, vol. 41, no. 1, pp. 83–95, Jan. 2011.

[8] G. D. Jay, J. R. Torres, D. K. Rhee, H. J. Helminen, M. M. Hytinnen, C.-J. Cha, K. Elsaid, K.-S. Kim, Y. Cui, and M. L. Warman, “Association between friction and wear in diarthrodial joints lacking lubricin.,” *Arthritis Rheum.*, vol. 56, no.

11, pp. 3662–9, Nov. 2007.

[9] K. A. Waller, L. X. Zhang, K. A. Elsaid, B. C. Fleming, M. L. Warman, and G. D. Jay, “Role of lubricin and boundary lubrication in the prevention of chondrocyte apoptosis.,” *Proc. Natl. Acad. Sci. U. S. A.*, vol. 110, no. 15, pp. 5852–7, Apr. 2013.

[10] E. A. Balazs, D. Watson, I. F. Duff, and S. Roseman, “Hyaluronic acid in synovial fluid. I. Molecular parameters of hyaluronic acid in normal and arthritic human fluids,” *Arthritis Rheum.*, vol. 10, no. 4, pp. 357–376, Aug. 1967.

[11] G. D. Jay, K. Haberstroh, and C. J. Cha, “Comparison of the boundary-lubricating ability of bovine synovial fluid, lubricin, and Healon.,” *J. Biomed. Mater. Res.*, vol. 40, no. 3, pp. 414–8, Jun. 1998.

[12] K. A. Elsaid, G. D. Jay, M. L. Warman, D. K. Rhee, and C. O. Chichester, “Association of articular cartilage degradation and loss of boundary-lubricating ability of synovial fluid following injury and inflammatory arthritis.,” *Arthritis Rheum.*, vol. 52, no. 6, pp. 1746–55, Jun. 2005.

[13] A. R. C. Jones, J. P. Gleghorn, C. E. Hughes, L. J. Fitz, R. Zollner, S. D. Wainwright, B. Caterson, E. A. Morris, L. J. Bonassar, and C. R. Flannery, “Binding and localization of recombinant lubricin to articular cartilage surfaces.,” *J. Orthop. Res.*, vol. 25, no. 3, pp. 283–92, Mar. 2007.

[14] C. R. Flannery, R. Zollner, C. Corcoran, A. R. Jones, A. Root, M. A. Rivera-Bermúdez, T. Blanchet, J. P. Gleghorn, L. J. Bonassar, A. M. Bendele, E. A.

Morris, and S. S. Glasson, “Prevention of cartilage degeneration in a rat model of osteoarthritis by intraarticular treatment with recombinant lubricin.,” *Arthritis Rheum.*, vol. 60, no. 3, pp. 840–7, Mar. 2009.

[15] G. D. Jay, B. C. Fleming, B. A. Watkins, K. A. McHugh, S. C. Anderson, L. X. Zhang, E. Teeple, K. A. Waller, and K. A. Elsaid, “Prevention of cartilage degeneration and restoration of chondroprotection by lubricin tribosupplementation in the rat following anterior cruciate ligament transection.,” *Arthritis Rheum.*, vol. 62, no. 8, pp. 2382–91, Aug. 2010.

[16] Z. Cui, C. Xu, X. Li, J. Song, and B. Yu, “Treatment with recombinant lubricin attenuates osteoarthritis by positive feedback loop between articular cartilage and subchondral bone in ovariectomized rats.,” *Bone*, vol. 74, pp. 37–47, May 2015.

[17] D. A. Swann, E. L. Radin, M. Nazimiec, P. A. Weisser, N. Curran, and G. Lewinnek, “Role of hyaluronic acid in joint lubrication.,” *Ann. Rheum. Dis.*, vol. 33, no. 4, pp. 318–26, Jul. 1974.

[18] G. W. Greene, X. Banquy, D. W. Lee, D. D. Lowrey, J. Yu, and J. N. Israelachvili, “Adaptive mechanically controlled lubrication mechanism found in articular joints.,” *Proc. Natl. Acad. Sci. U. S. A.*, vol. 108, no. 13, pp. 5255–9, Mar. 2011.

[19] S. Das, X. Banquy, B. Zappone, G. W. Greene, G. D. Jay, and J. N. Israelachvili, “Synergistic interactions between grafted hyaluronic acid and lubricin provide enhanced wear protection and lubrication.,”

Biomacromolecules, vol. 14, no. 5, pp. 1669–77, May 2013.

[20] E. A. Balazs and J. L. Denlinger, "Viscosupplementation: a new concept in the treatment of osteoarthritis.," *J. Rheumatol. Suppl.*, vol. 39, pp. 3–9, Aug. 1993.

[21] B. Widner, R. Behr, S. Von Dollen, M. Tang, T. Heu, A. Sloma, D. Sternberg, P. L. Deangelis, P. H. Weigel, and S. Brown, "Hyaluronic acid production in Bacillus subtilis.," *Appl. Environ. Microbiol.*, vol. 71, no. 7, pp. 3747–52, Jul. 2005.

[22] F. C. Linn, "Lubrication of animal joints," *J. Biomech.*, vol. 1, no. 3, pp. 193–205, Aug. 1968.

[23] J. J. Kwiecinski, S. G. Dorosz, T. E. Ludwig, S. Abubacker, M. K. Cowman, and T. A. Schmidt, "The effect of molecular weight on hyaluronan's cartilage boundary lubricating ability--alone and in combination with proteoglycan 4.," *Osteoarthritis Cartilage*, vol. 19, no. 11, pp. 1356–62, Nov. 2011.

[24] S. E. Majd, R. Kuijer, A. Köwitsch, T. Groth, T. A. Schmidt, and P. K. Sharma, "Both hyaluronan and collagen type II keep proteoglycan 4 (lubricin) at the cartilage surface in a condition that provides low friction during boundary lubrication.," *Langmuir*, vol. 30, no. 48, pp. 14566–72, Dec. 2014.

[25] M. D. Hersey, "The laws of lubrication of horizontal journal bearings," *J. Washingt. Acad. Sci.*, vol. 4, no. August, pp. 542–552, 1914.

[26] A. C. Dunn, W. G. Sawyer, and T. E. Angelini, "Gemini Interfaces in Aqueous Lubrication with Hydrogels," *Tribol. Lett.*, vol. 54, no. 1, pp. 59–66, Mar. 2014.

[27] I. Finelli, E. Chiessi, D. Galesso, D. Renier, and G. Paradossi, "Gel-like

structure of a hexadecyl derivative of hyaluronic acid for the treatment of osteoarthritis.," *Macromol. Biosci.*, vol. 9, no. 7, pp. 646–53, Jul. 2009.

[28] A. Unsworth, "Tribology of human and artificial joints," *Arch. Proc. Inst. Mech. Eng. Part H J. Eng. Med. 1989-1996 (vols 203-210)*, vol. 205, no. 38, pp. 163–172, Jun. 1991.

[29] G. E. Yakubov, J. McColl, J. H. H. Bongaerts, and J. J. Ramsden, "Viscous boundary lubrication of hydrophobic surfaces by mucin.," *Langmuir*, vol. 25, no. 4, pp. 2313–21, Feb. 2009.

[30] J. P. Gleghorn and L. J. Bonassar, "Lubrication mode analysis of articular cartilage using Stribeck surfaces.," *J. Biomech.*, vol. 41, no. 9, pp. 1910–8, Jan. 2008.

[31] K. Worden, C. X. Wong, U. Parlitz, A. Hornstein, D. Engster, T. Tjahjowidodo, F. Al-Bender, D. D. Rizos, and S. D. Fassois, "Identification of pre-sliding and sliding friction dynamics: Grey box and black-box models," *Mech. Syst. Signal Process.*, vol. 21, no. 1, pp. 514–534, Jan. 2007.

[32] J. P. Gleghorn, A. R. C. Jones, C. R. Flannery, and L. J. Bonassar, "Boundary mode lubrication of articular cartilage by recombinant human lubricin.," *J. Orthop. Res.*, vol. 27, no. 6, pp. 771–7, Jun. 2009.

[33] E. D. Bonnevie, J. L. Puetzer, and L. J. Bonassar, "Enhanced boundary lubrication properties of engineered menisci by lubricin localization with insulin-like growth factor I treatment.," *J. Biomech.*, vol. 47, no. 9, pp. 2183–8, Jun. 2014.

[34] G. D. Jay, J. R. Torres, M. L. Warman, M. C. Laderer, and K. S. Breuer, "The role of lubricin in the mechanical behavior of synovial fluid.," *Proc. Natl. Acad. Sci. U. S. A.*, vol. 104, no. 15, pp. 6194–9, Apr. 2007.

[35] X. Banquy, D. W. Lee, S. Das, J. Hogan, and J. N. Israelachvili, "Shear-Induced Aggregation of Mammalian Synovial Fluid Components under Boundary Lubrication Conditions," *Adv. Funct. Mater.*, vol. 24, no. 21, pp. 3152–3161, Jun. 2014.

[36] J.-Y. Park, C.-T. Duong, A. R. Sharma, K.-M. Son, M. S. Thompson, S. Park, J.-D. Chang, J.-S. Nam, S. Park, and S.-S. Lee, "Effects of Hyaluronic Acid and γ-Globulin Concentrations on the Frictional Response of Human Osteoarthritic Articular Cartilage.," *PLoS One*, vol. 9, no. 11, p. e112684, Jan. 2014.

[37] G. D. Jay, B. P. Lane, and L. Sokoloff, "Characterization of a bovine synovial fluid lubricating factor III. The interaction with hyaluronic acid," Jul. 2009.

[38] D. A. Gibbs, E. W. Merrill, K. A. Smith, and E. A. Balazs, "Rheology of hyaluronic acid.," *Biopolymers*, vol. 6, no. 6, pp. 777–91, Jun. 1968.

[39] K. Hyun, S. H. Kim, K. H. Ahn, and S. J. Lee, "Large amplitude oscillatory shear as a way to classify the complex fluids," *J. Nonnewton. Fluid Mech.*, vol. 107, no. 1–3, pp. 51–65, Dec. 2002.

[40] W. M. Lai, S. C. Kuei, and V. C. Mow, "Rheological Equations for Synovial Fluids," *J. Biomech. Eng.*, vol. 100, no. 4, p. 169, Nov. 1978.

[41] M. Caligaris and G. A. Ateshian, "Effects of sustained interstitial fluid pressurization under migrating contact area, and boundary lubrication by

synovial fluid, on cartilage friction.," *Osteoarthritis Cartilage*, vol. 16, no. 10, pp. 1220–7, Oct. 2008.

[42] S. Abubacker, S. G. Dorosz, D. Ponjevic, G. D. Jay, J. R. Matyas, and T. A. Schmidt, "Full-Length Recombinant Human Proteoglycan 4 Interacts with Hyaluronan to Provide Cartilage Boundary Lubrication.," *Ann. Biomed. Eng.*, Jul. 2015.

[43] C. Ragan and K. Meyer, "THE HYALURONIC ACID OF SYNOVIAL FLUID IN RHEUMATOID ARTHRITIS.," *J. Clin. Invest.*, vol. 28, no. 1, pp. 56–9, Jan. 1949.

[44] E. Teeple, K. A. Elsaid, G. D. Jay, L. Zhang, G. J. Badger, M. Akelman, T. F. Bliss, and B. C. Fleming, "Effects of supplemental intra-articular lubricin and hyaluronic acid on the progression of posttraumatic arthritis in the anterior cruciate ligament-deficient rat knee.," *Am. J. Sports Med.*, vol. 39, no. 1, pp. 164–72, Jan. 2011.

[45] D. L. Burris and W. G. Sawyer, "Addressing Practical Challenges of Low Friction Coefficient Measurements," *Tribol. Lett.*, vol. 35, no. 1, pp. 17–23, Apr. 2009.

[46] I. Finelli, E. Chiessi, D. Galesso, D. Renier, and G. Paradossi, "A new viscosupplement based on partially hydrophobic hyaluronic acid: A comparative study," *Biorheology*, vol. 48, no. 5–6, pp. 263–275, 2011.

[47] E. D. Bonnevie, V. J. Baro, L. Wang, and D. L. Burris, "Fluid load support during localized indentation of cartilage with a spherical probe.," *J. Biomech.*,

vol. 45, no. 6, pp. 1036–41, Apr. 2012.

CHAPTER 3

IL-1β Inhibits the Lubricating Mechanisms of Articular Cartilage[2]

Abstract

Objective: This study analyzed the effect of IL-1β treatment on the lubrication mechanisms of articular cartilage explants. By analyzing friction as a function of the Sommerfeld number, which accounts for sliding speed, lubricant viscosity, normal load, and contact geometry, lubrication modes of cartilage were mapped and related to other tissue changes.

Method: Cartilage explants were cultured up to 8 days with 10 ng/mL IL-1β and compared to controls. The samples were examined histologically, immunohistochemically, biochemically, mechanically, topographically, and tribologically. The tribological testing utilized a recently developed framework to analyze lubrication mechanisms of soft, permeable materials by varying the Sommerfeld number over 6 orders of magnitude (4 orders of magnitude in lubricant viscosity and 2 orders of magnitude in sliding speed).

Results: After culture with IL-1β, cartilage lost lubricin localized to the surface and proteoglycan content throughout the tissue. The cartilage became progressively softer and more permeable in addition to becoming significantly rougher. Consequently, lubrication mechanisms were significantly altered. After the first 4 days, boundary friction was elevated, but after 8 days, boundary friction remained high and the

[2] To be published with coauthors: Bonnevie, ED, Galesso, D, Secchieri, C, Bonassar, LJ.

transition away from boundary friction was hindered.

Conclusion: This study revealed two distinct degradation-dependent mechanisms by which the lubrication of cartilage explants was altered. Early degradation mainly involved loss of lubricin, which affected boundary friction while further degradation involved significant loss of ECM and surface roughening, which affected the transition away from boundary friction. The occurrence of distinct mechanisms at different stages of degradation may point to targeted therapeutic strategies at different stages of disease.

Introduction

Healthy articular cartilage is one of nature's most efficient bearing materials. This tissue that promotes both load support and lubrication within the body's diarthrodial joints typically provides a low friction interface over decades of constant use. In both rheumatoid arthritis (RA) and osteoarthritis (OA) the failure of this tissue is linked to both inflammatory and mechanical changes [1], [2]. While it is well known that inflammation alters cartilage compositionally and mechanically [2], it is not fully understood how lubrication is affected. Consequently, understanding how mechanisms of lubrication are altered in inflammation can shed light on the mechanical processes of cartilage damage propagation and could point to new therapies.

The lubrication mechanisms of articular cartilage have been examined closely over the past century, and several distinct lubrication mechanisms appear to operate in concert. Although these mechanisms of lubrication have been called by several names (e.g., boosted, weeping, boundary, hydrodynamic, and elastohydrodynamic lubrication), two common processes emerge through examination of the theories [3]–[8]: the lubrication of solid-on-solid, asperity contacts (e.g., boundary lubrication by lubricin[9]) and reduction of stresses of solid-on-solid contacts through fluid pressurization [3], [8], [10].

The role of fluid pressurization in cartilage lubrication is considered a key natural mechanism that provides cartilage with its exceptionally low friction coefficients, at times lower than μ=0.01 [3]. Specifically, fluid pressurization near the cartilage surface can arise from two sources: interstitial fluid pressurization and

viscous interfacial films [3], [8], [11]. While interstitial fluid pressurization is a main contributor to the low friction measured in cartilage bearings [12], viscous molecules in synovial fluid also reduce friction under certain contact conditions. The relationship between contact conditions and friction were classically described by use of the Stribeck curve that mapped lubrication modes from high friction in boundary mode lubrication to low friction in hydrodynamic lubrication as a function of variables such as sliding speed, lubricant viscosity, normal load, and surface roughness. Recently, however, we have reported on a similar curve for cartilage lubrication called the elastoviscous transition [13] that maps lubrication modes for soft permeable materials (Fig. 3.1A) [11]. Utilizing this curve enables distinction between lubrication mechanisms that can be altered for cartilage in processes such as injury or disease. Specifically, alterations in boundary lubrication (Fig. 3.1B) and the transition away from boundary lubrication to a regime dictated by viscous films (Fig. 3.1C) can be revealed by changes in this lubrication curve.

Key lubricating components of synovial fluid, lubricin and hyaluronic acid (HA), are the leading options in lubricant injections. While HA has been used clinically for decades [14], lubricin has shown promise in animal models of arthritis [15]–[17]. It is necessary to note, however, that these two molecules lubricate by distinct mechanisms. While lubricin adsorbs to the articular surface [18] and reduces the boundary friction coefficient[9], lubrication by HA is dependent on its viscosity [11] and is likely effective through the formation of viscous surface layers. While the lubrication mechanisms of the molecules have been studied extensively, their roles in lubricating degraded cartilage are still not fully understood.

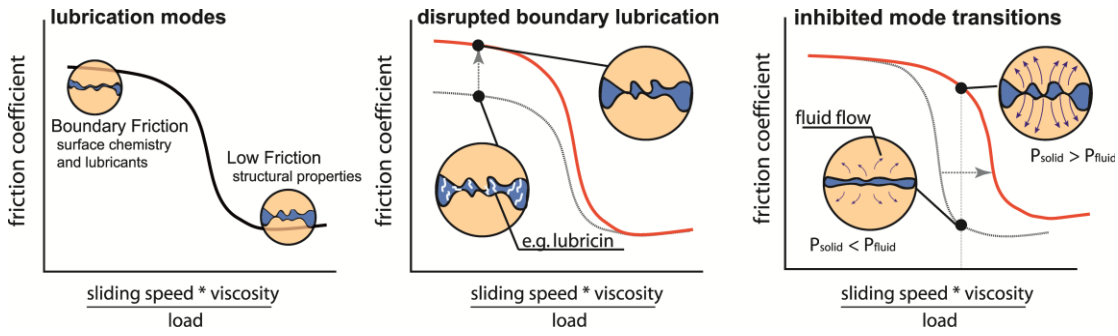

Figure 3.1 Elastoviscous lubrication mechanisms of articular cartilage. (A) Presentation of friction as a function of sliding speed, viscosity, and load (parameters captured by the Sommerfeld number, equation 1) reveals modes of lubrication. In the regime of boundary friction, solid on solid contact dominates the mechanics and consequently friction and wear are high. In the low friction mode, the friction is dictated by both viscous fluid films and contacting asperities [13], [41]. (B) Disruption of boundary lubrication is revealed by an increase in the left asymptote of the friction curve. (C) When the balance between viscous effects and solid contact is disrupted, the low friction mode and the transition towards low friction can be altered.

Interleukin-1β (IL-1β) is key catabolic cytokine in cartilage biology. For cartilage, IL-1β stimulation reduces lubricin expression [19] and increases the expression of cathepsin B [20], which is known to cleave the lubricin core protein [21]. As a result, IL-1β raises the boundary friction coefficients [22] of cartilage explants, however the effect that IL-1β has on other mechanisms of lubrication is not known. Stimulation by this cytokine causes proteoglycan release, through activation of aggrecanases [23], [24], and this biochemical consequence has effects structurally and mechanically. Cartilage explants exposed to IL-1β typically become softer and more permeable [22], and increased surface roughness has also been connected to IL-1β exposure [25]. These alterations in tissue structure likely have tribological consequences that affect more than boundary lubrication, but such effects have never been reported. Consequently, the goal of this study was to explore the role that biochemical and mechanical changes in cartilage after IL-1β exposure have on the lubrication mechanisms of cartilage.

Methods

In Vitro Degradation Model and Tissue Characterization

In order to evaluate lubrication changes after IL-1β treatment, we utilized culture conditions previously shown to alter the boundary friction coefficients of cartilage [22]. Briefly, we obtained neonatal bovine cartilage from the patellofemoral groove. Cartilage samples were obtained from 6 animals, cut into 6 mm in diameter by 2 mm thick disks and either sent to testing (0 day control group) or to 4 or 8 day culture with or without IL-1β. Explants were cultured in DMEM (Mediatech,

Manassas VA) supplemented with 10% fetal bovine serum (Mediatech, Manassas VA), 100 U/mL penicillin and 100 μg/mL streptomycin (Mediatech, Manassas VA), and with or without 10 ng/mL rhIL-1β (PeproTech, Rocky Hill NJ) with media refreshed every 2 or 3 days at 37 °C and 5% CO_2.

The effects of IL-1β exposure were revealed by testing explants biochemically, histologically, topographically and mechanically. For biochemical analysis, explants were tested in a modified DMMB assay for glycosaminoglycan content [26]. Both cultured and healthy explants were weighed, lyophilized and weighed again to obtain sample wet and dry weights. Samples were then digested overnight at 60°C in 1.25 mg/ml papain buffer, and compared to a standard curve obtained using shark fin C-6-S (Sigma).

For the histological analysis, 3 samples were fixed in 10% buffered formalin, embedded into paraffin blocks, and sectioned. Slide-mounted sections were cleared with xylene and rehydrated with steps of progressively weaker ethanol prior to staining. Samples were then stained with Safranin-O and Fast Green, dehydrated with steps of progressively stronger ethanol, cleared with xylene then coverslipped, and viewed on a light microscope.

Similarly, sections were tested for localization of lubricin at the surface using a previously reported immunohistochemistry procedure [27]. Briefly, after rehydration of mounted sections, antigen retrieval was conducted using citric acid (pH 6.0) for 20 minutes at 90°C. Slides were washed twice for 5 min in TRIS buffered saline with 0.5% TWEEN-20 (pH 7.4), incubated for 30 min in 0.01% hyaluronidase, 30 min in 3% hydrogen peroxide, and 60 min in a blocking solution containing normal serum,

bovine serum albumin, Triton X-100, and TWEEN-20. Between each step, slides were washed twice for 5 min in PBS. The primary antibody was applied overnight (Lubricin, Abcam product ab28484) at 4°C inside a humidity chamber. The secondary antibody (Vector, Burlingame, CA) was applied for 30 min followed by 30 min incubation with an avidin–biotin complex (Vectastain ABC, Vector). Staining was then carried out with a peroxidase substrate (ImmPACT DAB, Vector) for up to 3 min.

The mechanical effects of degradation were tested using a confined compression set-up on a Bose Enduratc testing frame. Briefly, 3 samples were placed in a confining chamber and compressed in four strain increments of 10% strain. The stress-relaxation curves were fit to a poroelastic model to calculate aggregate modulus and hydraulic permeability [28].

To determine alterations of the surface roughness and topography, 3 samples were analyzed using a white light interferometer (ADE Phase Shift MicroXAM Optical interferometric profiler). Four scans analyzing the height distribution in a 209 μm x 179 μm window were collected for each sample. The distributions of heights were fit to a Gaussian curve and the standard deviation, S_q, was calculated and presented as a roughness value.

Lubrication Analysis

Using a previously described, custom-built tribometer the friction coefficients of healthy and cultured cartilage were collected [8], [11]. Cylindrical cartilage 4 to 6 samples were mated against a polished glass flat counterface while bathed in lubricant baths of varying viscosities. The lubricants were PBS (1 mPas), 10 mg/mL 700 kDa

HA (156 mPas, Hyalgan®), and 8 mg/ml HYADD4 (72,000 mPas, Hymovis®) [29]. To mitigate the effects of interstitial fluid pressurization on friction coefficient measurements, samples were tested in a stationary contact area configuration [13], [30]. Before friction testing, samples were compressed to 25% strain and allowed to depressurize over the course of 1 hour. After fluid pressure dropped to the ambient pressure, the glass counterface was reciprocated at predetermined speeds ranging from 0.1 to 10 mm/s. Friction coefficients were recorded as the ratio of shear load to normal load measured by a biaxial load cell. Coefficients were calculated at the end of sliding when friction had reached an equilibrium value and averaged for both the forward and reverse sliding directions. After collection of friction coefficients, they were presented as a function of the Sommerfeld number, *S*, given by:

$$S = {}^{V\eta a}/_{F_n} \qquad \text{(equation 1)}$$

where V is sliding speed, η is lubricant viscosity, a is contact width, and F_n is normal load. As described previously[11], data were fit to a model curve where friction coefficient, μ, transitioned from a boundary friction coefficient, $\mu_{B,}$ to a minimum friction coefficient, μ_{min}, and allowed the determination of a transition number, S_t, that is representative of the Sommerfeld number at the midpoint of the transition. This equation was given by:

$$\mu(S) = \mu_{min} + (\mu_B - \mu_{min})e^{-(S/S_t)^d} \qquad \text{(equation 2)}$$

where d is a fitting parameter controlling the slope of the transition.

Rheological Analysis

The lubricant viscosities were measured using a commercial rheometer (TA

Instruments DHR3 Rheometer, New Castle DE). For the 10 mg/ml HA, a 40 mm diameter cone-plate set up with a 2° angle was used and viscosity was interpolated at a shear rate of $\dot{\gamma} = 1\ s^{-1}$. For HYADD4 a custom sandblasted 25mm plate-plate set up was used to mitigate wall slip due to elevated viscosity and conducted at the same shear rate. Viscosities were measured at 156 mPas for 10 mg/mL HA, 72,000 mPas for 8 mg/mL HYADD4.

Statistical Analysis

Results for mechanical, biochemical, and surface roughness analyses were determined to be normally distributed and analyzed between culture duration with a one way ANOVA with Tukey post-hoc. For the tribological characterization, a Monte Carlo analysis was conducted to determine uncertainty in the curve fit coefficients (μ_B, μ_{min}, and S_t) [11]. Briefly, the measurement standard deviations were used point by point and refit to the model curve by minimizing the RMS error using a custom Excel program. The results from 15 simulations provided the uncertainty in the curve fit coefficients and the coefficients were compared with a two-way ANOVA and Bonferroni post-hoc. For the transition number, a log transform was taken to normalize the data. For all analyses, significance was set at $p < 0.05$. Data is represented as mean ± standard deviation.

Results

Alterations in Tissue Structure and Composition

After culture for 4 and 8 days in the presence of 10 ng/mL IL-1β, proteoglycan loss throughout the tissue was revealed by the Safranin O staining (Fig. 3.2 A-C), and

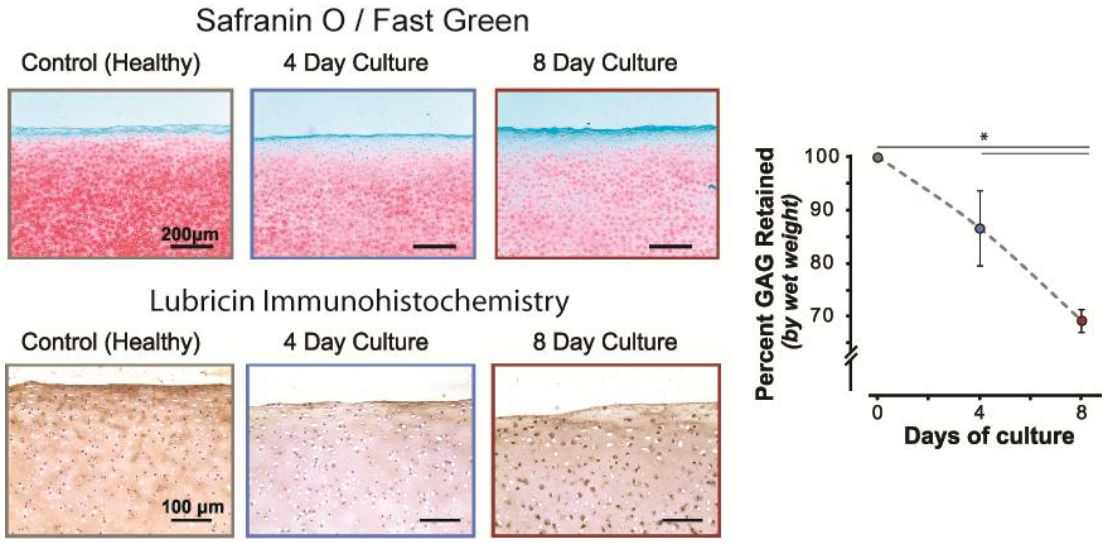

Figure 3.2 (A-C) Cartilage explants progressively lost proteoglycan content over the course of the 8 days of culture as revealed by Safranin O staining. (D) The proteoglycan loss was confirmed with the DMMB assay where up to 30% proteoglycan content was lost over the 8 day culture period. (E-G) Similarly, lubricin localization was altered after culture; both 4 and 8 days of culture with IL-1β led to decreased lubricin content present at the tissue surface as revealed through immunohistochemical staining. (* denotes $p < 0.05$, $n = 3$-4)

time-of-culture dependent proteoglycan loss was confirmed from biochemical analyses (Fig. 3.2 D). After 8 days of culture, the tissue lost over 30% of proteoglycan content compared to 0 day control tissue and 17% compared to tissue from 4 days of culture ($p<0.05$) (n=3-4).

Mechanically, the cartilage explants became both softer and more permeable after culture with IL-1β (Figure 3.3). The aggregate modulus decreased 30% (from 642 kPa to 385 kPa) after 4 days ($p<0.05$, n=3), and 50% after 8 days (to 315 kPa; $p<0.01$). Further, permeabilities trended 100% higher after 4 days compared to controls ($p=0.06$), and increased over 170% after 8 days of culture ($p<0.05$).

Topographically, cartilage surfaces were rougher after degradation by IL-1β, but this effect was not evident until after 8 days of culture (Figure 3.4). The roughness of control cartilage at day 0 was S_q = 2.29 μm. After 4 days the roughness was not significantly different (S_q = 3.02 μm), whereas after 8 days cartilage was significantly rougher. Roughness increased 158% to 5.91 μm ($p < 0.05$, Fig 3.4E).

Degradation-dependent Alterations in Lubrication Mechanisms

Stribeck-like behavior was noted for both control and degraded cartilage, with curves of friction as a function of Sommerfeld number that fit equation 5 robustly (Figure 3.5AB). Coefficients of variation of the Root Mean Square Deviation were: 4.6% for uncultured control cartilage, 10.0% for 4 day culture without IL-1 β, 4.1% for 4 day culture with IL-1 β, 12.3% for 8 day culture without IL-1 β, and 3.8% for 8 day culture with IL-1 β. The boundary friction coefficient, μ_B, increased after culture with IL-1β from 0.21 in control tissue to 0.26 and 0.25 for the 4 and 8 day IL-1β cultures, respectively ($p <0.05$). The transition number, S_t, did not significantly

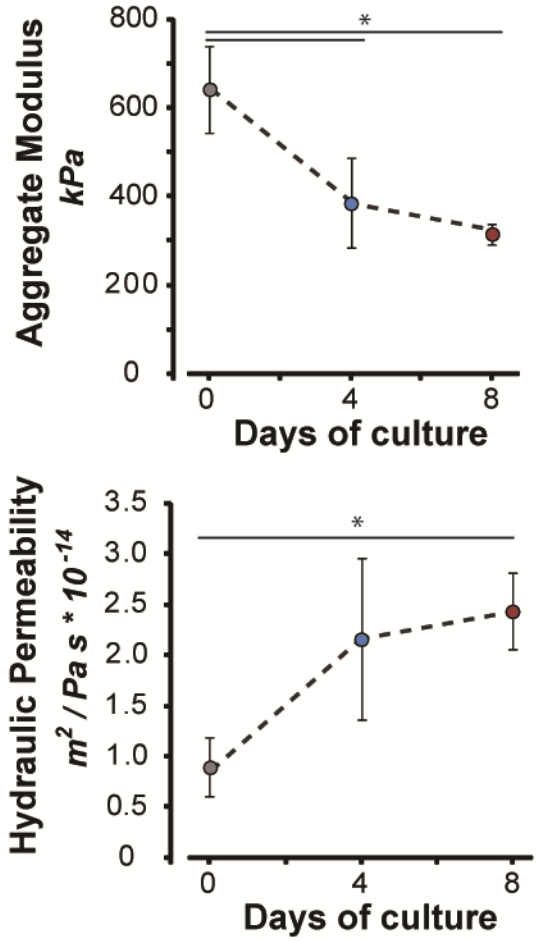

Figure 3.3 (A) The cartilage explants became softer over the 4 and 8 days of culture. The modulus dropped by almost 50% after 8 days of culture. (B) The hydraulic permeability of the tissue rose after culture with IL-1β. After 8 days in culture, the permeability rose over 150%. (* denotes $p < 0.05$, $n = 3$)

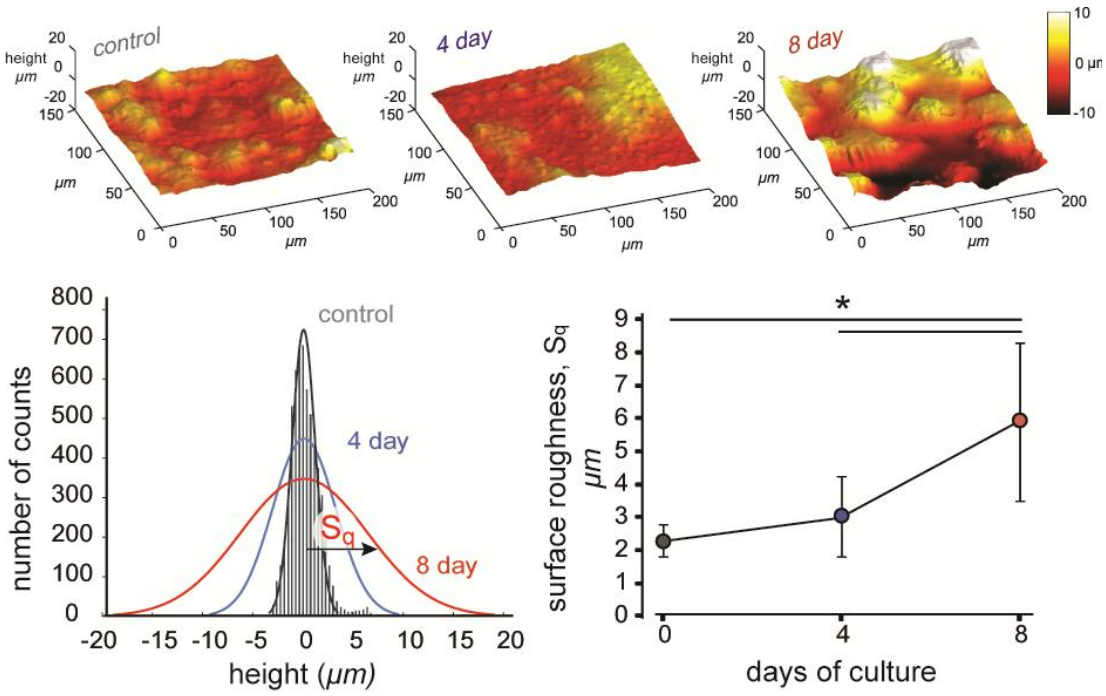

Figure 3.4 (A-C) Representative surface scans of control, 4 day, and 8 day samples. (D) Representative histogram of pixel counts per height measurements for control tissue with Gaussian fit to the data. Representative Gaussian fits are also shown for 4 day and 8 day groups, with the roughness measure, S_q, highlighted for the 8 day curve. (E) Surface roughness increased as a function of culture duration with the 8 day group having a significantly higher roughness than both control tissue and 4 day culture (* denotes $p < 0.05$, $n = 3$, 4 scans per sample).

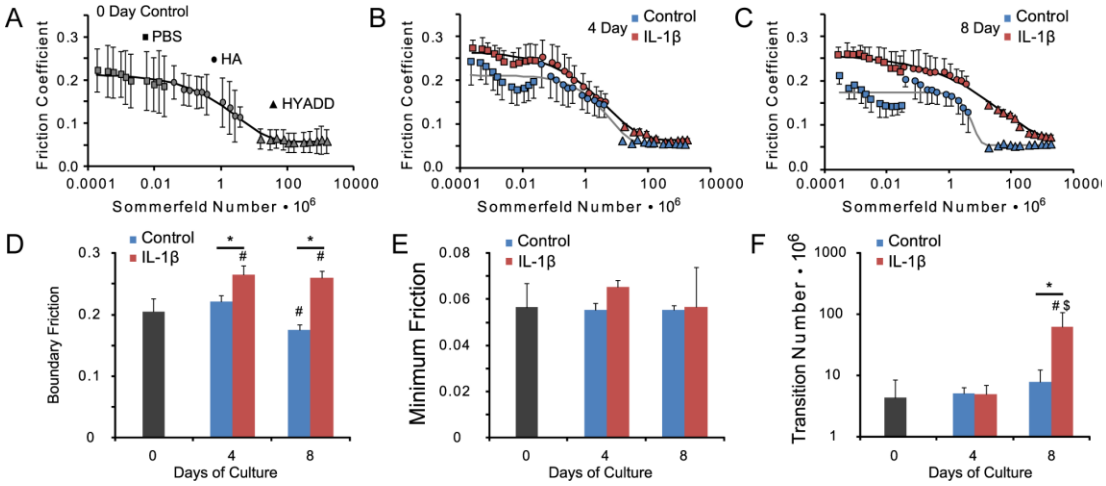

Figure 3.5 (A) Elastoviscous transition curves for cartilage were obtained by sliding in three lubricants with different viscosities (PBS, 1 mPas; HA ,150 mPas; and HYADD4, 72000 mPas). (B) Elastoviscous transitions of cartilage cultured for 4 days with and without IL-1β. (C) Elastoviscous transitions of cartilage cultured for 8 days with and without IL-1β. (D) Boundary friction increased after 4 days of culture and remained at a similar elevated level after 8 days. (E) The minimum friction coefficient was overall higher for the IL-1β-treated cartilage. (F) The transition number was not significantly higher after 4 days, but after 8 days, the transition number rose by an order of magnitude compared to controls. (* denotes $p < 0.05$, # denotes $p<0.05$ to 0 day control, $ denotes $p<0.05$ to 4 day; n=4-6)

increase after four days of culture ($4.94*10^{-6}$ compared to $4.25*10^{-6}$ for 0 day control tissue, $p > 0.05$). But after 8 days of culture, the transition number increased by over an order of magnitude to $63.0*10^{-6}$ at 8 days ($p<0.01$). Additionally, the minimum friction coefficient, μ_{min}, rose by over 10% between controls and IL-1β treated tissue ($p<0.05$), but there were no individually significant differences at either the 4 or 8 day cultures.

Discussion

This paper presented the degradation-dependent changes in cartilage lubrication mechanisms after exposure to IL-1β. Specifically, we utilized a Stribeck-like framework, the elastoviscous transition [11], [13], to examine how mechanisms of lubrication are altered under varying degrees of degradation. By altering both lubricant viscosity and sliding speed, we examined transitions between lubrication modes as we have recently reported [11]. Capturing the friction coefficient transition from a high value in boundary mode to a low friction coefficient consistent with theories of lubrication by viscous films [11], [13], [31] allowed the extraction of valuable information concerning the mechanisms of lubrication after degradation.

First, the boundary mode friction coefficient, μ_B, increased between 0 and 4 days of culture and was not increased further after 8 days of culture. During this same period, proteoglycan content, lubricin localization, permeability, and aggregate modulus were all altered. Although a decrease in modulus may increase the true area of contact through asperity flattening, it is likely that the depletion of lubricin is the dominant factor in the increase in boundary friction. The relative increase in friction

was consistent with changes in boundary friction for cartilage with its endogenous lubricin removed [9], [11]. Interestingly, there was no further increase in boundary friction between 4 and 8 days, when surface roughness increased. This result is in agreement with observations that surface roughness does not play a major role in the lubrication of hydrogels when roughness exceeds ~1μm [32]. Hence, the increase in the boundary friction coefficient may not correlate well with the increase in surface roughness, but likely depends more on the biochemical makeup of the tissue surface.

The novelty of this analysis framework enables calculation of the transition number, S_t, a measure of how effective viscous lubricants are in reducing friction. Analysis of the curve fitting parameters revealed that the transition to low, viscous friction occurred at higher values of the Sommerfeld number after 8 days of culture with IL-1β (Figure 3.5F). Similarly in this time frame from 4 to 8 days, the surface roughness increased significantly (Figure 3.4). While surface roughness may not be a dominant factor in boundary lubrication, it is likely that the surface roughness plays a large role in shifting the lubricating conditions away from relying on boundary lubrication. In theory, the roughening of cartilage can alter the mechanics of viscous lubricating fluids at the interface [31], [32]. For smooth surfaces, viscous films can be trapped at the interface and can pressurize to reduce the frictional stresses. In contrast, for a sufficiently rough surface the fluid at the interface is drainable as the increase in roughness may create channels through which viscous films can flow away from areas of high pressure [32]. This phenomenon was captured by the increase in the transition number between 4 and 8 days corresponding to the timeframe when surface roughness increased. Further, this may be a phenomenon with critical consequences for cartilage

in vivo, where joints with increased surface roughness in OA [33] are forced to rely more on effective boundary lubrication.

Similarly to the transition number, the minimum friction coefficient, μ_{min}, revealed changes in the lubrication mechanisms at the cartilage surface. The presence of a minimum friction coefficient which is substantially above μ=0.01 is an indication that the cartilage does not follow a typical Stribeck curve, a tool used to map changes in lubrication modes from boundary to hydrodynamic (where a fluid film fully separates the contacting surfaces). Recent work suggests that soft and permeable materials like cartilage follow different trends where a full fluid film is difficult to form and maintain at the interface due to both contact compliance and the ability of fluid to flow into and out of the bearing material [13]. This divergence from the classical lubrication mechanisms is called the elastoviscous transition and may reveal cartilage's ability to form or maintain a lubricating fluid film at the interface. Overall, μ_{min} for the IL-1β-treated cartilage was higher than control tissue (Figure 3.5E). Simply, it is possible that as cartilage becomes more permeable, it may not support viscous films at the interface as well. Consequently, a larger portion of the normal stress would be applied to the solid-on-solid contact of opposing asperities. As a result, elevated minimum friction during sliding may predispose cartilage to propagation of damage.

For boundary lubrication, the samples cultured without IL-1β exhibited a decrease in boundary friction that was significant after 8 days of culture. This decrease in boundary friction was not previously observed for serum-free media [22]. It is likely that either the cells within the explants in the serum-supplemented media are

active in producing lubricating molecules, or proteins within the serum adsorb to the articular surface and reduce friction. Interestingly, friction increased between the PBS and HA lubricated group (at $S \approx 0.02*10^{-6}$) for the controls cultured for 8 days. While lubricin in serum [34] may account for the boundary friction decrease, it is possible that albumin adsorption may account for this discontinuity. Albumin, which can localize to type II collagen, can block the interaction of HA with the articular surface [35] and may account for this discontinuity within the friction curve.

We have noted in this paper that alterations in both boundary mode lubrication and the transition away from boundary mode lubrication may have functional consequences in both cartilage disease and treatment. It is noteworthy that the two viscous lubricants used in this study are hyaluronic acid formulations approved for clinical use (Hyalgan® and Hymovis®). It is clear that both act as viscous lubricants, but changes in tissue properties after degradation affect the friction coefficients of cartilage lubricated by these lubricants. In the practice of viscosupplementation, lubrication is considered dependent on a supplement's viscosity [14]. As expected, the most viscous of the lubricants (HYADD4; η = 72,000 mPas) resulted in consistently lower friction than the other lubricants (PBS, 1 mPas; and HA, 156 mPas). However with degradation (i.e., after 8 days with IL-1β), friction was systematically higher across the friction curve. After localized lubricin was lost from the articular surface and the boundary friction coefficient rose, at low speeds friction was higher in IL-1β-exposed tissue when lubricated by HA, but this effect was muted at elevated speeds and viscosities. Similarly, when surface roughness was increased, even higher speeds and viscosities were necessary to mute the effect of increased friction of degraded

tissue compared to control. While there are regions of the friction curves where HA and HYADD lubricate degraded cartilage similarly to healthy cartilage, overall there are key conditions where these lubricants do not reduce friction to levels of healthy cartilage.

The conditions where HA did not lubricate degraded cartilage as well correspond to slow speeds after lubricin has been lost (i.e., 4 days of culture) and high speeds when surface roughness has increased (i.e., 8 days of culture). It is interesting to note that severe damage to cartilage causes lubrication changes such that medium viscosity lubricants are not very effective in reducing friction, and a sufficiently high viscosity is need to reduce friction to the low, viscous friction regime. To restore friction at low speeds, it is likely that the addition of a boundary lubricant would be effective. While not yet applied to clinical practice, tribosupplementation with lubricin has shown efficacy in animal trials [15]–[17]. It is likely that lubricin, which is an effective boundary lubricant [9], [11], [36] can restore lubricating function at low speeds for early cartilage damage. For more severe damage, it is currently unclear how to most effectively restore healthy lubricating function to cartilage because both boundary lubrication and viscous lubrication are hindered, but a combination approach to tribosupplementation emerges as a possible option. With the more thorough understanding of how lubrication is altered in degraded cartilage presented here, researchers can aim to produce tribosupplements that can restore healthy function to damaged cartilage.

While this study sheds new light on the role of IL-1β in cartilage lubrication, there are several limitations that should be acknowledged. While neonatal bovine

cartilage has been used in many studies with IL-1β (e.g., [22], [37], [38]), it is possible that there are catabolic and anabolic differences between young bovine and adult human. However, hallmarks of IL-1β stimulation, aggrecan and lubricin loss, are consistently observed in different aged bovine and adult human [19], [22], [37], [39]. Further, the use of neonatal tissue helps to eliminate confounding effects of preexisting cartilage damage in measurements of friction coefficient. Finally, the use of a polished glass counterface against cartilage provides similar boundary friction coefficients to cartilage on cartilage [6], [8], [9], [11], [40] and may be less susceptible to effects of interstitial fluid pressurization as cartilage on cartilage provides two compliant, permeable surfaces.

In conclusion, this study revealed how the inflammatory cytokine, IL-1β, can negatively influence the lubrication of cartilage. The observed changes in the mechanics of the tissue, lubricin localization, and surface roughness observed all likely play a role in compromising cartilage's natural lubricating mechanisms. While boundary lubrication increased after cytokine exposure, more pronounced changes were observed in the lubrication of cartilage by viscous lubricants likely due to the softening and roughening of the cartilage surface.

REFERENCES

[1] E. H. Choy and G. S. Panayi, “Cytokine pathways and joint inflammation in rheumatoid arthritis.,” *N. Engl. J. Med.*, vol. 344, no. 12, pp. 907–16, Mar. 2001.

[2] S. R. Goldring and M. B. Goldring, “The role of cytokines in cartilage matrix degeneration in osteoarthritis.,” *Clin. Orthop. Relat. Res.*, no. 427 Suppl, pp. S27–36, Oct. 2004.

[3] G. A. Ateshian, “The role of interstitial fluid pressurization in articular cartilage lubrication.,” *J. Biomech.*, vol. 42, no. 9, pp. 1163–76, Jun. 2009.

[4] C. W. McCutchen, “The frictional properties of animal joints,” *Wear*, vol. 5, no. 1, pp. 1–17, Jan. 1962.

[5] G. W. Greene, X. Banquy, D. W. Lee, D. D. Lowrey, J. Yu, and J. N. Israelachvili, “Adaptive mechanically controlled lubrication mechanism found in articular joints.,” *Proc. Natl. Acad. Sci. U. S. A.*, vol. 108, no. 13, pp. 5255–9, Mar. 2011.

[6] T. A. Schmidt, N. S. Gastelum, Q. T. Nguyen, B. L. Schumacher, and R. L. Sah, “Boundary lubrication of articular cartilage: role of synovial fluid constituents.,” *Arthritis Rheum.*, vol. 56, no. 3, pp. 882–91, Mar. 2007.

[7] P. S. Walker, D. Dowson, M. D. Longfield, and V. Wright, “‘Boosted lubrication’ in synovial joints by fluid entrapment and enrichment.,” *Ann. Rheum. Dis.*, vol. 27, no. 6, pp. 512–20, Nov. 1968.

[8] J. P. Gleghorn and L. J. Bonassar, “Lubrication mode analysis of articular

cartilage using Stribeck surfaces.," *J. Biomech.*, vol. 41, no. 9, pp. 1910–8, Jan. 2008.

[9] J. P. Gleghorn, A. R. C. Jones, C. R. Flannery, and L. J. Bonassar, "Boundary mode lubrication of articular cartilage by recombinant human lubricin.," *J. Orthop. Res.*, vol. 27, no. 6, pp. 771–7, Jun. 2009.

[10] E. D. Bonnevie, V. Baro, L. Wang, and D. L. Burris, "In-situ studies of cartilage microtribology: roles of speed and contact area.," *Tribol. Lett.*, vol. 41, no. 1, pp. 83–95, Jan. 2011.

[11] E. D. Bonnevie, D. Galesso, C. Secchieri, I. Cohen, and L. J. Bonassar, "Elastoviscous Transitions of Articular Cartilage Reveal a Mechanism of Synergy between Lubricin and Hyaluronic Acid.," *PLoS One*, vol. 10, no. 11, p. e0143415, Jan. 2015.

[12] R. Krishnan, M. Kopacz, and G. A. Ateshian, "Experimental verification of the role of interstitial fluid pressurization in cartilage lubrication.," *J. Orthop. Res.*, vol. 22, no. 3, pp. 565–70, May 2004.

[13] A. C. Dunn, W. G. Sawyer, and T. E. Angelini, "Gemini Interfaces in Aqueous Lubrication with Hydrogels," *Tribol. Lett.*, vol. 54, no. 1, pp. 59–66, Mar. 2014.

[14] E. A. Balazs and J. L. Denlinger, "Viscosupplementation: a new concept in the treatment of osteoarthritis.," *J. Rheumatol. Suppl.*, vol. 39, pp. 3–9, Aug. 1993.

[15] G. D. Jay, B. C. Fleming, B. A. Watkins, K. A. McHugh, S. C. Anderson, L. X. Zhang, E. Teeple, K. A. Waller, and K. A. Elsaid, "Prevention of cartilage degeneration and restoration of chondroprotection by lubricin

tribosupplementation in the rat following anterior cruciate ligament transection.," *Arthritis Rheum.*, vol. 62, no. 8, pp. 2382–91, Aug. 2010.

[16] E. Teeple, K. A. Elsaid, G. D. Jay, L. Zhang, G. J. Badger, M. Akelman, T. F. Bliss, and B. C. Fleming, "Effects of supplemental intra-articular lubricin and hyaluronic acid on the progression of posttraumatic arthritis in the anterior cruciate ligament-deficient rat knee.," *Am. J. Sports Med.*, vol. 39, no. 1, pp. 164–72, Jan. 2011.

[17] C. R. Flannery, R. Zollner, C. Corcoran, A. R. Jones, A. Root, M. A. Rivera-Bermúdez, T. Blanchet, J. P. Gleghorn, L. J. Bonassar, A. M. Bendele, E. A. Morris, and S. S. Glasson, "Prevention of cartilage degeneration in a rat model of osteoarthritis by intraarticular treatment with recombinant lubricin.," *Arthritis Rheum.*, vol. 60, no. 3, pp. 840–7, Mar. 2009.

[18] A. R. C. Jones, J. P. Gleghorn, C. E. Hughes, L. J. Fitz, R. Zollner, S. D. Wainwright, B. Caterson, E. A. Morris, L. J. Bonassar, and C. R. Flannery, "Binding and localization of recombinant lubricin to articular cartilage surfaces.," *J. Orthop. Res.*, vol. 25, no. 3, pp. 283–92, Mar. 2007.

[19] A. R. C. Jones and C. R. Flannery, "Bioregulation of lubricin expression by growth factors and cytokines.," *Eur. Cell. Mater.*, vol. 13, pp. 40–5; discussion 45, Jan. 2007.

[20] A. Baici and A. Lang, "Effect of interleukin-1 beta on the production of cathepsin B by rabbit articular chondrocytes.," *FEBS Lett.*, vol. 277, no. 1–2, pp. 93–6, Dec. 1990.

[21] K. A. Elsaid, G. D. Jay, and C. O. Chichester, “Reduced expression and proteolytic susceptibility of lubricin/superficial zone protein may explain early elevation in the coefficient of friction in the joints of rats with antigen-induced arthritis.,” *Arthritis Rheum.*, vol. 56, no. 1, pp. 108–16, Jan. 2007.

[22] J. P. Gleghorn, A. R. C. Jones, C. R. Flannery, and L. J. Bonassar, “Alteration of articular cartilage frictional properties by transforming growth factor beta, interleukin-1beta, and oncostatin M.,” *Arthritis Rheum.*, vol. 60, no. 2, pp. 440–9, Feb. 2009.

[23] E. C. Arner, C. E. Hughes, C. P. Decicco, B. Caterson, and M. D. Tortorella, “Cytokine-induced cartilage proteoglycan degradation is mediated by aggrecanase.,” *Osteoarthritis Cartilage*, vol. 6, no. 3, pp. 214–28, May 1998.

[24] J. D. Sandy, V. Thompson, C. Verscharen, and D. Gamett, “Chondrocyte-mediated catabolism of aggrecan: evidence for a glycosylphosphatidylinositol-linked protein in the aggrecanase response to interleukin-1 or retinoic acid.,” *Arch. Biochem. Biophys.*, vol. 367, no. 2, pp. 258–64, Jul. 1999.

[25] G. DuRaine, C. P. Neu, S. M. T. Chan, K. Komvopoulos, R. K. June, and A. H. Reddi, “Regulation of the friction coefficient of articular cartilage by TGF-beta1 and IL-1beta.,” *J. Orthop. Res.*, vol. 27, no. 2, pp. 249–56, Feb. 2009.

[26] R. W. Farndale, C. A. Sayers, and A. J. Barrett, “A Direct Spectrophotometric Microassay for Sulfated Glycosaminoglycans in Cartilage Cultures,” *Connect. Tissue Res.*, vol. 9, no. 4, pp. 247–248, Jul. 1982.

[27] E. D. Bonnevie, J. L. Puetzer, and L. J. Bonassar, “Enhanced boundary

lubrication properties of engineered menisci by lubricin localization with insulin-like growth factor I treatment.," *J. Biomech.*, vol. 47, no. 9, pp. 2183–8, Jun. 2014.

[28] V. L. Cross, Y. Zheng, N. Won Choi, S. S. Verbridge, B. A. Sutermaster, L. J. Bonassar, C. Fischbach, and A. D. Stroock, "Dense type I collagen matrices that support cellular remodeling and microfabrication for studies of tumor angiogenesis and vasculogenesis in vitro.," *Biomaterials*, vol. 31, no. 33, pp. 8596–607, Nov. 2010.

[29] I. Finelli, E. Chiessi, D. Galesso, D. Renier, and G. Paradossi, "Gel-like structure of a hexadecyl derivative of hyaluronic acid for the treatment of osteoarthritis.," *Macromol. Biosci.*, vol. 9, no. 7, pp. 646–53, Jul. 2009.

[30] M. Caligaris and G. A. Ateshian, "Effects of sustained interstitial fluid pressurization under migrating contact area, and boundary lubrication by synovial fluid, on cartilage friction.," *Osteoarthritis Cartilage*, vol. 16, no. 10, pp. 1220–7, Oct. 2008.

[31] G. E. Yakubov, J. McColl, J. H. H. Bongaerts, and J. J. Ramsden, "Viscous boundary lubrication of hydrophobic surfaces by mucin.," *Langmuir*, vol. 25, no. 4, pp. 2313–21, Feb. 2009.

[32] S. Yashima, N. Takase, T. Kurokawa, and J. P. Gong, "Friction of hydrogels with controlled surface roughness on solid flat substrates.," *Soft Matter*, vol. 10, no. 18, pp. 3192–9, May 2014.

[33] V. K. Shekhawat, M. P. Laurent, C. Muehleman, and M. A. Wimmer, "Surface

topography of viable articular cartilage measured with scanning white light interferometry.," *Osteoarthritis Cartilage*, vol. 17, no. 9, pp. 1197–203, Sep. 2009.

[34] M. Ai, Y. Cui, M.-S. Sy, D. M. Lee, L. X. Zhang, K. M. Larson, K. C. Kurek, G. D. Jay, and M. L. Warman, "Anti-lubricin monoclonal antibodies created using lubricin-knockout mice immunodetect lubricin in several species and in patients with healthy and diseased joints.," *PLoS One*, vol. 10, no. 2, p. e0116237, Jan. 2015.

[35] S. E. Majd, R. Kuijer, A. Köwitsch, T. Groth, T. A. Schmidt, and P. K. Sharma, "Both hyaluronan and collagen type II keep proteoglycan 4 (lubricin) at the cartilage surface in a condition that provides low friction during boundary lubrication.," *Langmuir*, vol. 30, no. 48, pp. 14566–72, Dec. 2014.

[36] G. D. Jay, D. A. Harris, and C.-J. Cha, "Boundary lubrication by lubricin is mediated by O-linked β(1-3)Gal-GalNAc oligosaccharides," *Glycoconj. J.*, vol. 18, no. 10, pp. 807–815, Oct. 2001.

[37] Y. Li, Y. Wang, S. Chubinskaya, B. Schoeberl, E. Florine, P. Kopesky, and A. J. Grodzinsky, "Effects of insulin-like growth factor-1 and dexamethasone on cytokine-challenged cartilage: relevance to post-traumatic osteoarthritis.," *Osteoarthritis Cartilage*, vol. 23, no. 2, pp. 266–74, Feb. 2015.

[38] S. Kar, D. W. Smith, B. S. Gardiner, Y. Li, Y. Wang, and A. J. Grodzinsky, "Modeling IL-1 induced degradation of articular cartilage.," *Arch. Biochem. Biophys.*, Feb. 2016.

[39] S. Y. Lee, T. Niikura, and A. H. Reddi, “Superficial zone protein (lubricin) in the different tissue compartments of the knee joint: modulation by transforming growth factor beta 1 and interleukin-1 beta.,” *Tissue Eng. Part A*, vol. 14, no. 11, pp. 1799–808, Nov. 2008.

[40] S. Abubacker, S. G. Dorosz, D. Ponjevic, G. D. Jay, J. R. Matyas, and T. A. Schmidt, “Full-Length Recombinant Human Proteoglycan 4 Interacts with Hyaluronan to Provide Cartilage Boundary Lubrication.,” *Ann. Biomed. Eng.*, Jul. 2015.

[41] M. D. Hersey, “The laws of lubrication of horizontal journal bearings,” *J. Washingt. Acad. Sci.*, vol. 4, no. August, pp. 542–552, 1914.

CHAPTER 4

Characterization of Tissue Response to Impact Loads Delivered Using a Hand-Held Instrument for Studying Articular Cartilage Injury[3]

Abstract

Objective: The objective of this study was to fully characterize the mechanics of an *in vivo* impactor and correlate the mechanics with superficial cracking of articular surfaces.

Design: A spring-loaded impactor was used to apply energy-controlled impacts to the articular surfaces of neonatal bovine cartilage. The simultaneous use of a load cell and displacement sensor provided measurements of stress, stress rate, strain, strain rate, and strain energy density. Application of India ink post impact was used to correlate the mechanical inputs during impact with the resulting severity of tissue damage. Additionally, a signal processing method to deconvolve inertial stresses from impact stresses was developed and validated.

Results: Impact models fit the data well (RMSE average ~0.09) and provided a fully characterized impact. Correlation analysis between mechanical inputs and degree of superficial cracking made visible through India ink application provided significant positive correlations for stress and stress rate with degree of surface cracking (R^2 = 0.7398 and R^2 = 0.5262, respectively). Ranges of impact parameters were 7-21 MPa, 6-40 GPa/s, 0.16-0.38, 87-236 s^{-1}, and 0.3-1.1 MJ/m^3 for stress, stress rate, strain, strain rate, and strain energy density, respectively. Thresholds for damage for all

[3] Published as: Bonnevie, ED, Delco, ML, Fortier, LA, Alexander, PG, Tuan, RS, Bonassar, LJ, Characterization of tissue response to impact loads delivered using a hand-held instrument for studying articular cartilage injury. *Cartilage* 2015 6(4) 226-232

inputs were determined at 13 MPa, 15 GPa/s, 0.23, 160 s^{-1}, and 0.59 MJ/m^3 for this system.

Conclusions: This study provided the mechanical basis for use of a portable, sterilizable, and maneuverable impacting device. Use of this device enables controlled impact loads *in vitro* or *in vivo* to connect mechanistic studies with long term monitoring of disease progression.

Introduction

Osteoarthritis (OA) is the leading cause of chronic disability in the United States, and a significant fraction of OA cases are attributable to previous joint trauma (i.e., post-traumatic osteoarthritis, PTOA) [1]–[3]. No therapies currently exist that prevent or slow progression of PTOA, and mounting evidence suggests that interventions must occur in the acute time frame after injury to effectively modify the course of the disease [4]. Therefore, research models that allow interrogation of pathologic mechanisms immediately following impact injury are critical to the development of preventative therapies. Both *in vitro* and *in vivo* impact models have been applied to native articular cartilage. Common methods to deliver impact injury include drop towers [5]–[7], pendulums [8], and more recently spring-loaded impactors [9]–[12]. Unlike stress or strain controlled impact systems [13]–[15], the impacting methods deliver a quick, single impact where energy input is correlated to the initial height of a weight or pendulum or to the stretch of a spring. With such systems, it is difficult to fully characterize an insult mechanically as both stress and strain data are difficult to capture with such quick insults that occur during time scales on the order of milliseconds.

In previous work, an *in vivo* impactor [9] consisting of a spring-loaded missile attached to a load cell was used to measure impact force, while pressure sensitive film provided an estimate of contact area and impact stress. This device has major advantages for use *in vivo* including compact design (allowing sterilization and intraarticular positioning of the impactor tip) and rapid impact delivery. Limitations of the design include a lack of information on the deformations that occur during

impact, as well as inertial effects of having a mounted load cell accelerate prior to impact that may confound real time measurements of load during impact. In the present study, we have modified the impactor to more fully characterize the insult. Addition of a displacement sensor provided real time displacement data. In addition to providing impact strain data, this allowed the calculation of the strain energy density, a possible metric for predicting surface damage [16].

The goals of this study were three-fold: (1) present a fully characterized insult that is capable of correlating stress, stress rate, strain, strain rate, and strain energy density to severity of damage (i.e., surface cracking), (2) provide a method to reduce inertial artifacts that occur when a load cell is mounted to a moving section of an impactor, and (3) determine which mechanical inputs correlate most strongly with measured surface damage.

Materials and Methods

Impactor Modification

A spring-loaded impactor presented by Alexander *et al.* [9] was modified in this study to simultaneously provide stress and strain data (Figure 4.1). In short, a 12 mm diameter impacting head was mounted in line with the axis of a spring which was compressed to produce energy-controlled impacts. The impact force was measured at 50 kHz by a load cell (PCBPiezotronics, Depew, NY) attached to the impactor tip. A linear variable differential transducer (LVDT; RDP Electronics, Pottstown PA) was mounted in parallel with the impactor and attached to the impactor tip to measure the depth of penetration of the impactor tip into a sample in real time.

Sample Preparation and Analysis

In these validation studies, neonatal bovine cartilage was impacted and analyzed. Femoral condyle cartilage was explanted from 1-3 day old bovids within 48 hours of sacrifice and sectioned into 6 mm diameter by 3 mm thick cylinders with the articular surface intact. Samples contained the majority of the deep zone tissue but no subchondral bone. Twelve samples were impacted under 6 different stretches of the internal spring, and voltages from the load cell and LVDT were recorded simultaneously with a custom LabVIEW program (NI, Austin TX). In the present study, a plane-ended impactor tip was used resulting in an impact configuration consistent with unconfined compression.

After impact, India ink was applied to the articular surfaces to detect superficial cracking and fibrillation. Consistently for all samples, several drops from a transfer pipette were applied to the surface and allowed to sit for no more than 3 minutes, after this time the samples were rinsed in PBS and wiped with a PBS-soaked Kimwipe to remove unbound dye. To quantify the amount of surface damage, photographs of the stained surfaces were imported into ImageJ (NIH, Bethesda MD) and converted to binary images. The area percent of surface staining was recorded as a measure of surface damage.

Signal Analysis and Processing

Throughout all twelve impacts, the recorded voltage from the load cell resembled a two-peaked impulse while the LVDT voltage resembled a one-peak impulse. This two peak impulse, considered an artifact of accelerating the load cell along with the impacting head prior to impact, can systematically confound further

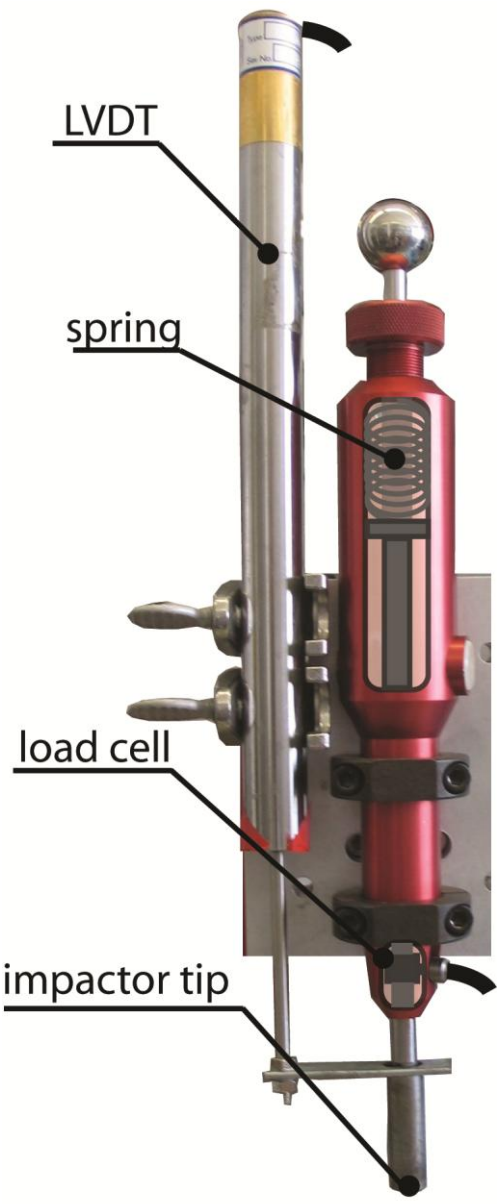

Figure 4.1 The spring-loaded impactor used in this study was modified from previous studies [9], [10] to include a displacement sensor (LVDT). This sensor was added in parallel with the impactor tip.

mechanical analyses such as calculations of peak stress and stress rate. The first voltage peak is a result of the spring hitting the load cell and accelerating it downward.

This portion of the impact is not directly applied to the cartilage surface. Here, we present a method of data analysis to remove the inertial artifact.

Assuming that the load cell signal is composed of two impulses, one peak when the load cell accelerated downward and one when the cartilage was impacted, the raw stress data were fitted to the sum of two Gaussian impulses given by the equation:

$$\sigma(t) = a_1 \left(exp(\frac{-(b_1-t)^2}{2\,c_1^2})\right) + a_2 \left(exp(\frac{-(b_2-t)^2}{2\,c_2^2})\right) \qquad \text{eq. 1}$$

Where, σ is the stress signal from the load cell, *a*, *b*, and *c* are constant fit parameters and *t* is time. The constants *a*, *b*, and *c* correspond to the amplitudes of the impacts, the times when the impact peaks occur, and the durations (i.e., the standard deviation) of the impacts, respectively. The subscripts 1 and 2 correspond to the first and second impulses, respectively. The model constants were obtained by minimizing RMS error between the model and data using a custom developed Excel program (available upon request). By subtracting the first impulse from the raw data we obtained a corrected raw data set and corrected model curve:

$$\sigma_{corrected}(t) = \sigma_{raw}(t) - a_1 \left(exp(\frac{-(b_1-t)^2}{2\,c_1^2})\right) \qquad \text{eq. 2}$$

$$\sigma_{model}(t) = a_2 \left(exp(\frac{-(b_2-t)^2}{2\,c_2^2})\right) \qquad \text{eq. 3}$$

The corrected data and model fit (eqns. 2 and 3) are shown in Figure 4.2B where the

parameters *a* and *c* from equation 3 are highlighted for clarity. Obtaining a corrected data set and model fit allowed for calculation of stress rate both numerically and from differentiation of the model (Fig 4.2C). The equations for both the numerical and explicit stress rates are given by:

$$d\sigma/_{dt} = \frac{\sigma_t - \sigma_{t-5}}{5\Delta t} \qquad \text{eq. 4}$$

$$\dot{\sigma}(t) = d\sigma(t)/_{dt} = a_1 \frac{(b_1 - t)}{c_1^2}\left(\exp\left(\frac{-(b_1 - t)^2}{2\,c_1^2}\right)\right) \qquad \text{eq. 5}$$

Where a numerical derivative is taken over 5 data points to minimize noise and an explicit derivative of the model is taken with respect to time. Similar precautions were not necessary for strain and strain-rate taken from the LVDT due to the one peak nature of the raw data. The strain model was similar to the stress model in equation 3 and given by:

$$\epsilon_{model}(t) = a_3\left(exp\left(\frac{-(b_3 - t)^2}{2\,c_3^2}\right)\right) \qquad \text{eq. 6}$$

Where ϵ is strain and a_3, b_3, and c_3 are distinct constants. Strain rates were then calculated in a similar way to stress rates.

Impact Strain Energy Density

With both stress and strain data available for each impact, the data was parametrically presented on a stress-strain curve. With this relationship, the strain energy density applied during an impact may be calculated from the following equation:

$$e = \int_0^{\epsilon_{max}} \sigma \, d\epsilon \cong \sum_{\epsilon=0}^{\epsilon_{max}} \sigma_t * (\epsilon_t - \epsilon_{t-1}) \qquad \text{eq. 7}$$

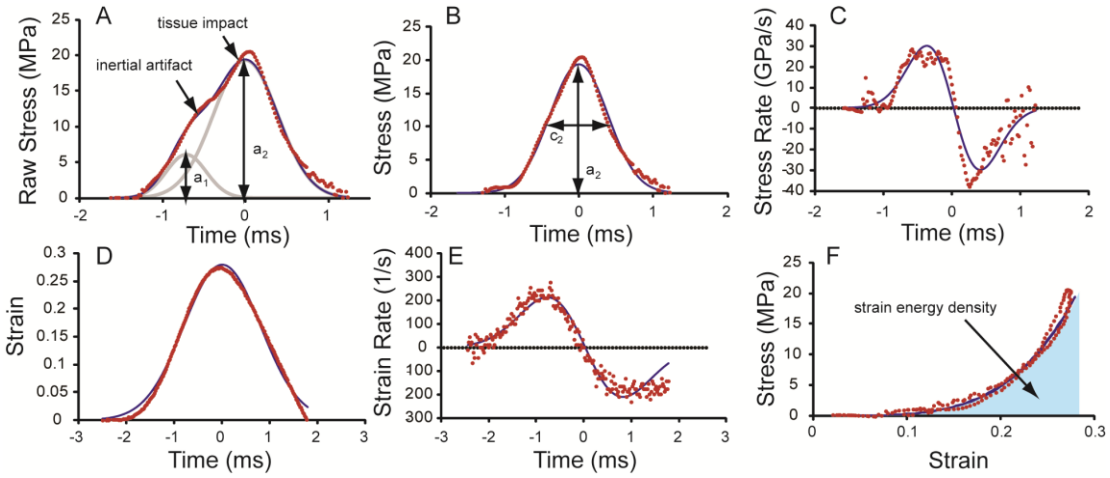

Figure 4.2 (A) The raw (unmodified) stress signal resembled a two-peaked impulse for all impacts and fit well to the impact model (eqn 1). (B) The corrected stress signal fit well to a single impulse model (eqns. 2-3). The constants *a* and *c* are shown for clarity. (C) Stress rate data of both the data and explicit derivative of the model (eqns. 4-5). (D) Strain data fit well to a single impulse model (eqn. 6). (E) Strain rate obtained similarly to stress rate. (F) Integration of the stress-strain curve provides a value for strain energy density.

Where e is the strain energy density (energy applied per unit volume), ϵ is strain, and ϵ_{max} is the maximum strain during an impact. For the impacts in this study, a right rectangular approximation of the integral was used to determine the amount of energy applied during an impact. The strain energy density is shaded in the stress strain curve for clarity (Figure 4.2F). Due to the high frequency of data collection and using different sensors for stress and strain, the data were inconsistently out of phase, although the strain rates would imply an elastic response due to deformations greatly exceeding the gel diffusion rate in cases where there is minimal energy dissipation through viscous losses or damage initiation [13], [17] (Peclet number ~ 10^6). Due to this drawback in data acquisition, an elastic response was modeled where the peak stress and strain were assumed to occur at the same time.

Results

A representative fit of equation 1 is presented in Figure 4.2A, where raw data are dotted, the full fit is the solid line, and the two Gaussian impulses are shaded in the background. Representative data and fits for stress, stress rate, strain, strain rate, and stress-strain are shown in Figure 4.2B-F, where strain energy density is the shaded area in Figure 4.2F. Impacts with varying spring deflections provided a range of stress, stress rate, strain, strain rate, and impact energy values (Figure 4.3). Peak impact stresses ranged from 7 to 22 MPa with peak stress rates ranging from 6 to 40 GPa/s. The raw data fit well to the impulse models with average (± standard deviation, n=12) coefficients of variation of the RMSE equal to 0.087±0.028 and 0.103±0.041 for the

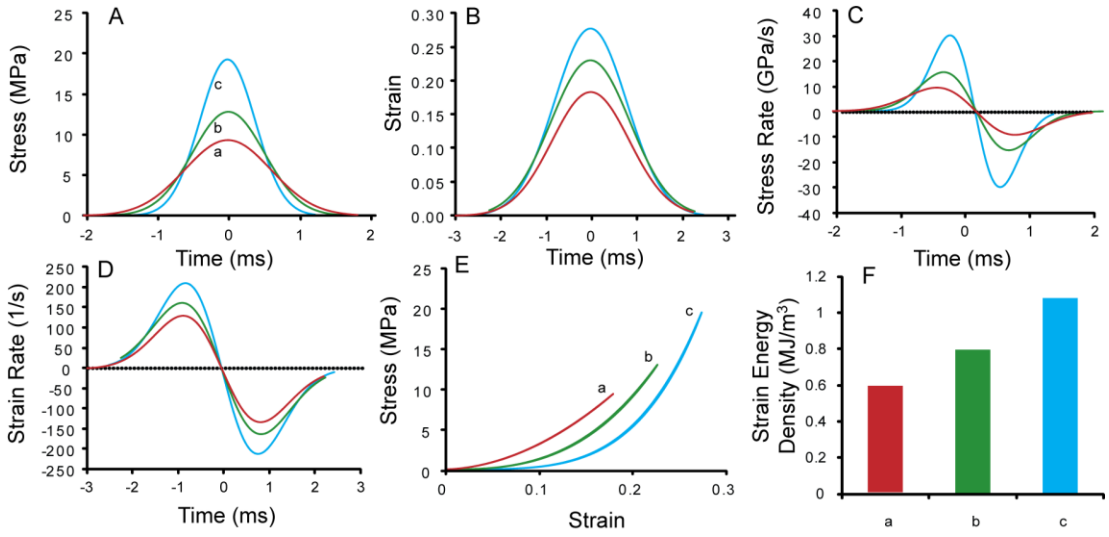

Figure 4.3 (A) Typical model traces for (A) stress, (B) strain, (C) stress rate, (D) strain rate, (E) stress-strain, and (F) strain energy density. The letters a, b, and c denote data corresponding to impacts conducted at three different deflections of the internal spring.

fits of equations 1 and 3, respectively. Similarly, peak strains ranged from 0.16 to 0.38 and peak strain rates ranged from 87 to 240 s^{-1}. As with the stress data, all of the strain data fit well to the impulse models with average coefficient of variation of the RMSE equal to 0.084±0.032. Relating stress and strain through the energy density relationship (equation 7), peak strain energy density varied from 0.302 to 1.08 MJ/m^3. Both peak stress and peak strain had a significant positive correlation with strain energy density ($p<0.05$, data not shown). Further, in 8 independent impacts at the same spring deflection, the coefficients of variation for stress, stress rate, strain, strain rate, and strain energy density were 0.066, 0.11, 0.088, 0.045, and 0.062, respectively (Figure 4.4, n=8).

Image analysis of the articular surfaces revealed significant cracking (arbitrarily determined at >1% staining by area) in samples with higher energy impacts. No significant surface damage was observed for peak stresses, stress rates, strains, strain rates, and strain energy densities below 13 MPa, 15 GPa/s, 0.23, and 160 s^{-1}, and 0.59 MJ/m^3, respectively (Figure 4.5). Stress and stress rate correlated significantly with surface damage (Figure 4.5, $p<0.05$), while strain, strain rate, and strain energy density did not. These fits predicted damage thresholds of 14.4 MPa and 13.9 GPa/s for stress and stress rate, respectively for this impacting system and tissue.

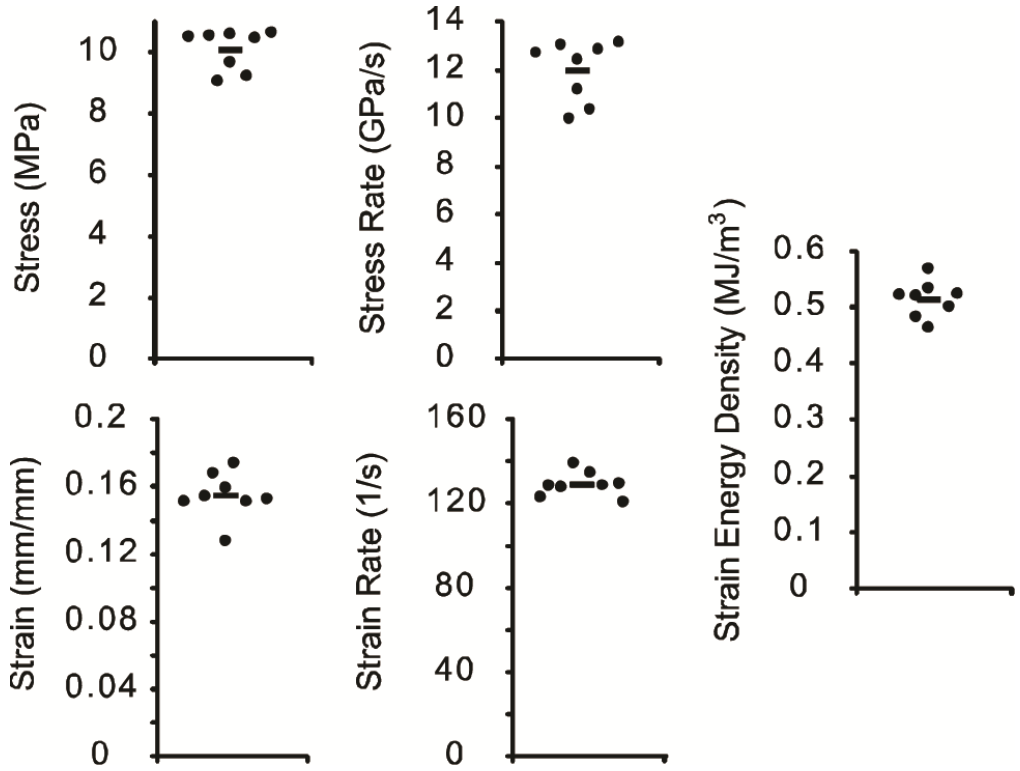

Figure 4.4 The repeatability of the impactor was shown through independent impacts at one spring deflection (n = 8, bars denote mean).

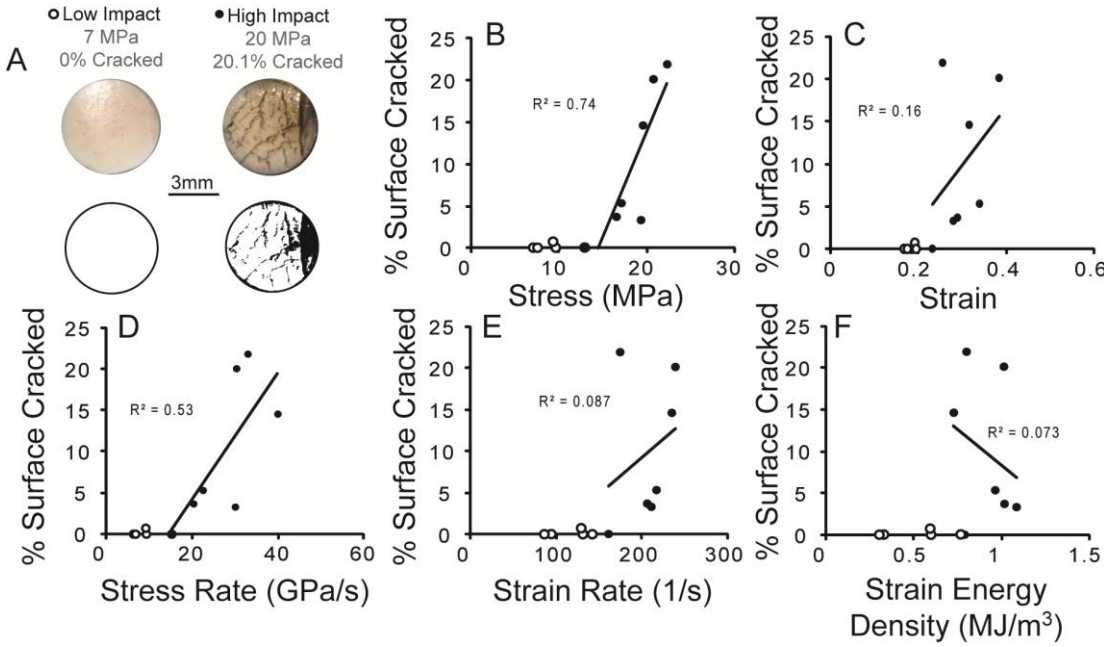

Figure 4.5 Twelve samples were impacted at six different deflections of the internal spring. (A) Representative photographs and binary images of the 6 mm diameter surface for low (below damage threshold) and high impact (above damage threshold) samples after application of India ink. (B-F) Correlations between surface cracking and mechanical aspects of impact were determined from closed circle data points, which included all data points with >1% cracking and the highest point that did not reveal cracking. Only stress (B) and stress rate (D) provided significant correlations with surface cracking ($p<0.05$).

Discussion

This study describes the characterization of mechanical consequences of impact injuries to articular cartilage delivered with a hand-held instrument. This instrument, which has been previously used to deliver impact injuries *in vivo*[9] delivers impacts with peak stresses up to 20 MPa on a time scale of 2 ms, producing stress rates up to 40 GPa/s and macro-scale strains and strain rates of 0.4 and 200/s, respectively. Use of this instrument enabled the identification of thresholds of mechanical inputs above which visible fissures were induced in the articular surfaces of cartilage explants. The mechanical factors that most strongly correlated with the development of tissue cracks were stress and stress rate.

The characterization of this model enables more mechanistic studies of PTOA *in vivo*. The ability to easily move and sterilize the impactor allows it to be used within the operating room. Furthermore, the ability to perform the impacts at arbitrary angles, as opposed to the vertical angles necessary for drop towers and horizontal angles necessary for pendulum systems, makes this system easier to use for *in vivo* studies where animal positioning may become a limiting factor. In addition to these innovations, the impacts have been shown to be fully characterized and controllable. This system enables controlled impacts *in vitro* and *in vivo* that may enable direct comparisons of mechanistic studies with long term monitoring of disease progression.

The fully characterized mechanical insult resulted from the addition of a displacement sensor that provided the basis for measuring strain, strain rate, and also strain energy density. By correlating all of the mechanical aspects of the impact with observed surface damage, we unexpectedly found that only stress and stress rate

significantly correlated with degree of surface damage. Although the correlations provided threshold values for only stress and stress rate, threshold values for strain, strain rate, and strain energy density were evident in the surface cracking plots (Figure 4.5). Due to inherent variability between samples it is likely that strain, strain rate, and strain energy density are not sensitive metrics for predicting degree of surface damage. In addition to inter-sample variation, the finding that stress and stress rate are more predictive of damage than strain, strain rate, or strain energy density, may be because they are more directly related to internal fluid pressure, which is known to be an important factor in the failure of poroelastic/biphasic materials through hydraulic fracturing [18]. Consistent with other studies [13], this study suggests that stress and stress rate are the most sensitive metrics for predicting cartilage surface damage.

In the context of other studies, this device provides a set of impact parameters that fall in range of those previously reported. Other spring-loaded systems estimated peak stresses of 17 – 80 MPa, but did not provide data on stress rates or tissue strains [12]. In a drop tower system peak stresses of 60 MPa [19] were observed while a strain-controlled system provided peak stresses of 14 MPa [13]. Between those studies, peak strain rates ranged from 1000 s^{-1} to 0.07 s^{-1}, respectively. Similarly, stress rates from other studies have varied from 35 MPa/s to 2.5 GPa/s for a strain controlled system and a pendulum system, respectively [8], [20], but stress rate was not reported for the drop tower study. Previous *in vitro* studies using this system reported correlations between peak stress, cell death, proteoglycan release, and surface fissuring in a range similar to the one reported here (~17 MPa peak stress) [10]. It should be noted, however that contact geometry and boundary conditions can also

affect comparisons, where the results in this study utilize explants with no subchondral bone and are impacted in unconfined compression may differ from other configurations.

The stress and stress rate values determined in this study were obtained from fitting the data to a modified Gaussian impulse model. This model (equations 1-5) was used to deconvolve inertial and impact signals from the mounted load cell. *In vivo* impact systems that operate using a mounted load cell that accelerates during impact may also have an inertial artifact present during the impulse force trace. The method used here corrects for this inertial artifact allowing calculation of stresses and stress rates that are not confounded by inertial effects. Simply put, the inertial artifact would overestimate the strain energy density and may also result in higher stresses and stress rates in cases where the inertial peak exceeds or occurs faster than the tissue impact peak, respectively.

This study suggests that stress and stress rate may be sufficient to predict severity of impact after full characterization of an impact system. Future *in vivo* studies utilizing this system and analysis framework may reduce the current knowledge gap surrounding the mechanical and biological aspects of PTOA and provide information necessary to develop preventative strategies following cartilage injury.

REFERENCES

[1] D. D. Anderson, S. Chubinskaya, F. Guilak, J. A. Martin, T. R. Oegema, S. A. Olson, and J. A. Buckwalter, "Post-traumatic osteoarthritis: improved understanding and opportunities for early intervention.," *J. Orthop. Res.*, vol. 29, no. 6, pp. 802–9, Jun. 2011.

[2] J. A. Buckwalter, C. Saltzman, and T. Brown, "The impact of osteoarthritis: implications for research.," *Clin. Orthop. Relat. Res.*, no. 427 Suppl, pp. S6–15, Oct. 2004.

[3] T. D. Brown, R. C. Johnston, C. L. Saltzman, J. L. Marsh, and J. A. Buckwalter, "Posttraumatic osteoarthritis: a first estimate of incidence, prevalence, and burden of disease.," *J. Orthop. Trauma*, vol. 20, no. 10, pp. 739–44, Jan. .

[4] C. R. Chu, B. D. Beynnon, J. A. Buckwalter, W. E. Garrett, J. N. Katz, S. A. Rodeo, K. P. Spindler, and R. A. Stanton, "Closing the gap between bench and bedside research for early arthritis therapies (EARTH): report from the AOSSM/NIH U-13 Post-Joint Injury Osteoarthritis Conference II.," *Am. J. Sports Med.*, vol. 39, no. 7, pp. 1569–78, Jul. 2011.

[5] J. E. Jeffrey, D. W. Gregory, and R. M. Aspden, "Matrix damage and chondrocyte viability following a single impact load on articular cartilage.," *Arch. Biochem. Biophys.*, vol. 322, no. 1, pp. 87–96, Sep. 1995.

[6] L. V Burgin and R. M. Aspden, "A drop tower for controlled impact testing of biological tissues.," *Med. Eng. Phys.*, vol. 29, no. 4, pp. 525–30, May 2007.

[7] J. B. Finlay and R. U. Repo, “Cartilage impact in vitro: Effect of bone and cement,” *J. Biomech.*, vol. 11, no. 8–9, pp. 379–388, Jan. 1978.

[8] J. Borrelli, M. E. Burns, W. M. Ricci, and M. J. Silva, “A method for delivering variable impact stresses to the articular cartilage of rabbit knees.,” *J. Orthop. Trauma*, vol. 16, no. 3, pp. 182–8, Mar. 2002.

[9] P. G. Alexander, J. A. McCarron, M. J. Levine, G. M. Melvin, P. J. Murray, P. A. Manner, and R. S. Tuan, “An In Vivo Lapine Model for Impact-Induced Injury and Osteoarthritic Degeneration of Articular Cartilage,” *Cartilage*, vol. 3, no. 4, pp. 323–333, May 2012.

[10] P. G. Alexander, Y. Song, J. M. Taboas, F. H. Chen, G. M. Melvin, P. A. Manner, and R. S. Tuan, “Development of a Spring-Loaded Impact Device to Deliver Injurious Mechanical Impacts to the Articular Cartilage Surface,” *Cartilage*, vol. 4, no. 1, pp. 52–62, Aug. 2012.

[11] A. Changoor, J. P. Coutu, M. Garon, E. Quenneville, M. B. Hurtig, and M. D. Buschmann, “Streaming potential-based arthroscopic device is sensitive to cartilage changes immediately post-impact in an equine cartilage injury model.,” *J. Biomech. Eng.*, vol. 133, no. 6, p. 061005, Jun. 2011.

[12] C. J. Bolam, M. B. Hurtig, A. Cruz, and B. J. E. McEwen, “Characterization of experimentally induced post-traumatic osteoarthritis in the medial femorotibial joint of horses.,” *Am. J. Vet. Res.*, vol. 67, no. 3, pp. 433–47, Mar. 2006.

[13] V. Morel and T. M. Quinn, “Cartilage injury by ramp compression near the gel diffusion rate.,” *J. Orthop. Res.*, vol. 22, no. 1, pp. 145–51, Jan. 2004.

[14] T. M. Quinn, A. J. Grodzinsky, E. B. Hunziker, and J. D. Sandy, “Effects of injurious compression on matrix turnover around individual cells in calf articular cartilage explants.,” *J. Orthop. Res.*, vol. 16, no. 4, pp. 490–9, Jul. 1998.

[15] R. L.-Y. Sah, J.-Y. H. Doong, A. J. Grodzinsky, A. H. K. Plaas, and J. D. Sandy, “Effects of compression on the loss of newly synthesized proteoglycans and proteins from cartilage explants,” *Arch. Biochem. Biophys.*, vol. 286, no. 1, pp. 20–29, Apr. 1991.

[16] G. C. Sih, “Strain-energy-density factor applied to mixed mode crack problems,” *Int. J. Fract.*, vol. 10, no. 3, pp. 305–321, Sep. 1974.

[17] E. D. Bonnevie, V. J. Baro, L. Wang, and D. L. Burris, “Fluid load support during localized indentation of cartilage with a spherical probe.,” *J. Biomech.*, vol. 45, no. 6, pp. 1036–41, Apr. 2012.

[18] M. K. Hubbert and D. G. W. Willis, “Mechanics of Hydraulic Fracturing,” *Trans. Am. Inst. Mining, Metall. Pet. Eng. Inc.*, vol. 210, pp. 153–168, 1957.

[19] J. B. Finlay and R. U. Repo, “Instrumentation and procedure for the controlled impact of articular cartilage.,” *IEEE Trans. Biomed. Eng.*, vol. 25, no. 1, pp. 34–9, Jan. 1978.

[20] J. Borrelli, P. A. Torzilli, R. Grigiene, and D. L. Helfet, “Effect of impact load on articular cartilage: development of an intra-articular fracture model.,” *J. Orthop. Trauma*, vol. 11, no. 5, pp. 319–26, Jul. 1997.

CHAPTER 5

Sub-Critical Impact Inhibits the Lubricating Mechanisms of Articular Cartilage[4]

Abstract

Although post-traumatic osteoarthritis accounts for a significant proportional of all osteoarthritis, the understanding of both biological and mechanical phenomena that lead to cartilage degeneration in the years to decades after trauma is still lacking. In this study, we evaluate how cartilage lubrication is altered after a sub-critical impact (i.e., an impact to the cartilage surface that produces surface cracking but not full thickness fissuring). Through utilizing a Stribeck-like framework, the elastoviscous transition, we evaluated changes to both the innate boundary lubricating ability of cartilage after impact and also the effectiveness of viscous lubricants to lower friction after impact. Increases in boundary friction were linked to observed changes in lubricin localization and surface roughness after impact. But, more prominent changes were observed in the low, viscous friction regime of lubrication, and were connected to topological changes to the cartilage surface after impact. The data here reveal distinct mechanisms of cartilage lubrication that can fail after traumatic impact and may explain a key mechanical phenomenon that predisposes cartilage to development of osteoarthritis after injury.

[4] To be published with co-authors: Bonnevie, ED, Delco, ML, Galesso, D, Sechieri, C, Fortier, LA, Bonassar, LJ.

Introduction

Although articular cartilage is commonly regarded as one of the most remarkable bearing surfaces found in nature, the failure of this tissue in osteoarthritis (OA) is the leading cause of severe disability within the United States [1]. For most OA cases, the mechanisms of initiation and progression of this disease are not well understood; however, a significant portion of cases (~12%) are connected to an earlier traumatic injury [2]. These cases of secondary OA are considered post-traumatic OA (PTOA), and it is highly likely a traumatic injury such as an anterior cruciate ligament tear will lead to PTOA. In fact, 78% of anterior cruciate ligament tears resulted in radiographic changes consistent with OA 14 years post-injury [3]. Although traumatic injury is considered an initiating event in cases of PTOA, the mechanisms by which this disease manifests are not fully understood. Both mechanical and biological factors are known to play a role with significant interaction between these factors [4], [5].

To study the complex etiology of PTOA, both *in vivo* and *in vitro* post-traumatic models have been developed to investigate the mechanical and biological events following trauma. Strategies for controlling cartilage injury include imposing specific loads, displacements, and impact energies on the tissue [6]–[14]. Biologically, impact stresses on the order of 15-20 MPa and local strains on the order of 0.10 are known to cause significant cell death [6], [15], and impacts below these thresholds can often induce matrix damage [16], catabolic responses [17], and mitochondrial depolarization leading to chondrocyte apoptosis [18]. While the acute biological consequences of trauma have been studied extensively, there is less known about the direct mechanical consequences of cartilage trauma. Impacts on the order of 20 MPa

are known to cause catastrophic matrix fissuring and can alter the water content of the tissue [19], which can influence the mechanics of cartilage [20]. Recently, we have reported superficial cartilage cracking at impact stresses as low as 14 MPa when delivered by a spring-loaded impacting device [14]. These superficial cracks, which may be on the order of tens of microns wide, would be very difficult to visualize or observe *in vivo* using conventional imaging practice [21], and it is not currently known whether these types of cracks have any functional consequences to the tissue.

Functional changes to the naturally low friction and shear environment of cartilage can have profound biological consequences for tissue health. Increased friction has been linked to chondrocyte apoptosis [22], mitochondrial dysfunction [23], loss of superficial zone cellularity [24], and matrix wear and degradation [25]. However, it is currently unknown if cartilage trauma affects lubrication and what role inferior lubrication may have in the initiation and progression of PTOA.

The naturally low friction of cartilage is due to cooperation of several mechanisms leading to some of the lowest friction coefficients found in nature [26]. Fluid pressurization within the cartilage matrix is a key factor that reduces friction by supporting a substantial portion of the contact load and consequently reducing the stresses on contacting solid asperities [27]–[29]. Additionally, the frictional stresses on the contacting asperities are reduced by lubricating molecules found in synovial fluid [30]. Lubricin, a boundary lubricant, reduces frictional stresses under high load and low motion [31], [32], and hyaluronic acid, a viscous boundary lubricant, reduces friction at higher speeds due to formation of viscous films [33], [34]. However, it is not currently known how a traumatic impact to cartilage can affect the efficacy of

these lubricants to reduce cartilage friction.

In this study, we explore the effects of sub-critical impact on the lubricating behavior of cartilage. Specifically, we focused on the intrinsic boundary lubricating ability of the tissue and the role of viscous lubricants in reducing friction after cartilage impact. By using a Stribeck-like framework [35], the elastoviscous transition [34], [36], we deconvolved the lubrication contributions of boundary and viscous lubricants, such as lubricin and hyaluronic acid, respectively. By analyzing specific mechanisms of cartilage lubrication and assessing cartilage structure by histology, optical profilometry, mechanical testing we identified key structural alterations that lead to compromised lubrication.

Methods

Tissue Source

Neonatal bovine stifles were obtained from a local abbatoir within 24 hours of sacrifice. Cartilage plugs (6 mm diameter by 3 mm thick) were extracted aseptically from the femoral condyles and frozen at -20°C. All samples were used within one month of freezing.

Impacting Device and data acquisition

A previously validated, custom-built, spring-loaded impactor was used in this study [13], [14]. Briefly, an 8 mm diameter cylindrical impacting missile was used to impact articular cartilage plugs in unconfined compression at a stress level previously determined to produce surface fissure without full thickness cracks [14]. Impact loads were collected using a load cell mounted in parallel to the impacting missile at 50 kHz

(PCBPiezotronics, Depew, NY). A linear variable differential transducer (LVDT; RDP Electronics, Pottstown PA) was mounted in parallel with the impacting tip to measure the deformation of the cartilage plug in real time.

India ink staining and histology

To reveal the extent of surface fissuring inflicted by the impact, cartilage was impacted, and exposed to india ink before being wiped with a kimwipe to remove unbound dye and surface photographs were recorded. Also, impacted and non impacted cartilage plugs were fixed in buffered 10% formalin for 48 hours, dehydrated in ethanol, embedded in paraffin, and mounted on slides. For histological staining, slides were cleared with xylene and rehydrated in progressively weaker ethanol before staining with either Safranin-O or Picrosirius Red. Samples were imaged on a light microscope and images were captured with a camera. Picrosirius Red-stained slides were viewed under crossed polarizers to view collagen organization.

Lubricin IHC

Lubricin immunohistochemical staining was conducted as previously described [37]. Briefly, samples were cleared and rehydrated as above. Antigen retrieval was conducted at 90°C for 20 minutes in citric acid followed by rinses in TRIS buffered saline with 0.5% TWEEN-20. Blocking was conducted using a solution containing normal serum, bovine serum albumin, Triton X-100, and TWEEN-20. Primary lubricin antibodies (Abcam: ab28484) were applied overnight at 4°C. Biotinylated Secondary antibodies (Vectastain ABC, Vector) were applied for 30 minutes followed by 30 minute incubation in avidin-biotin complex (Vectastain ABC, Vector). Staining was conducted using a peroxidase substrate (ImmPACT DAB, Vector) for 2 minutes.

Surface Profilometry

Surface topology of non-impacted and impacted cartilage was analyzed using a noncontact, scanning white light profilometer (ADE Phase Shift MicroXAM Optical interferometric profiler). Scans analyzing the height distribution in a 209 μm x 179 μm window were collected for each sample. The surface roughness, S_q, was calculated for each sample, and the window size was chosen to minimize effects of curvature on roughness values.

Compression Testing

The bulk mechanical effects sub-critical impact were tested using a confined compression set-up mounted on a Bose Enduratc testing frame. Briefly, samples were placed in a confining chamber bathed in PBS and compressed in four strain increments of 5% strain. The stress-relaxation curves were fit to a poroelastic model to calculate aggregate modulus and hydraulic permeability [38].

Friction Analysis

Cartilage lubricating properties were analyzed using a custom-built tribometer [31], [34], [37]. Using a recently described framework, the boundary mode friction coefficient and the transition to low, viscous friction were mapped using an array of three different lubricants with viscosities that varied by over five orders of magnitude [34]: phosphate buffered saline (PBS, 1 mPas), 10 mg/ml 630 kDa hyaluronic acid (HA, 151 mPas), and a hydrophobicized HA derivative, (HYADD4, 72,000 mPas) [39]. Friction coefficients were recorded over a range of sliding speeds for each sample ranging from 0.1 mm/s to 10 mm/s. Friction coefficients were presented as a function of the Sommerfeld number, *S*, which takes into account the sliding speed (V),

applied normal load (F_N), lubricant viscosity (η), and the contact width (a = 6 mm) [36], [40]:

$$S = {}^{V\eta a}/_{F_n} \quad \text{(equation 1)}$$

The boundary mode friction coefficient, μ_B, the minimum friction coefficient, μ_{min}, and the Sommefeld number at the midpoint between high and low friction, S_t, were all determined through fitting the friction data of impacted and non-impacted cartilage combined for all three viscosities by using the following equation of friction coefficient, μ, as a function of the Sommerfeld number, S [34]:

$$\mu(S) = \mu_{min} + (\mu_B - \mu_{min})e^{-(S/S_t)^d} \quad \text{(equation 2)}$$

Statistical Analysis

Statistical analysis for comparisons between non-impacted and impacted cartilage were conducted using a Student's t-test for significance. Uncertainties for the curve fit parameters in equation 2 were determined through 15 Monte Carlo simulations based on the point-by-point standard deviations of friction coefficient. Curve fits parameters for equation 2 were determined through RMS error minimization, and goodness of fit for equation 2 to friction coefficients were determined through coefficient of variation of the RMS error. Significance was set at $p < 0.05$.

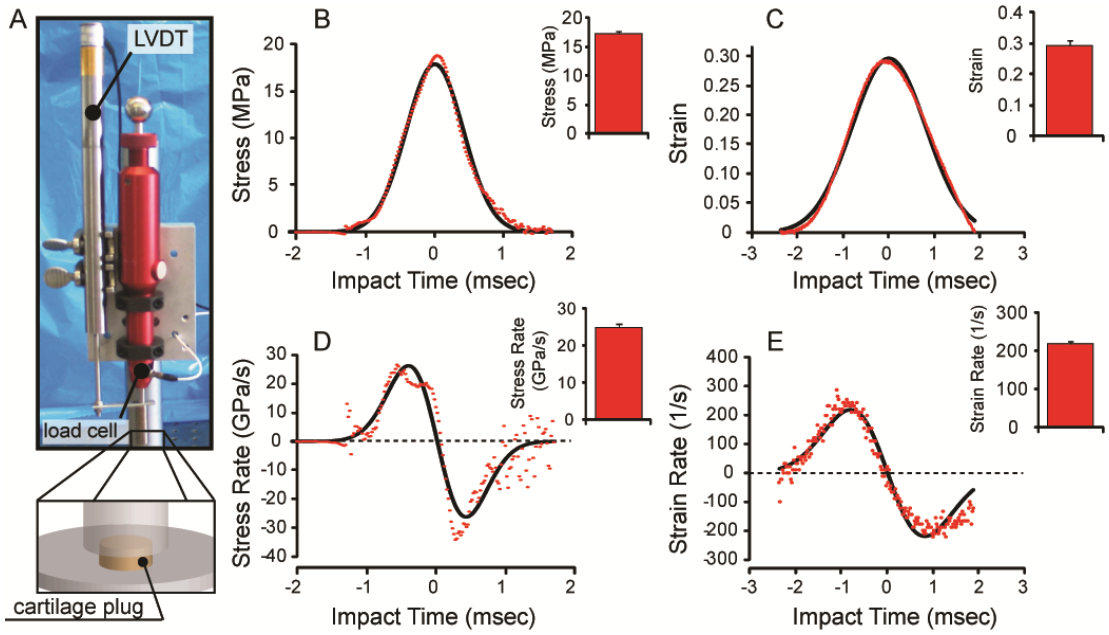

Figure 5.1 (A) The spring-loaded impacting device utilizes both a linear variable displacement transducer and load cell to quantify the strains and stresses, respectively. (B-E) Applied impacts resulted in peak impact stresses of 17.2 ± 0.49 MPa, peak stress rates of 24.8 ± 1.0 GPa/s, peak strains of 0.29 ± 0.019, and peak strain rates of 218 ± 8.1 s^{-1} as determined from Gaussian model fits using a recently described model to eliminate inertial artifacts from accelerating a load cell mounted on the impacting piston. Insets reveal typical deviations of impact parameters.

Results

The applied impacts to cartilage were considerably repeatable. For stress, stress rate, strain, and strain rate, the coefficients of variation were all less than 7% for 4 representative samples. These impacts resulted in peak impact stresses of 17.2 ± 0.49 MPa, peak stress rates of 24.8 ± 1.0 GPa/s, peak strains of 0.29 ± 0.019, and peak strain rates of 218 ± 8.1 s^{-1} as determined from Gaussian model fits [14] (Figure 5.1).

India ink application to the articular surface after impact revealed surface fissuring that was not present in non-impacted cartilage (Figure 5.2A). Further, lubricin immunohistochemical staining revealed less localized lubricin in the impacted cartilage, but not total loss of lubricin localization at the tissue surface (Figure 5.2B). Structurally, Safranin O and Pircosirius red staining viewed under polarized light revealed fibrillation of the cartilage matrix at the articular surface without cracks extending deeper than the superficial zone (Figure 5.2 F and H, arrows). Impact did not affect either protgeoglycan localization or collagen organization based on histological staining (Figure 5.2 C and D).

To better understand the topological changes to the articular surface after mechanical impact, scanning light white profiles were collected of non-impacted and impacted cartilage. For non-impacted cartilage, surfaces were relatively smooth. The height distribution was roughly Gaussian and average RMS roughness, S_q, was 2.23 ± 0.43 μm. In contrast, a representative surface scan of impacted cartilage displayed a crack running along the length of the scan. Consequently, the height distribution was no longer Guassian, but followed the form of a bi-modal distribution. For impacted cartilage, RMS roughnesses were 72% higher with average roughness of 3.85 ± 1.2

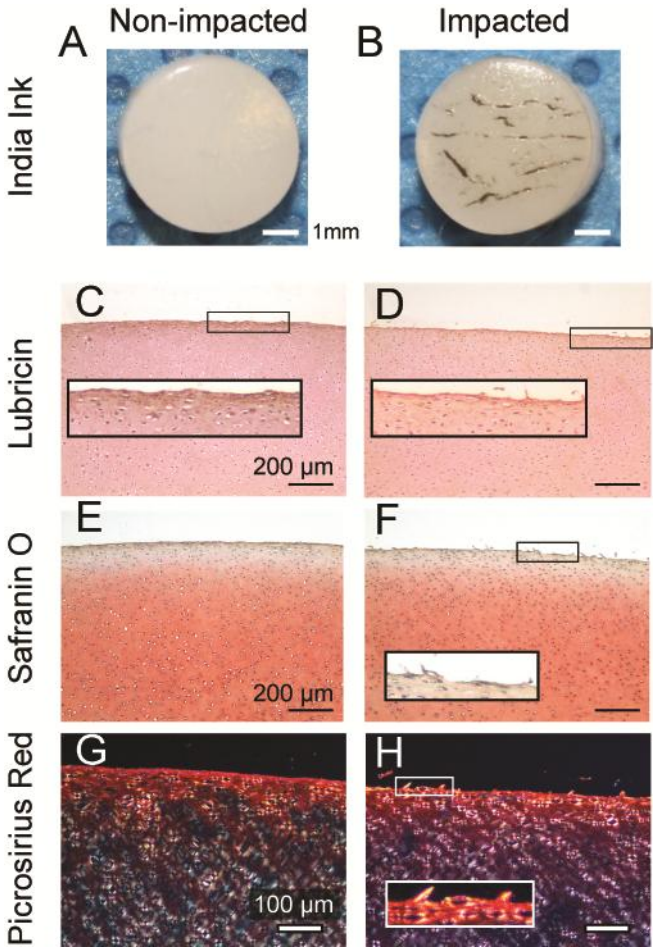

Figure 5.2 (AB) Surface fissuring in impacted cartilage was visualized after India ink application. (CD) Less lubricin was localized to the surfaces of impacted cartilage. (EF) Safranin O staining exposed no macroscopic changes in proteoglycan localization. (GH) Picrosirius red staining visualized under polarized light revealed no macroscopic changes to collagen structure and organization. Insets in (F) and (H) highlight local areas of cartilage fissuring.

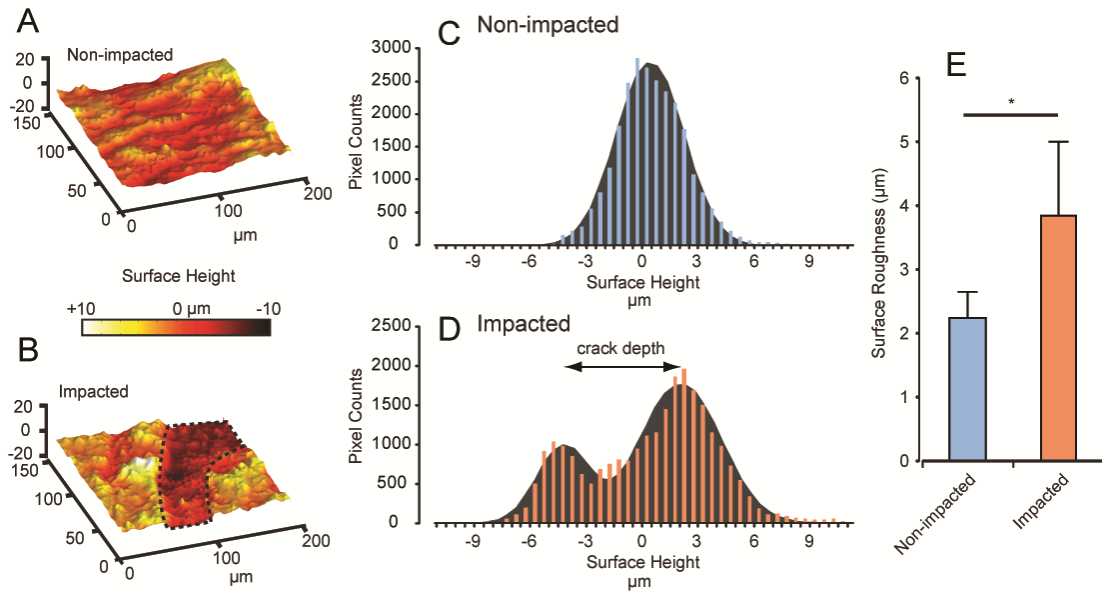

Figure 5.3 (AB) Representative surface scans of non-impacted and impacted cartilage revealed relatively smooth surfaces in non-impacted cartilage, but fissuring in impacted cartilage, with fissures on the order of 50 µm wide (outlined region). (C) Non-impacted cartilage had a normal Gaussian surface height distribution, but (D) impacted cartilage had a bimodal height distribution. The difference in heights between the two modes of surface heights revealed surface fissures were on the order of 8 µm deep. (E) The average surface roughness of impacted cartilage was 72% higher than non-impacted cartilage (*$p < 0.05$, $n = 4$-5).

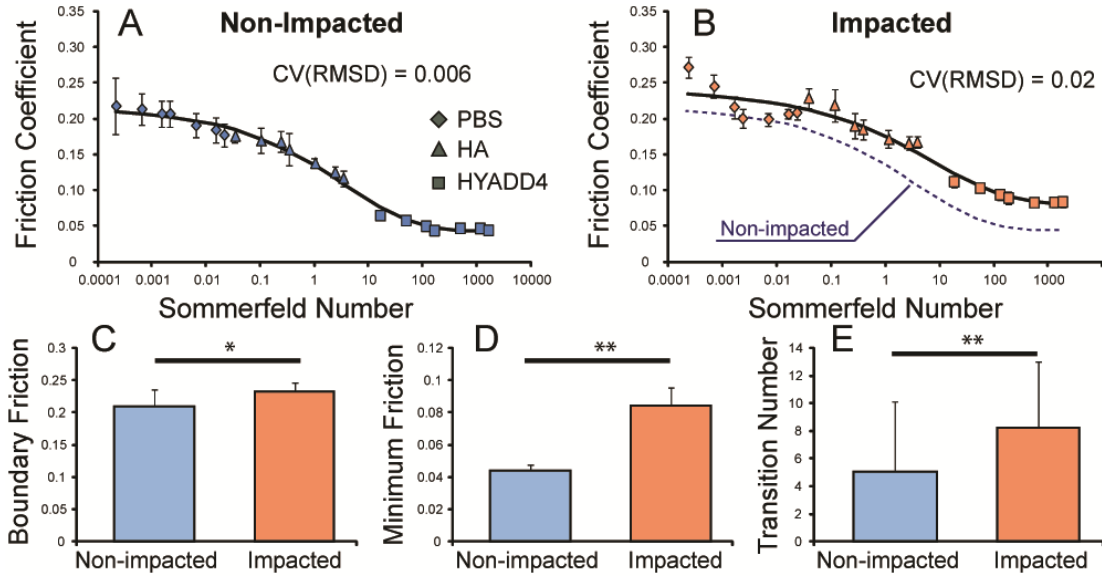

Figure 5.4 (AB) Friction coefficients as a function of Sommerfeld number fit very well to elastoviscous transition curves for both non-impacted and impacted cartilage (CV < 2% for both, n = 4). (C-E) Fit parameters from the model curve (equation 2) revealed how mechanisms of lubrication were altered after cartilage impact. (C) Boundary friction coefficient rose 11% after impact (*p < 0.05). (D) Minimum friction coefficient rose 94% after impact (**p < 0.01). (E) Transition number rose 62% after impact (**p < 0.01).

μm (n = 4-5, p = 0.02). Further, the surface profile of impacted cartilage revealed that the surface fissures were on the order of 50 μm wide (Figure 5.3 B). Fitting the height profile to a bimodal distribution of surface heights revealed that surface fissures were on the order of 8 μm deep, determined from the distance between the two maxima in the distribution (gray shaded regions, Figure 5.3 D).

Bulk mechanical compression revealed no changes in the aggregate modulus or hydraulic permeability. Moduli for non-impacted cartilage and impacted cartilage were 640 ± 130 kPa and 760 ± 150 kPa, respectively (n = 10-11, p = 0.064). Hydraulic permeability for non-impacted and impacted cartilage were 3.60 ± 1.4 m^2/Pa/s and 3.40 ± 1.2 m^2/Pa/s, respectively (n = 10-11, p = 0.73).

Both non-impacted and impacted cartilage fit well to an elastoviscous transition curve that presented friction transition from a high boundary friction plateau to a low, viscous friction regime. For non-impacted and impacted cartilage the coefficients of variation of the RMS error were 0.62% and 2.6%, respectively. Overall, the friction coefficients for impacted cartilage were 41% higher than non-impacted cartilage. In the boundary regime of lubrication, impacted cartilage friction was 11% higher than non-impacted controls (Figure 5.4 C). However, in the low, viscous friction regime of lubrication, friction for impacted cartilage was 94% higher than non-impacted controls (Figure 5.4 D). Additionally, the transition number, $S_{t,}$ increased 63% percent after impact (Figure 5.4 E). Collectively these data revealed that although boundary friction coefficicents rose, the most drastic changes occurred in the low viscous regime of lubrication and the transition towards it.

Discussion

This study revealed a connection between structural changes to articular cartilage after a sub-critical traumatic impact and changes to the effectiveness of viscous lubricants in reducing cartilage friction. While the intrinsic boundary lubricating ability of the cartilage was altered after impact (Figure 5.4 C), the most pronounced changes were discovered in the viscous regime of lubrication and the transition away from boundary to low, viscous friction (Figure 5.4 DE). This altered tribological behavior not only has implications concerning cartilage homeostasis after impact injury, but also in understanding how therapeutics may function to restore proper joint lubrication.

The most drastic changes to the intrinsic lubrication of cartilage after trauma were observed in the lubrication by viscous lubricants. Both the minimum friction coefficient and the transition away from boundary friction were significantly altered after impact (Figure 5.4 DE). Two key structural changes that may play a role in these friction changes were the loss of lubricin from the articular surface (Figure 5.2 CD) and increased surface roughness (Figure 5.3). We have recently observed that lubricin localization at the tissue surface interacts with viscous lubricants, such as hyaluronic acid, and serves to promote effective lubrication in a manner similar to viscous boundary lubrication [34], [41]. In this mechanism of lubrication, adsorbed, viscous surface layers promote the transition away from boundary friction to a low, viscous friction regime. Decreased lubricin localization after impact may be one structural change that hinders the viscous boundary lubrication of cartilage in this study. While we have recently observed that lubricin removal hinders the transition to low friction,

we did not observe the minimum friction coefficient increase substantially after lubricin removal [34], and likely, another structural change is responsible for the increase in the minimum friction coefficient.

The factor which likely plays a major role in the increased minimum friction ceofficient was the alteration of surface topology and roughness as a consequence of impact. For a soft, impermeable material lubricated by viscous mucin films, increased surface roughness inhibited the mechanism of viscous boundary lubrication [41], which is hypothesized to be the mechanism by which hyaluronic acid lubricates cartilage [33], [34]. Additionally, a study on the lubrication mechanisms of hydrogels hypothesized that increased surface roughness allows lubricating films at the interface to be drainable [42]. In this case, the minimum friction increase observed in the present study may be due to the viscous hyaluronic acid lubricant becoming drainable into the surface fissures, which can consequenty transfer higher stresses to the contacting asperities increasing the friction coefficient.

Not only was the low, viscous friction of impacted cartilage altered, but the boundary plateau was affected as well. The lubricin staining revealed less lubricin localized at the tissue surface, consistent with previous studies, the boundary friction coefficient, especially at low speed, increased on the order of ~20% [31], [34]. While the present study focused on the intrinsic lubricating ability of cartilage after trauma, it is important to note that lubricin within synovial fluid also plays a key role in the low friction of cartilage. However, in cases of trauma such as ACL rupture, lubricin concentration can fall by ~80% as early as 32 days after injury and take a full year to rebound to baseline levels [43]. With this in mind, the loss of intrinsic boundary

lubricating ability, along with the possibility of detrimental changes to synovial fluid composition highlights that while boundary lubrication was not altered on level equal to that of viscous friction, its importance should not be understated.

These changes in both the intrinsic boundary lubrication and viscous lubrication of cartilage after trauma may have functional consequences fueling the progression of damage consistent with development of PTOA. Cartilage homeostasis is dependent on a balance of frictional forces that can stimulate chondrocytes without causing detrimental effects [22], [44]. Shear stimulus of synovial fluid and chondrocytes, and active deformation of the cartilage matrix are pivotal to the transport of nutrients to deeper tissue and also to the stimulation of important genes such as proteoglycan 4 (i.e., lubricin encoding gene) [44] and the activation of signaling molecules, such as transforming growth factors [45]. However, overstimulation of cartilage in the form of elevated friction can acutely lead to chondrocyte apoptosis and necrosis [22], and mitochondrial dysfunction [23]. In the longer term, increased friction can lead to a loss of cellularity in the cartilage superficial zone [24]. The question remains as to whether the lubrication changes observed here are drastic enough to initiate any of these biological consequences. However, it is important to note that even in cases where trauma may not cause frictional changes that can lead to adverse effects such as chondrocyte apoptosis acutely, degeneration due to the elevated friction [25] may lead to adverse effects later on and may be a factor in the long, in some cases decades long, incubation period of PTOA.

From connecting structural changes to lubrication changes, it is very likely that the surface cracking plays a key role in inhibiting lubrication. In this study, we specifically explored a sub-critical impact model, that is, a model that causes surface damage to cartilage in the absence of full-thickness fissuring. These injuries would be impossible to detect through imaging modalities such as MRI or contrast-enhanced CT, and they would be difficult to detect even through arthroscopy especially compared to the detection of full–thickness cartilage lesions [21]. However, we have seen here that these surface fissures which can be on the order of only 50 μm wide and 10 μm deep, can have drastic effects on the lubricating environment. They may pose a target in developing *in vivo* imaging modalities that can detect defects on their size scale, and after their detection, suitable therapeutics may be applied.

One avenue for therapeutic intervention is tribosupplementation, the process of supplementing the joint with an exogenous lubricant injection [46]–[48]. In the form of viscosupplementation, injecting hyaluronic acid is currently a $1B industry world-wide, with varying results depending on many factors. It appears traumatic cartilage is destined for higher friction, while hyaluronic acid can decrease the friction of non-impacted cartilage over 50% compared to PBS, the friction of impacted cartilage is still 50% higher than non-impacted cartilage when lubricated by HA but 60% lower than impacted cartilage lubricated by PBS. It is possible that post-traumatic cartilage is predisposed to friction-mediated degeneration and the variation between lubricant efficacy on fissured and non-fissured cartilage may describe one mechanism by which HA is or isn't effective on a case-by-case basis.

Viscous friction was not the only regime of lubrication altered in the present

model, but the boundary mode friction coefficient was elevated as well. Consequently, boundary lubrication by lubricin poses a promising path for tribosupplementation [47], [48]. Lubricin replenishment can not only restore lubricating ability in boundary mode friction, but it also enhances the lubrication of HA through viscous boundary lubrication [33], [34]. Likely for these reasons, lubricin has proven effective at limiting cartilage degeneration in multiple animal models of traumatic OA.

While this study has revealed multiple paths through which the intrinsic lubricating mechanisms of cartilage are altered after traumatic impact, there are several limitations to be discussed. While the use of neonatal bovine cartilage provided a consistent source of healthy cartilage, it is likely that the surface damage seen in this study would happen at different stress and strain levels in both different aged animals and in different species. Additionally, the boundary conditions of the impact (i.e., cartilage plugs without subchondral bone, and flat ended impacter tip) may change thresholds for damage as well. Nevertheless, the effect of damage on lubrication would likely be similar. Further, due to a lack of availability of post-traumatic synovial fluid and exogenous lubricin, this study focused on the innate lubricating mechanisms of cartilage and the role of viscous lubricants. Future studies should evaluate the role replenishing boundary lubricants on the lubrication of post-traumatic cartilage and also post-traumatic *in vivo* studies should focus on the lubricating ability of synovial fluid after trauma.

REFERENCES

[1] L. Murphy, T. A. Schwartz, C. G. Helmick, J. B. Renner, G. Tudor, G. Koch, A. Dragomir, W. D. Kalsbeek, G. Luta, and J. M. Jordan, "Lifetime risk of symptomatic knee osteoarthritis.," *Arthritis Rheum.*, vol. 59, no. 9, pp. 1207–13, Sep. 2008.

[2] T. D. Brown, R. C. Johnston, C. L. Saltzman, J. L. Marsh, and J. A. Buckwalter, "Posttraumatic osteoarthritis: a first estimate of incidence, prevalence, and burden of disease.," *J. Orthop. Trauma*, vol. 20, no. 10, pp. 739–44, Jan. .

[3] A. von Porat, "High prevalence of osteoarthritis 14 years after an anterior cruciate ligament tear in male soccer players: a study of radiographic and patient relevant outcomes," *Ann. Rheum. Dis.*, vol. 63, no. 3, pp. 269–273, Mar. 2004.

[4] J. A. Buckwalter, D. D. Anderson, T. D. Brown, Y. Tochigi, and J. A. Martin, "The Roles of Mechanical Stresses in the Pathogenesis of Osteoarthritis: Implications for Treatment of Joint Injuries.," *Cartilage*, vol. 4, no. 4, pp. 286–294, Oct. 2013.

[5] D. D. Anderson, S. Chubinskaya, F. Guilak, J. A. Martin, T. R. Oegema, S. A. Olson, and J. A. Buckwalter, "Post-traumatic osteoarthritis: improved understanding and opportunities for early intervention.," *J. Orthop. Res.*, vol. 29, no. 6, pp. 802–9, Jun. 2011.

[6] V. Morel and T. M. Quinn, "Cartilage injury by ramp compression near the gel diffusion rate.," *J. Orthop. Res.*, vol. 22, no. 1, pp. 145–51, Jan. 2004.

[7] T. M. Quinn, A. J. Grodzinsky, E. B. Hunziker, and J. D. Sandy, “Effects of injurious compression on matrix turnover around individual cells in calf articular cartilage explants.,” *J. Orthop. Res.*, vol. 16, no. 4, pp. 490–9, Jul. 1998.

[8] R. L.-Y. Sah, J.-Y. H. Doong, A. J. Grodzinsky, A. H. K. Plaas, and J. D. Sandy, “Effects of compression on the loss of newly synthesized proteoglycans and proteins from cartilage explants,” *Arch. Biochem. Biophys.*, vol. 286, no. 1, pp. 20–29, Apr. 1991.

[9] L. V Burgin and R. M. Aspden, “A drop tower for controlled impact testing of biological tissues.,” *Med. Eng. Phys.*, vol. 29, no. 4, pp. 525–30, May 2007.

[10] J. B. Finlay and R. U. Repo, “Instrumentation and procedure for the controlled impact of articular cartilage.,” *IEEE Trans. Biomed. Eng.*, vol. 25, no. 1, pp. 34–9, Jan. 1978.

[11] J. E. Jeffrey, D. W. Gregory, and R. M. Aspden, “Matrix damage and chondrocyte viability following a single impact load on articular cartilage.,” *Arch. Biochem. Biophys.*, vol. 322, no. 1, pp. 87–96, Sep. 1995.

[12] J. Borrelli, M. E. Burns, W. M. Ricci, and M. J. Silva, “A method for delivering variable impact stresses to the articular cartilage of rabbit knees.,” *J. Orthop. Trauma*, vol. 16, no. 3, pp. 182–8, Mar. 2002.

[13] P. G. Alexander, Y. Song, J. M. Taboas, F. H. Chen, G. M. Melvin, P. A. Manner, and R. S. Tuan, “Development of a Spring-Loaded Impact Device to Deliver Injurious Mechanical Impacts to the Articular Cartilage Surface,” *Cartilage*, vol. 4, no. 1, pp. 52–62, Aug. 2012.

[14] E. D. Bonnevie, M. L. Delco, L. A. Fortier, P. G. Alexander, R. S. Tuan, and L. J. Bonassar, “Characterization of Tissue Response to Impact Loads Delivered Using a Hand-Held Instrument for Studying Articular Cartilage Injury.,” *Cartilage*, vol. 6, no. 4, pp. 226–32, Oct. 2015.

[15] L. R. Bartell, L. A. Fortier, L. J. Bonassar, and I. Cohen, “Measuring microscale strain fields in articular cartilage during rapid impact reveals thresholds for chondrocyte death and a protective role for the superficial layer,” *J. Biomech.*, vol. 48, no. 12, pp. 3440–3446, Sep. 2015.

[16] T. M. Quinn, R. G. Allen, B. J. Schalet, P. Perumbuli, and E. B. Hunziker, “Matrix and cell injury due to sub-impact loading of adult bovine articular cartilage explants: effects of strain rate and peak stress.,” *J. Orthop. Res.*, vol. 19, no. 2, pp. 242–9, Mar. 2001.

[17] R. M. Natoli, C. C. Scott, and K. A. Athanasiou, “Temporal effects of impact on articular cartilage cell death, gene expression, matrix biochemistry, and biomechanics.,” *Ann. Biomed. Eng.*, vol. 36, no. 5, pp. 780–92, May 2008.

[18] C. A. M. Huser and M. E. Davies, “Calcium signaling leads to mitochondrial depolarization in impact-induced chondrocyte death in equine articular cartilage explants.,” *Arthritis Rheum.*, vol. 56, no. 7, pp. 2322–34, Jul. 2007.

[19] P. A. Torzilli, R. Grigiene, J. Borrelli, and D. L. Helfet, “Effect of Impact Load on Articular Cartilage: Cell Metabolism and Viability, and Matrix Water Content,” *J. Biomech. Eng.*, vol. 121, no. 5, p. 433, Oct. 1999.

[20] V. C. Mow, S. C. Kuei, W. M. Lai, and C. G. Armstrong, “Biphasic Creep and Stress Relaxation of Articular Cartilage in Compression: Theory and

Experiments," *J. Biomech. Eng.*, vol. 102, no. 1, p. 73, Feb. 1980.

[21] K. D. Novakofski, S. L. Pownder, M. F. Koff, R. M. Williams, H. G. Potter, and L. A. Fortier, "High-Resolution Methods for Diagnosing Cartilage Damage In Vivo.," *Cartilage*, vol. 7, no. 1, pp. 39–51, Jan. 2016.

[22] K. A. Waller, L. X. Zhang, K. A. Elsaid, B. C. Fleming, M. L. Warman, and G. D. Jay, "Role of lubricin and boundary lubrication in the prevention of chondrocyte apoptosis.," *Proc. Natl. Acad. Sci. U. S. A.*, vol. 110, no. 15, pp. 5852–7, Apr. 2013.

[23] E. D. Bonnevie, M. L. Delco, N. Jasty, L. Bartell, L. A. Fortier, I. Cohen, and L. J. Bonassar, "Chondrocyte death and mitochondrial dysfunction are mediated by cartilage friction and shear strain," *Osteoarthr. Cartil.*, vol. 24, no. 24, p. S46, Apr. 2016.

[24] N. P. Karamchedu, J. N. Tofte, K. A. Waller, L. X. Zhang, T. K. Patel, and G. D. Jay, "Superficial zone cellularity is deficient in mice lacking lubricin: a stereoscopic analysis.," *Arthritis Res. Ther.*, vol. 18, no. 1, p. 64, Jan. 2015.

[25] G. D. Jay, J. R. Torres, D. K. Rhee, H. J. Helminen, M. M. Hytinnen, C.-J. Cha, K. Elsaid, K.-S. Kim, Y. Cui, and M. L. Warman, "Association between friction and wear in diarthrodial joints lacking lubricin.," *Arthritis Rheum.*, vol. 56, no. 11, pp. 3662–9, Nov. 2007.

[26] C. W. McCutchen, "The frictional properties of animal joints," *Wear*, vol. 5, no. 1, pp. 1–17, Jan. 1962.

[27] G. A. Ateshian, "The role of interstitial fluid pressurization in articular cartilage lubrication.," *J. Biomech.*, vol. 42, no. 9, pp. 1163–76, Jun. 2009.

[28] R. Krishnan, M. Kopacz, and G. A. Ateshian, “Experimental verification of the role of interstitial fluid pressurization in cartilage lubrication.,” *J. Orthop. Res.*, vol. 22, no. 3, pp. 565–70, May 2004.

[29] E. D. Bonnevie, V. Baro, L. Wang, and D. L. Burris, “In-situ studies of cartilage microtribology: roles of speed and contact area.,” *Tribol. Lett.*, vol. 41, no. 1, pp. 83–95, Jan. 2011.

[30] T. A. Schmidt, N. S. Gastelum, Q. T. Nguyen, B. L. Schumacher, and R. L. Sah, “Boundary lubrication of articular cartilage: role of synovial fluid constituents.,” *Arthritis Rheum.*, vol. 56, no. 3, pp. 882–91, Mar. 2007.

[31] J. P. Gleghorn, A. R. C. Jones, C. R. Flannery, and L. J. Bonassar, “Boundary mode lubrication of articular cartilage by recombinant human lubricin.,” *J. Orthop. Res.*, vol. 27, no. 6, pp. 771–7, Jun. 2009.

[32] G. D. Jay, D. A. Harris, and C.-J. Cha, “Boundary lubrication by lubricin is mediated by O-linked β(1-3)Gal-GalNAc oligosaccharides,” *Glycoconj. J.*, vol. 18, no. 10, pp. 807–815, Oct. 2001.

[33] S. Das, X. Banquy, B. Zappone, G. W. Greene, G. D. Jay, and J. N. Israelachvili, “Synergistic interactions between grafted hyaluronic acid and lubricin provide enhanced wear protection and lubrication.,” *Biomacromolecules*, vol. 14, no. 5, pp. 1669–77, May 2013.

[34] E. D. Bonnevie, D. Galesso, C. Secchieri, I. Cohen, and L. J. Bonassar, “Elastoviscous Transitions of Articular Cartilage Reveal a Mechanism of Synergy between Lubricin and Hyaluronic Acid.,” *PLoS One*, vol. 10, no. 11, p. e0143415, Jan. 2015.

[35] M. D. Hersey, “The laws of lubrication of horizontal journal bearings,” *J. Washingt. Acad. Sci.*, vol. 4, no. August, pp. 542–552, 1914.

[36] A. C. Dunn, W. G. Sawyer, and T. E. Angelini, “Gemini Interfaces in Aqueous Lubrication with Hydrogels,” *Tribol. Lett.*, vol. 54, no. 1, pp. 59–66, Mar. 2014.

[37] E. D. Bonnevie, J. L. Puetzer, and L. J. Bonassar, “Enhanced boundary lubrication properties of engineered menisci by lubricin localization with insulin-like growth factor I treatment.,” *J. Biomech.*, vol. 47, no. 9, pp. 2183–8, Jun. 2014.

[38] V. L. Cross, Y. Zheng, N. Won Choi, S. S. Verbridge, B. A. Sutermaster, L. J. Bonassar, C. Fischbach, and A. D. Stroock, “Dense type I collagen matrices that support cellular remodeling and microfabrication for studies of tumor angiogenesis and vasculogenesis in vitro.,” *Biomaterials*, vol. 31, no. 33, pp. 8596–607, Nov. 2010.

[39] I. Finelli, E. Chiessi, D. Galesso, D. Renier, and G. Paradossi, “Gel-like structure of a hexadecyl derivative of hyaluronic acid for the treatment of osteoarthritis.,” *Macromol. Biosci.*, vol. 9, no. 7, pp. 646–53, Jul. 2009.

[40] A. Unsworth, “Tribology of human and artificial joints,” *Arch. Proc. Inst. Mech. Eng. Part H J. Eng. Med. 1989-1996 (vols 203-210)*, vol. 205, no. 38, pp. 163–172, Jun. 1991.

[41] G. E. Yakubov, J. McColl, J. H. H. Bongaerts, and J. J. Ramsden, “Viscous boundary lubrication of hydrophobic surfaces by mucin.,” *Langmuir*, vol. 25, no. 4, pp. 2313–21, Feb. 2009.

[42] S. Yashima, N. Takase, T. Kurokawa, and J. P. Gong, “Friction of hydrogels

with controlled surface roughness on solid flat substrates.," *Soft Matter*, vol. 10, no. 18, pp. 3192–9, May 2014.

[43] K. A. Elsaid, B. C. Fleming, H. L. Oksendahl, J. T. Machan, P. D. Fadale, M. J. Hulstyn, R. Shalvoy, and G. D. Jay, "Decreased lubricin concentrations and markers of joint inflammation in the synovial fluid of patients with anterior cruciate ligament injury.," *Arthritis Rheum.*, vol. 58, no. 6, pp. 1707–15, Jun. 2008.

[44] G. E. Nugent, N. M. Aneloski, T. A. Schmidt, B. L. Schumacher, M. S. Voegtline, and R. L. Sah, "Dynamic shear stimulation of bovine cartilage biosynthesis of proteoglycan 4.," *Arthritis Rheum.*, vol. 54, no. 6, pp. 1888–96, Jun. 2006.

[45] M. B. Albro, A. D. Cigan, R. J. Nims, K. J. Yeroushalmi, S. R. Oungoulian, C. T. Hung, and G. A. Ateshian, "Shearing of synovial fluid activates latent TGF-β.," *Osteoarthritis Cartilage*, vol. 20, no. 11, pp. 1374–82, Nov. 2012.

[46] E. A. Balazs and J. L. Denlinger, "Viscosupplementation: a new concept in the treatment of osteoarthritis.," *J. Rheumatol. Suppl.*, vol. 39, pp. 3–9, Aug. 1993.

[47] C. R. Flannery, R. Zollner, C. Corcoran, A. R. Jones, A. Root, M. A. Rivera-Bermúdez, T. Blanchet, J. P. Gleghorn, L. J. Bonassar, A. M. Bendele, E. A. Morris, and S. S. Glasson, "Prevention of cartilage degeneration in a rat model of osteoarthritis by intraarticular treatment with recombinant lubricin.," *Arthritis Rheum.*, vol. 60, no. 3, pp. 840–7, Mar. 2009.

[48] E. Teeple, K. A. Elsaid, G. D. Jay, L. Zhang, G. J. Badger, M. Akelman, T. F. Bliss, and B. C. Fleming, "Effects of supplemental intra-articular lubricin and

hyaluronic acid on the progression of posttraumatic arthritis in the anterior cruciate ligament-deficient rat knee.," *Am. J. Sports Med.*, vol. 39, no. 1, pp. 164–72, Jan. 2011.

CHAPTER 6

Cartilage Friction Influences Depth-Dependent Shear Strain, Cell Death, Mitochondrial Depolarizaiton, and Apoptosis[5]

Abstract

Friction in cartilage disease has classically been thought to have negative consequences through a wear and tear mechanism of fibrillating the cartilage surface and causing matrix damage. However, recent evidence suggests that elevated friction can have the adverse effect of causing chondrocyte apoptosis. In this study live cartilage explants were subjected to either high friction or low friction by being slid in saline or synovial fluid, respectively. The depth-dependent shear strains during cartilage sliding were measured using confocal elastography. Additionally, the cellular responses to high friction in terms of cell death, mitochondrial depolarization, and caspase activation were all analyzed for high and low friction. Elevated friction was connected to increases in all three of cell death, mitochondrial depolarization, and caspase activation. Additionally, strong correlations between each of these cell responses and local frictional shear strain revealed a strong local mechanics dependence. Further, a strong correlation between mitochondrial depolarization and caspase activation was found. This study revealed a biological response to high friction that is due to local frictional strains and provides insight into probably mechanisms of damage initiation and progression as a function of improper lubrication of the cartilage surface.

[5] To be published with co-authors: E.D. Bonnevie, M.L. Delco, N. Jasty, L.R. Bartell, I. Cohen, L.A. Fortier, L.J. Bonassar

Introduction

Under typical conditions, articular cartilage provides the body's joints with the most efficient bearing surface found in nature. However, the failure of this tissue in osteoarthritis (OA) is the leading cause of severe disability in the United States [1]. Despite its widespread prevalence, the early incubation phases of OA and its progression are not well understood [2], [3]. Even in cases with a known initiating event such as a traumatic injury in post-traumatic OA, which accounts for ~12% of OA cases, the incubation phase can last decades [4]. This gap in knowledge in the initiation and progression of OA has been linked to not fully understanding both biological and mechanical factors that interact with each other [3].

The interaction between mechanical and biological factor has long been studied in cartilage research, but despite this previous work it remains a key aspect in the progression of OA that is still not fully understood. One source of mechanical stimulus to cartilage is frictional shear due to cartilage sliding against cartilage. The degree of mechanical stimulus is dependent on lubrication [5], and factors such as aging [6], traumatic injury [7], and disease [8] can all have drastic effects on cartilage lubrication. These factors can each affect the main lubricating molecules of synovial fluid, lubricin and hyaluronic acid, and consequently increase the friction coefficient at a cartilage surface [9], [10]. In fact, a traumatic ACL tear can cause lubricin concentrations to drop 90% below normal levels and take an entire year to rebound [7]. Similarly increased friction at the cartilage surface has been connected to increased depth-dependent shear strains [5] and surface wear independently [11], and is likely a key factor in the initiation or progression of cartilage degeneration.

Although the detrimental effects of cartilage lubrication have classically been considered mechanical in nature, recent experimental evidence suggests that altered lubrication can have drastic biological effects as well. Cartilage exposed to high friction exhibits significantly more chondrocyte apoptosis compared to cartilage lubricated by healthy synovial fluid [12]. However, the link between elevated friction, frictional shear strains, and adverse cellular responses has not been characterized.

While understudied with respect to lubrication lubrication, the link between mechanical stimulation through injurious compression and cellular responses is comparatively well characterized. In addition to upregulating inflammatory signals [13], traumatic impacts and compressions can induce acute chondrocyte necrosis at strains ~0.1 within hours after compression [14], [15]. Further, injurious compression induces chondrocyte apoptosis as well [16]. One avenue for mechanically-mediated apoptosis is through the mitochondria. Increases in calcium signaling have been connected to mitochondrial depolarization, and mitochondrial depolarization has been implicated in intitating the caspase cascade though cytochrom c release [16]. However, there is currently minimal insight on the mechanical thresholds necessary to elicit such a response.

Although the response of chondrocytes to mechanical loading has been comparatively well characterized for cartilage compression, mechanical stimulus in the form of frictional shear loading can elicit cellular responses that differ from those for compression [17]. Shear and compression loading of cartilage differentially regulate gene transcription. it is currently unclear whether these effects extend to factors such as necrosis and apoptosis.

Addressing the knowledge gap concerning the role of friction in cellular responses, the goals of the present study are 6-fold: 1) Determine the link between cartilage friction and depth-dependent shear deformation and strains, 2) Determine the link between cartilage friction and depth-dependent acute cell death, 3) Determine the link between cartilage friction and depth-dependent MT depolarization, 4) Determine the link between cartilage friction and depth-dependent apoptosis, 5) Determine the link between frictional shear strain and necrosis, MT dysfunction, and apoptosis, 6) Determine the link between acute MT dysfunction and apoptosis.

Methods

Tissue Harvest and Preparation

Cartilage from the femoral condyles of more than 10 neonatal bovine were collected within 24 hours of sacrifice. Cylindrical plugs (6 mm diameter by 2 mm thick) were extracted using sterile practices from the central region of the condyles along the major axis of articulation. Prior to any mechanical stimulus, samples were equilibrated for 90 minutes in DMEM at 37°C and 5% CO_2. Synovial fluid was extracted from adult equine and pooled from several joints to minimize sample to sample variability.

Frictional Sliding

Articular cartilage samples were slid against polished glass counterfaces in a custom-built tribometer[10], [18]. Samples were submerged in a lubricating bath of either phosphate buffered saline (Corning, Manassas VA) or equine synovial fluid. Samples were compressed to 15% axial compression using optical micrometer stages

before sliding 30 reciprocating cycles of ±6 cm. Both shear and normal loads were collected using a biaxial load cell and friction coefficient was calculated as the ration between shear load and normal load.

Depth-Dependent Shear Strain Measurements

A similar setup was mounted on a Zeiss Live 5 confocal microscope to measure depth-dependent frictional shear strains in a similar manner to previous studies that measured depth-dependent shear properties [19], [20]. Samples were biaxially cut to form hemicylindrical samples that were mounted via cyanoacrylate adhesive to a tissue deformation imaging stage as previously described [19]. Samples were stained in 7 μg/mL 5-DTAF for general protein florescence. Unlike previous studies, samples were bathed in either PBS or synovial fluid and compressed to 15% axial strain against polished glass. In a similar manner to frictional testing, the glass slide was reciprocated against the cartilage surface. Depth-dependent shear deformations were tracked by analyzing the displacements photobleached lines perpendicular to the articular surface. The local shear strains were calculated from differentiation of the local displacements as previously described [19].

Cellular Imaging

Unfixed, hydrated, and intact cartilage explants were imaged on a Zeiss LSM 710 confocal microscope to determine the cellular responses to repeated frictional shear. After 30 cycles of frictional sliding, samples were either incubated in DMEM for 2 hours before staining, or incubated for 24 hours in DMEM supplemented with 100 U/ml penicillin and 100 μg/ml streptomycin. Live/Dead staining was conducted 2 hours after sliding. Cylindrical samples were axially bisected into hemicylinders and

stained for 20 minutes with 4 μM Calcein AM and 2 μM Ethidium homodimer (Molecular Probes). Followed by rinses in PBS. Mitochondrial polarization was assessed 2 hours after sliding as well. Hemicylindrical sections were stained with Mitotracker MitoTracker Green (MTrG; 200 nM) for 40 minutes followed by 20 minutes with tetramethylrhodamine methyl ester perchlorate (TMRM; 10 nM) added as well. Briefly, MTrG staining was used as a general MT stain regardless of membrane polarity whereas TMRM staining was used to indicate functional (i.e., polarized) MT. Samples that were incubated for 24 hours were assessed similarly with the Live/Dead assay. Additionally, samples incubated for 24 hours after sliding were stained with CellEvent Caspase-3/7 Green. Staining for 30 minutes was conducted before imaging along with confocal reflectance.

Depth-dependent cellular responses were quantified using ImageJ. Briefly, 50 μm deep by 250 μm wide bins were analyzed to determine cell death (percentage of cells staining with ethidium homodimer and no Calcein AM), MT dysfunction (percentage of cells staining with only MTrG and no colocalization with TMRM), and apoptosis (number of caspase-positive cells).

Statisctial Analysis

Differences in equilibrium friction coefficient were determined by Student's t-test for the 30^{th} cycle of sliding and significance was set at $p < 0.05$. Differences in depth-dependent shear strain were determined at each depth similarly with a Student's t-test and average p value was reported for all depths in addition to the max p value. Cellular effects between lubrications groups and control were analyzed at each depth bin using a one-way ANOVA with Bonferroni post-hoc. Depth-dependence in cellular

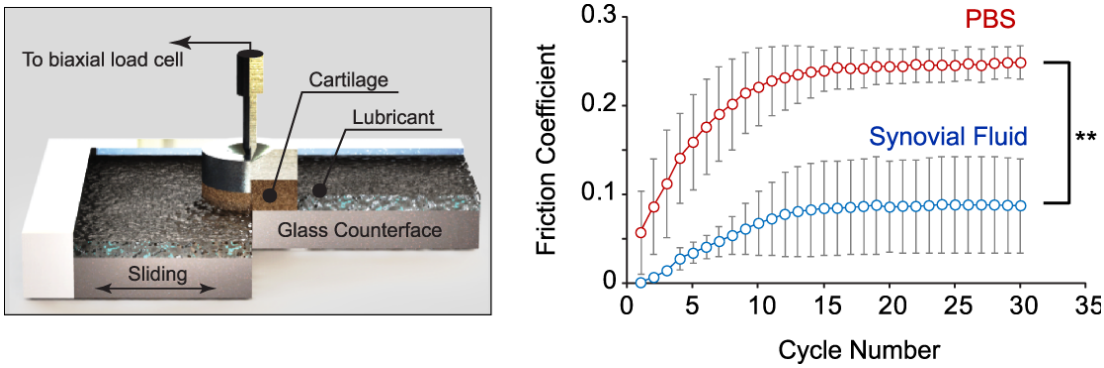

Figure 6.1 *Left* Cartilage samples were slid against polished glass in a custom tribometer while lubricated by either PBS or synovial fluid. *Right* PBS- and synovial fluid-lubricated cartilage exhibited time-dependent friction coefficients. The equilibrium friction coefficient for PBS was 2.8x that of synovial fluid (**$p < 0.01$, $n = 3$)

effects were determined by paired Student's t-test between adjacent depth bins. Correlations between measured parameters were determined using a Pearson correlation coefficient.

Results

The friction coefficient for cartilage lubricated by both PBS and synovial fluid displayed time dependence as expected [21] but reached equilibrium values after ~15 cycles (30 minutes of sliding) of the 30 sliding cycles. Equilibrium friction for PBS was 2.8X that of synovial fluid ($p < 0.008$, $n = 3$) The equilibrium friction coefficients were $\mu_{eq} = 0.25 \pm 0.02$ for PBS lubricated cartilage and $\mu_{eq} = 0.09 \pm 0.05$ for synovial fluid lubricated cartilage (Fig. 6.1).

A similar set up to the friction measurements was mounted on a confocal microscope and depth-dependent shear strains were measured for the two lubricating conditions (Fig. 6.1). Both PBS and synovial fluid lubricated cartilage exhibited depth-dependent shear strain as expected [5], [19]. Further, the shear strains in PBS lubricated cartilage were throughout the depth at least twice as high as those of synovial fluid lubricated cartilage ($p_{ave} < 0.001$, $p_{max} = 0.0026$, $n = 7$-8 samples at 96 depths). Maximum shear strains in PBS lubricated cartilage were $9.7 \pm 2.6\%$ and occured at the tissue surface, while shear strains in synovial fluid lubricated cartilage reached $4.5 \pm 1.9\%$ at the surface.

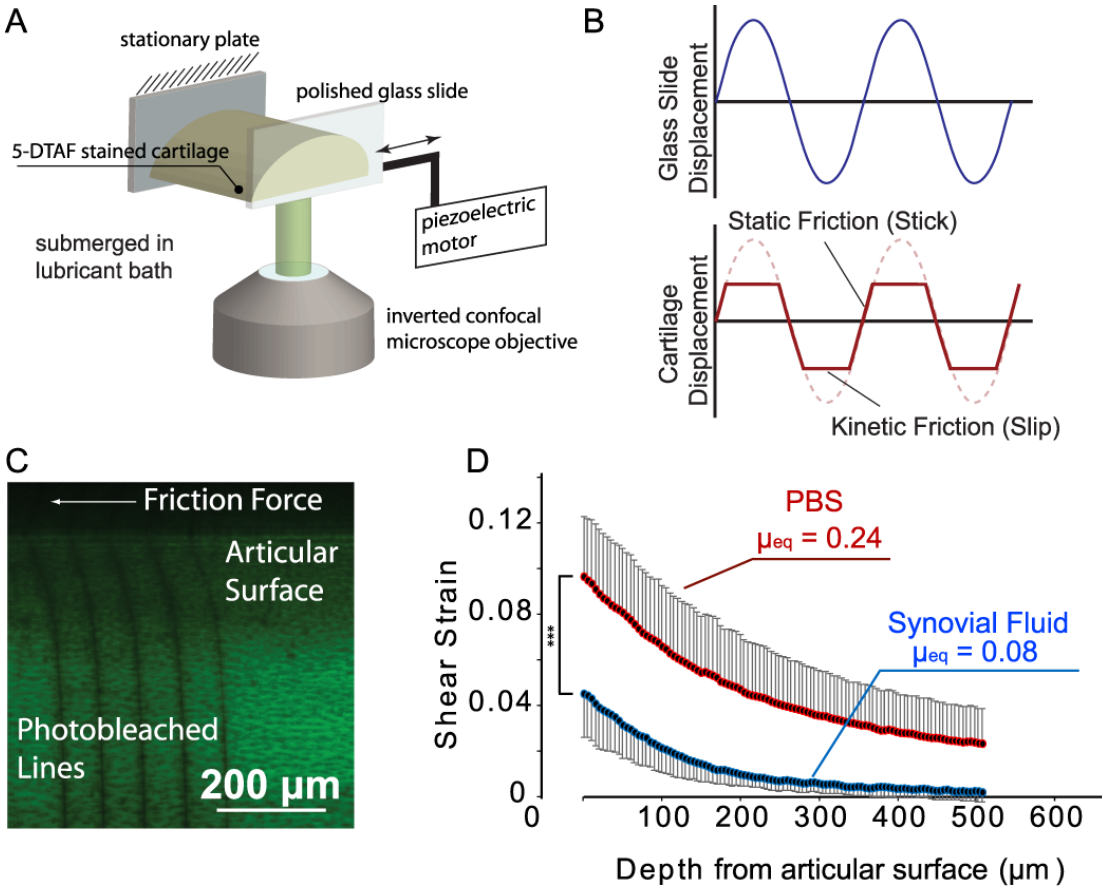

Figure 6.2 (A-B) Cartilage was mounted on an inverted confocal microscope and a glass slide was slid against the surface while depth-dependent deformations were tracked. (C) Photobleached lines provided depth-dependent deformations. (D) Shear strain for PBS was at least twice as high than synovial fluid throughout the cartilage depth (***$p < 0.005$, $n = 7$-8).

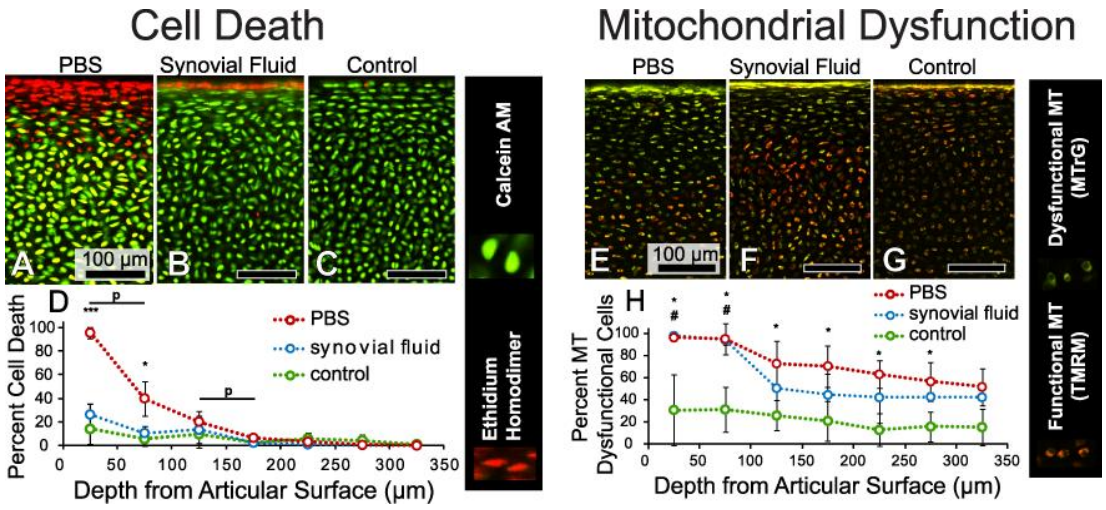

Figure 6.3 (A-C) Live/Dead staining of PBS, synovial fluid, and control cartilage revealed significant cell death in PBS-slid cartilage. (D) Percent cell death was significantly higher for PBS than the other two groups within 100 µm of the articular surface (*** $p < 0.005$, * $p < 0.05$, $n = 4$). PBS-lubricated cartilage displayed depth-depdendent cell death within 200 µm of the surface (*p* denotes $p < 0.05$ between depths). (E-G) Significant mitochondrial depolarization was revealed in the superficial most 100 µm of both PBS- and synovial fluid-lubricated cartilage. (H) Depth-dependence of MT depolarization (* denotes $p < 0.05$ for PBS vs control, # denotes $p < 0.05$ synovial fluid vs control, $n = 4$).

Samples that underwent 30 cycles of sliding over 1 hour in the tribometer were assayed after 2 hours incubation in DMEM for chondrocyte viability (Fig 6.3). Staining with both Calcein AM and ethidium homor dimer revealed little cell death in both control and synovial fluid lubricated tissue (viability >90%, except for the superficial most 50 μm of synovial fluid lubricated tissue where 26 ± 9% of cells were dead (n = 4). However, for PBS lubricated cartilage, a more distinct depth-dependent profile of viability as a function of tissue depth was evident. PBS lubricated tissue exhibited significantly more cell death than control and synovial fluid lubricated cartilage in the superficial 100 μm ($p < 0.05$) and also exhibited significant depth dependence. Within the first 50 μm of tissue, 95 ± 4% of cells were dead, and between 50 and 100 μm deep 40 ± 15% of cells were dead (n = 4).

Similarly to acute cell death, MT depolarization was both depth- and friction-dependent (Fig 6.3). Within the superficial-most 100 μm both PBS and synovial fluid lubricated cartilage presented a large proportion of cells displaying MT depolarization compard to controls (98 ± 2% and 94 ± 4% of cells for 0-50 μm and 50-100 μm for synovial fluid, and 96 ± 3% and 95 ± 14% of cells for 0-50 μm and 50-100 μm for PBS lubricated cartilage, $p < 0.05$, n = 4). Deeper than the superficial zone, MT depolarization dropped to 44% and 63% for synovial fluid and PBS lubricated cartilage respectively, between 100 and 350 μm deep.

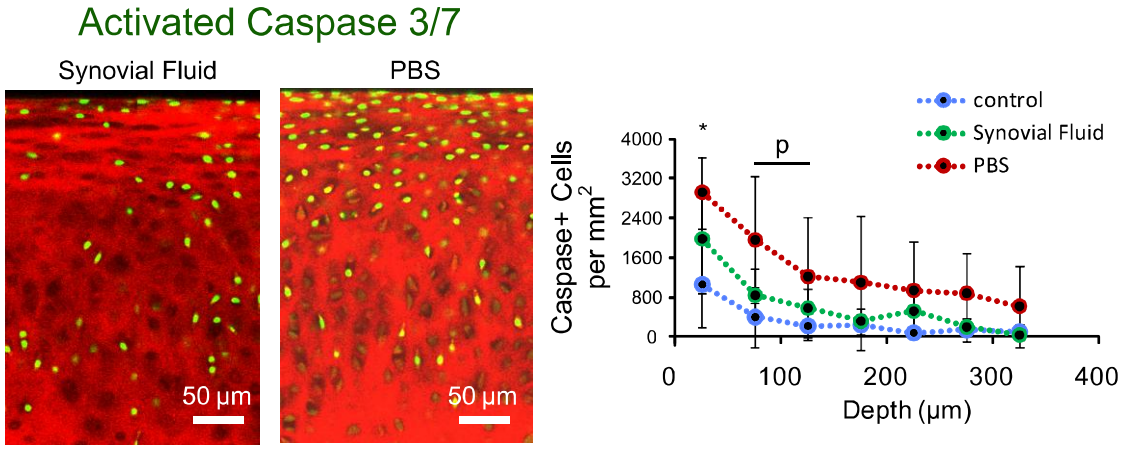

Figure 6.4 *Left* Representative images of activated caspase in synovial fluid- and PBS-lubricated cartilage 24 hours after sliding. *Right* PBS-lubricated cartilage displayed depth-dependence within 100 µm of the surface (*p* denotes $p < 0.05$ between times), and significantly more apoptotic cells than control within 50 µm of the surface (* denotes $p < 0.05$, PBS vs control).

Samples assayed 24 hours after sliding were analyzed for activated caspase 3/7 and counter-imaged using collagen reflectance. Overall more apoptotic cells were detected in PBS lubricated cartilage compared to controls (121 ± 88, 56 ± 30, and 28 ± 18 caspase-positive cells for PBS, synovial fluid, and control, respectively; $p < 0.05$, $n = 4$, Fig 6.4). Similarly to cell death and MT dysfunction, apoptosis was depth dependent for PBS lubricated cartilage within 100 μm of the surface ($p = 0.02$).

Connections between depth-dependent shear strains and cellular responses provide mechanistic insight into the roles of mechanical perturbations and cellular responses (Fig 6.5). Connecting the applied shear frictional shear strain and acute cell death provided a significant correlation between depth-dependent shear strain and fractional cell death ($R^2 = 0.61$, $p < 0.001$). To understand the role of local normal strain as well, local normal strains were calculated based off recent work using the same tissue source [22]. With a linear combination of shear and normal strain, the correlation with acute cell death was stronger ($R^2 = 0.78$, $p < 0.001$).

For MT dysfunction a similar correlation was made with local strains. However, in this case, the superficial-most 100 μm of tissue were not included in the analysis due to complications due to both cell death and compression alone (see supplemental material) having an effect of mitochondrial depolarization in the superficial zone. The correlation between shear strain and MT depolarization was very strong ($R^2 = 0.95$, $p < 0.00001$) revealing a strong connection between local mechanics and MT function. Similarly for apoptosis, correlation between caspase-positive cells and local shear strain provided a strong connection ($R^2 = 0.80$, $p = 0.000014$). Further, the correlation between number of apoptotic cells and MT

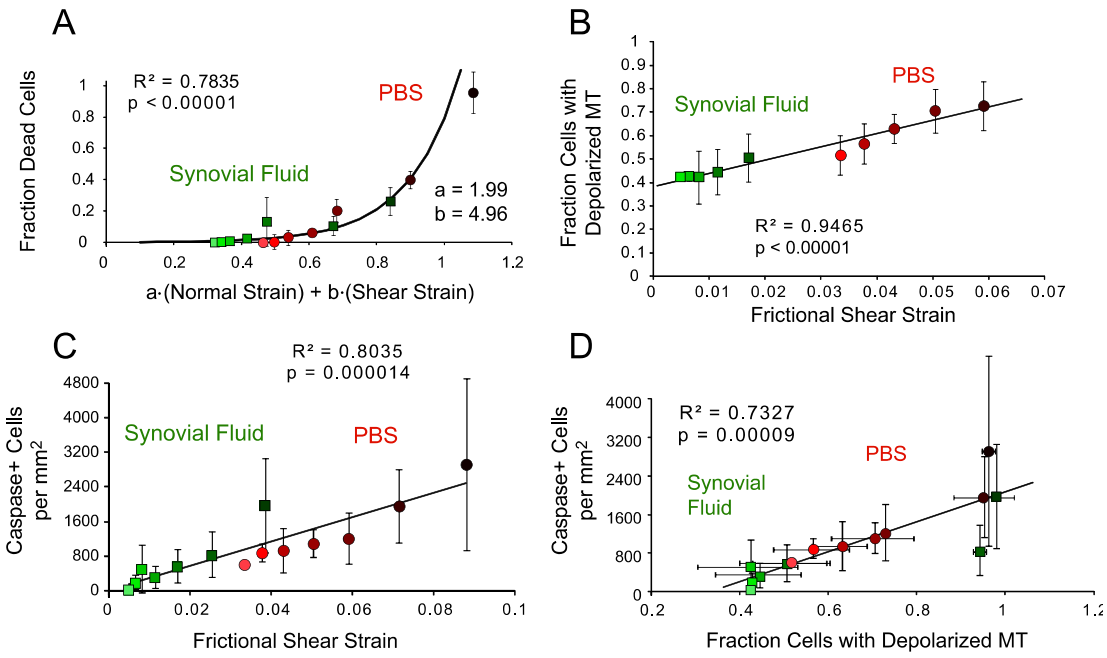

Figure 6.5 (A) Acute cell death correlated highly with a linear combination of local shear strain and normal strain for both PBS and synovial fluid lubricated cartilage (Exponential curve fit, $R^2 = 0.78$, $p < 0.00001$) . (B) MT dysfunction correlated highly with local frictional shear strain ($R^2 = 0.95$, $p < 0.00001$). (C) Number of apoptotic cells correlated highly with local frictional shear strain ($R^2 = 0.80$, $p = 0.000014$). (D) Number of apoptotic cells at 24 hours was predicted by MT depolarization at 2 hours ($R^2 = 0.73$, $p = 0.00009$).

depolarization was also strong ($R^2 = 0.73$, $p = 0.00009$) and solidified the connection between local mechanics, MT depolarization, and apoptosis due to friction in articular cartilage.

Discussion

This study explored the mechanical and biological effects of elevated friction on articular cartilage. Mechanically, the relationship between friction and local shear strains was determined through confocal elastography, and biologically, the connection between higher friction and chondrocyte death, MT depolarization, and apoptosis was established. Further, the dependence of these cellular responses on local shear strain was confirmed. Additionally, mechanically-driven MT depolarization 2 hours after friction exposure was a strong predictor of apoptosis 24 hours later. Together the data here provide insight into the mechanisms through which arthritis may initiate or progress, and reveal a potential therapeutic target in mitochondrial restabilization.

While the consequences of high cartilage friction are typically considered mechanical in nature, the evidence presented here suggests that the biological consequences are also critical to cartilage homeostasis. The correlation between frictional shear strain and MT depolarization (Figure 6.5B, $R^2 = 0.95$) suggests that biological consequences of high friction can diminish proper chondrocyte function. Outside of cartilage, MT depolarization is implicated in the progression of other diseases including cardiac and neurodegenerative diseases [23], [24]. By hindering the function of MT, not only are the energetics of a tissue hindered, but also these

dysfunctional cells are typically destined for apoptosis. In cartilage, where cell and matrix turnover is low, this may be a critical step in the incubation phases of cartilage diseases. Recent evidence suggests that MT dysfunction precedes histologic evidence of cartilage damage [25], and here we revealed a mechanically-driven mechanism through which MT depolarization can occur.

Due to its avascular nature, cartilage relies heavily on mechanical stimulus for proper function, but while most physiological stresses may be beneficial, it is likely that mechanical overload is a key initiator in chondrocyte dysfunction. MT depolarization can result from excess intracellular calcium influx through mechanically-opened ion channels following traumatic impact [16] and is connected to increased reactive oxygen species (ROS) concentrations [24]. Further, MT dysfunction itself is a source of in increased ROS levels [26]. While the biochemical pathway through which depolarization occurred in this study was not explicitly determined, depolarization was highly correlated with local shear strains (Figure 6.5B). The mechanical stimulus applied in this study, 30 cycles of sliding, was neither traumatic nor overtly chronic, however, the results are in agreement with both traumatic and chronic models of compressive loading [27], [28]. In contrast, the shear strains measured here (~5%) that induced mitochondrial depolarization are well below the compressive strains (between 20% and 40%) used in the chronic model of cartilage loading. These low frictional shear strains that induced MT depolarization may indicate that cartilage is more susceptible to shear strain mediated dysfunction compared to compression.

The full effects of MT depolarization are still to be seen in cartilage, but

connection to other tissues reveals the extent to which consequences may hinder cartilage function. In other cell types (e.g., neurons) mitochondrial depolarization is proven to be a pivotal step in apoptosis. Increased mitochondrial membrane permeability initiates cytochrome c release and may also initiate the release of apoptosis-initiating factor [29] leading to caspase activation. Connecting to cartilage, the effects of this cascade have been implicated in early signs of cartilage degeneration. Chondrocyte apoptosis is a known consequence of hindered boundary lubrication [12] and apoptosis is also an effect of traumatic impact to cartilage [30]. Considering lower cellularity is a hallmark of early OA progression, previous research has attempted to inhibit chondrocyte death through intraarticular caspase inhibitor treatment; however with minimal success. Considering the large role of MT in regulating the energetics of cells, a downstream target such as caspase inhibition may inhibit cell death but it is unclear whether such a treatment can restore proper function to dysfunctional cells.

With a mitochondrial-mediated aspect of OA progression clear in the form of both apoptosis, ROS production, and inflammation, MT stabilization emerges as a viable candidate for a disease modifying OA drug. MT stabilization is currently used as a treatment in several other diseases to prevent cell death and restore respiratory function [31]–[33]. This treatment has only recently been applied to cartilage [34], but may provide advantages over apoptosis prevention through caspase inhibition [35]. Caspase inhibition in a posttraumatic model facilitated smaller cartilage lesions, but had minimal effects, if any, on proteoglycan content and cellularity. It is likely that a therapeutic target upstream of caspase activation such as mitochondrial depolarization

may pose a more viable target to rescue chondrocytes. Szeto-Schiller peptides are synthetic peptides with high affinity to the inner mitochondrial membrane that have MT stabilizing properties. In non-chondrocyte models, these drugs have reduced ROS levels, MT depolarization, caspase activation, and cell death [31]. Recently, in a PTOA model using cartilage explants, we have reported on both apoptosis inhibition and reduced matrix damage and cell death. With theses promising findings, it is likely a similar treatment may prove effective for the friction-mediated MT depolarization and apoptosis revealed in the present study.

In addition to apoptosis, acute non-specific cell was also revealed here as a function of mechanical overloading. While MT depolarization was revealed deeper than the most superficial 100 μm, the majority of acute non-specific cell death was localized within the superficial most 100 μm from the articular surface. We found that depth-dependant shear strain alone was not a very strong predictor of cell death (R^2 = 0.61). Consequently, using local strains calculated from previously reported displacements using the same tissue source and deformation system as the one used in this study [22] we found a stronger predictor of cell death than shear strain alone. Correlating cell death with a linear combination of normal and shear strains (i.e., $a \cdot \varepsilon_{normal} + b \cdot \varepsilon_{shear}$) provided this stronger predictor of acute cell death (R^2 = 0.78, a = 1.99, b = 4.98). The coefficients may indicate chondrocyte death is relatively more sensitive to shear strain; however, it should be noted that in the case of this study the shear strain was cyclically applied while the normal strain was held constant. Nevertheless, the current study confirms that superficial chondrocytes are more prone to mechanically-mediated cell death [14], [15] even in this case of frictional shear

strain.

The biological effects of elevated friction from the present study provide insight into the wear mechanisms of cartilage. Typically, the effects of high friction in cartilage are considered to be mechanical in nature. Dozens of studies have analyzed the role of friction in the mechanical degradation, or "wearing," of cartilage [36]–[38]. Sliding cartilage against surfaces like the glass used in this study have reported proteoglycan and collagen loss from the cartilage matrix[39], and other studies have analyzed the morphological changes of the cartilage surface after friction to elucidate the mechanisms through which the "wear and tear" of OA progresses. The data in this study reveal, however, that biological mechanisms may be more sensitive to increases in friction.

While this study provided strong evidence for the role of frictional shear strains on detrimental cellular reponses in articular cartilage, there are several limitations that should be both acknowledged and addressed. While neonatal bovine tissue was used in this study to mitigate the probability of preexisting damage or degradation in the tissue, there are differences between both cellular density and local mechanics in different aged tissues that may alter the damage thresholds revealed in this study. Further, while the time points evaluated were based on previous work, there is still likely time-dependence in the cellular responses not fully characterized by our two time points, and future work should be conducted to understand how spatio-temporal cellular responses evolve based on cartilage friction. Also regarding cellular responses, shearing of synovial fluid may activate signal molecules that can affect the cells, however despite this possibility, we still dicovered strong correlations with local

mechanics and cellular responses consistent for both PBS and synovial fluid as a lubricant. Finally, while this study bookended the friction coefficients in health and disease (i.e., PBS is a worst case friction scenario) future work on the role of synovial fluid from injury or disease can shed light on the role of decreased lubrication and the responses of chondrocytes.

In summary, this study revealed a biological mechanism through which elevated friction can disrupt chondrocyte homeostasis. With severely altered boundary lubricating ability, the shear strains in cartilage can significantly increase. The heterogeneity of cartilage causes distinct depth-dependent trends of local shear strains and these local strains effect chondrocyte function through non-specific cell death, mitochondrial depolarization, and apoptosis. These biological responses to high friction may be initiating events that cause damage to initiate and propagate throughout a joint.

REFERENCES

[1] L. Murphy, T. A. Schwartz, C. G. Helmick, J. B. Renner, G. Tudor, G. Koch, A. Dragomir, W. D. Kalsbeek, G. Luta, and J. M. Jordan, "Lifetime risk of symptomatic knee osteoarthritis.," *Arthritis Rheum.*, vol. 59, no. 9, pp. 1207–13, Sep. 2008.

[2] D. D. Anderson, S. Chubinskaya, F. Guilak, J. A. Martin, T. R. Oegema, S. A. Olson, and J. A. Buckwalter, "Post-traumatic osteoarthritis: improved understanding and opportunities for early intervention.," *J. Orthop. Res.*, vol. 29, no. 6, pp. 802–9, Jun. 2011.

[3] J. A. Buckwalter, D. D. Anderson, T. D. Brown, Y. Tochigi, and J. A. Martin, "The Roles of Mechanical Stresses in the Pathogenesis of Osteoarthritis: Implications for Treatment of Joint Injuries.," *Cartilage*, vol. 4, no. 4, pp. 286–294, Oct. 2013.

[4] T. D. Brown, R. C. Johnston, C. L. Saltzman, J. L. Marsh, and J. A. Buckwalter, "Posttraumatic osteoarthritis: a first estimate of incidence, prevalence, and burden of disease.," *J. Orthop. Trauma*, vol. 20, no. 10, pp. 739–44, Jan. .

[5] B. L. Wong, W. C. Bae, J. Chun, K. R. Gratz, M. Lotz, and R. L. Robert L. Sah, "Biomechanics of cartilage articulation: Effects of lubrication and degeneration on shear deformation," *Arthritis Rheum.*, vol. 58, no. 7, pp. 2065–2074, Jul. 2008.

[6] M. M. Temple-Wong, S. Ren, P. Quach, B. C. Hansen, A. C. Chen, A. Hasegawa, D. D. D'Lima, J. Koziol, K. Masuda, M. K. Lotz, and R. L. Sah, "Hyaluronan concentration and size distribution in human knee synovial fluid: variations with age and cartilage degeneration," *Arthritis Res. Ther.*, vol. 18, no. 1, p. 18, Dec. 2016.

[7] K. A. Elsaid, B. C. Fleming, H. L. Oksendahl, J. T. Machan, P. D. Fadale, M. J. Hulstyn, R. Shalvoy, and G. D. Jay, "Decreased lubricin concentrations and markers of

joint inflammation in the synovial fluid of patients with anterior cruciate ligament injury.," *Arthritis Rheum.*, vol. 58, no. 6, pp. 1707–15, Jun. 2008.

[8] M. K. Kosinska, T. E. Ludwig, G. Liebisch, R. Zhang, H.-C. Siebert, J. Wilhelm, U. Kaesser, R. B. Dettmeyer, H. Klein, B. Ishaque, M. Rickert, G. Schmitz, T. A. Schmidt, and J. Steinmeyer, "Articular Joint Lubricants during Osteoarthritis and Rheumatoid Arthritis Display Altered Levels and Molecular Species," *PLoS One*, vol. 10, no. 5, p. e0125192, May 2015.

[9] T. A. Schmidt, N. S. Gastelum, Q. T. Nguyen, B. L. Schumacher, and R. L. Sah, "Boundary lubrication of articular cartilage: role of synovial fluid constituents.," *Arthritis Rheum.*, vol. 56, no. 3, pp. 882–91, Mar. 2007.

[10] E. D. Bonnevie, D. Galesso, C. Secchieri, I. Cohen, and L. J. Bonassar, "Elastoviscous Transitions of Articular Cartilage Reveal a Mechanism of Synergy between Lubricin and Hyaluronic Acid.," *PLoS One*, vol. 10, no. 11, p. e0143415, Jan. 2015.

[11] G. D. Jay, J. R. Torres, D. K. Rhee, H. J. Helminen, M. M. Hytinnen, C.-J. Cha, K. Elsaid, K.-S. Kim, Y. Cui, and M. L. Warman, "Association between friction and wear in diarthrodial joints lacking lubricin.," *Arthritis Rheum.*, vol. 56, no. 11, pp. 3662–9, Nov. 2007.

[12] K. A. Waller, L. X. Zhang, K. A. Elsaid, B. C. Fleming, M. L. Warman, and G. D. Jay, "Role of lubricin and boundary lubrication in the prevention of chondrocyte apoptosis.," *Proc. Natl. Acad. Sci. U. S. A.*, vol. 110, no. 15, pp. 5852–7, Apr. 2013.

[13] K. D. Novakofski, L. C. Berg, I. Bronzini, E. D. Bonnevie, S. G. Poland, L. J. Bonassar, and L. A. Fortier, "Joint-dependent response to impact and implications for post-traumatic osteoarthritis.," *Osteoarthritis Cartilage*, vol. 23, no. 7, pp. 1130–7, Jul.

2015.

[14] T. M. Quinn, R. G. Allen, B. J. Schalet, P. Perumbuli, and E. B. Hunziker, “Matrix and cell injury due to sub-impact loading of adult bovine articular cartilage explants: effects of strain rate and peak stress.,” *J. Orthop. Res.*, vol. 19, no. 2, pp. 242–9, Mar. 2001.

[15] L. R. Bartell, L. A. Fortier, L. J. Bonassar, and I. Cohen, “Measuring microscale strain fields in articular cartilage during rapid impact reveals thresholds for chondrocyte death and a protective role for the superficial layer,” *J. Biomech.*, vol. 48, no. 12, pp. 3440–3446, Sep. 2015.

[16] C. A. M. Huser and M. E. Davies, “Calcium signaling leads to mitochondrial depolarization in impact-induced chondrocyte death in equine articular cartilage explants.,” *Arthritis Rheum.*, vol. 56, no. 7, pp. 2322–34, Jul. 2007.

[17] J. B. Fitzgerald, M. Jin, and A. J. Grodzinsky, “Shear and Compression Differentially Regulate Clusters of Functionally Related Temporal Transcription Patterns in Cartilage Tissue,” *J. Biol. Chem.*, vol. 281, no. 34, pp. 24095–24103, Aug. 2006.

[18] J. P. Gleghorn and L. J. Bonassar, “Lubrication mode analysis of articular cartilage using Stribeck surfaces.,” *J. Biomech.*, vol. 41, no. 9, pp. 1910–8, Jan. 2008.

[19] M. R. Buckley, A. J. Bergou, J. Fouchard, L. J. Bonassar, and I. Cohen, “High-resolution spatial mapping of shear properties in cartilage,” 2010.

[20] D. J. Griffin, J. Vicari, M. R. Buckley, J. L. Silverberg, I. Cohen, and L. J. Bonassar, “Effects of enzymatic treatments on the depth-dependent viscoelastic shear properties of articular cartilage,” *J. Orthop. Res.*, vol. 32, no. 12, pp. 1652–1657, Dec. 2014.

[21] G. A. Ateshian, “The role of interstitial fluid pressurization in articular cartilage lubrication.,” *J. Biomech.*, vol. 42, no. 9, pp. 1163–76, Jun. 2009.

[22] J. L. Silverberg, A. R. Barrett, M. Das, P. B. Petersen, L. J. Bonassar, and I. Cohen, “Structure-Function Relations and Rigidity Percolation in the Shear Properties of Articular Cartilage,” *Biophys. J.*, vol. 107, no. 7, pp. 1721–1730, 2014.

[23] M. T. Lin and M. F. Beal, “Mitochondrial dysfunction and oxidative stress in neurodegenerative diseases,” *Nature*, vol. 443, no. 7113, pp. 787–795, Oct. 2006.

[24] J. Levraut, H. Iwase, Z.-H. Shao, T. L. Vanden Hoek, and P. T. Schumacker, “Cell death during ischemia: relationship to mitochondrial depolarization and ROS generation.,” *Am. J. Physiol. Heart Circ. Physiol.*, vol. 284, no. 2, pp. H549–58, Feb. 2003.

[25] J. E. Goetz, M. C. Coleman, D. C. Fredericks, E. Petersen, J. A. Martin, T. O. McKinley, and Y. Tochigi, “Time-dependent loss of mitochondrial function precedes progressive histologic cartilage degeneration in a rabbit meniscal destabilization model,” *J. Orthop. Res.*, Jun. 2016.

[26] W. Goodwin, D. McCabe, E. Sauter, E. Reese, M. Walter, J. A. Buckwalter, and J. A. Martin, “Rotenone prevents impact-induced chondrocyte death,” *J. Orthop. Res.*, vol. 28, no. 8, p. n/a–n/a, 2010.

[27] M. L. Delco, “Acute mitochondrial dysfunction in cartilage following mechanical injury,” *Osteoarthr. Cartil.*, vol. 23, pp. A288–A289, Apr. 2015.

[28] M. C. Coleman, P. S. Ramakrishnan, M. J. Brouillette, and J. A. Martin, “Injurious Loading of Articular Cartilage Compromises Chondrocyte Respiratory Function,”

Arthritis Rheumatol., vol. 68, no. 3, pp. 662–671, Mar. 2016.

[29] A. C. Rego and C. R. Oliveira, "Mitochondrial Dysfunction and Reactive Oxygen Species in Excitotoxicity and Apoptosis: Implications for the Pathogenesis of Neurodegenerative Diseases," *Neurochem. Res.*, vol. 28, no. 10, pp. 1563–1574, 2003.

[30] C.-T. Chen, N. Burton-Wurster, C. Borden, K. Hueffer, S. E. Bloom, and G. Lust, "Chondrocyte necrosis and apoptosis in impact damaged articular cartilage," *J. Orthop. Res.*, vol. 19, no. 4, pp. 703–711, Jul. 2001.

[31] H. H. Szeto and P. W. Schiller, "Novel Therapies Targeting Inner Mitochondrial Membrane—From Discovery to Clinical Development," *Pharm. Res.*, vol. 28, no. 11, pp. 2669–2679, Nov. 2011.

[32] A. Eirin, B. Ebrahimi, X. Zhang, X.-Y. Zhu, J. R. Woollard, Q. He, S. C. Textor, A. Lerman, and L. O. Lerman, "Mitochondrial protection restores renal function in swine atherosclerotic renovascular disease.," *Cardiovasc. Res.*, vol. 103, no. 4, pp. 461–72, Sep. 2014.

[33] H. H. Szeto, "Mitochondria-Targeted Cytoprotective Peptides for Ischemia–Reperfusion Injury," *http://dx.doi.org/10.1089/ars.2007.1892*, 2008.

[34] M. L. Delco, E. D. Bonnevie, H. H. Szeto, L. J. Bonassar, and L. A. Fortier, "Mitoprotection as a strategy to prevent chondrocyte death and cartilage degeneration following mechanical injury," *Osteoarthr. Cartil.*, vol. 24, pp. S500–S501, Apr. 2016.

[35] D. D'Lima, J. Hermida, S. Hashimoto, C. Colwell, and M. Lotz, "Caspase inhibitors reduce severity of cartilage lesions in experimental osteoarthritis," *Arthritis Rheum.*, vol. 54, no. 6, pp. 1814–1821, Jun. 2006.

[36] S. R. Oungoulian, S. Chang, O. Bortz, K. E. Hehir, K. Zhu, C. E. Willis, C. T. Hung, and G. A. Ateshian, "Articular Cartilage Wear Characterization With a Particle Sizing and Counting Analyzer," *J. Biomech. Eng.*, vol. 135, no. 2, p. 024501, Feb. 2013.

[37] E. L. Radin and I. L. Paul, "Response of Joints to Impact Loading. I. In Vitro Wear," *Arthritis Rheum.*, vol. 14, no. 3, pp. 356–362, May 1971.

[38] H. Forster and J. Fisher, "The influence of continuous sliding and subsequent surface wear on the friction of articular cartilage," *Proc. Inst. Mech. Eng. Part H J. Eng. Med.*, vol. 213, no. 4, pp. 329–345, Apr. 1999.

[39] S. R. Oungoulian, K. M. Durney, B. K. Jones, C. S. Ahmad, C. T. Hung, and G. A. Ateshian, "Wear and damage of articular cartilage with friction against orthopedic implant materials," *J. Biomech.*, vol. 48, no. 10, pp. 1957–1964, 2015.

CHAPTER 7

Enhanced Boundary Lubrication Properties of Engineered Menisci by Lubricin Localization with Insulin-like Growth Factor I Treatment[6]

Abstract

In this study we analyzed the effects of IGF-I on the boundary lubricating ability of engineered meniscal tissue using a high density collagen gel seeded with meniscal fibrochondrocytes. Biochemical, histological, immunohistochemical, and tribological analyses were carried out to determine a construct's ability to functionally localize lubricin. Our study revealed that supplementation with IGF-I enhanced both the proliferation of cells within the construct as well as enhanced the anabolic activity of the seeded cells. Growth factor supplementation also facilitated the localization of ECM constituents (i.e. fibronectin and type II collagen) near the tissue surface that are important for the localization of lubricin, a boundary lubricant. Consequently, we found localized lubricin in the constructs supplemented with IGF-I. Tribologically, we demonstrated that lubricin serves as a boundary lubricant adsorbed to native meniscal surfaces. Lubricin removal from the native meniscus surface increased boundary friction coefficient by 40%. For the engineered constructs, the lubricin localization facilitated by growth factor supplementation also reduced friction coefficient by a similar margin, but similar results were not evident in control constructs. This study demonstrates that the use of growth factors in meniscal tissue engineering can enhance tribological properties by facilitating the localization of boundary lubricants at the

[6] This chapter is published: Bonnevie, Edward D., Jennifer L. Puetzer, and Lawrence J. Bonassar. "Enhanced boundary lubrication properties of engineered menisci by lubricin localization with insulin-like growth factor I treatment." Journal of biomechanics 47.9 (2014): 2183-2188.

surface of engineered tissue.

Introduction

The menisci play important mechanical roles within the knee. These wedge-shaped fibrocartilaginous tissues transmit load, dissipate energy, stabilize the joint, and promote effective lubrication [1]. After damage, the meniscus exhibits slow to no healing due to the avascular nature of the majority of the tissue [2], [3]. Consequently, injury can lead to either partial or full meniscectomy [1]. However, the removal of meniscus tissue is considered a major risk factor in developing osteoarthritis (OA) [4]. Removal of meniscus tissue affects several factors that lead to the onset of OA. The meniscal surfaces that interact with the femoral condyles and tibial plateau promote joint conformity, and by increasing the area of contact in the knee they lower the contact pressures [1].

It is suggested that menisci also promote boundary lubrication within the knee due to similarities in coefficients of friction with articular cartilage [5]–[8] and the presence of adsorbed lubricin [9]. As shown for articular cartilage, the presence of lubricin, a mucinous glycoprotein, reduces the measured friction coefficient of contacting surfaces in the boundary regime of lubrication [10], [11], where sliding speeds are slow, normal stresses are high, and friction coefficients are highest. The structure of lubricin is hypothesized to be essential in reducing boundary friction coefficients and mitigating the progression of surface damage [11], [12]. After attaching to the articular surface through the molecule's carboxy-terminus [13], the molecule's long hydrophilic mucin-like domain attracts water to the tissue surface which, in turn, serves to reduce boundary friction coefficients.

Although there have been recent advances in repairing focal meniscal injuries,

severe damage can still lead to meniscectomy. Because of the significantly altered lubrication environment after meniscectomy, treatments necessitate full replacement of meniscus tissue [14]. Allograft transplantation, the current practice, is limited by the availability of suitable allograft tissue, intrinsic anatomical variations, and risk of disease transmission [2], [3], [15].

Due to the drawbacks associated with allograft transplantation, recent efforts have turned towards tissue engineering total meniscal constructs to replace damaged meniscal tissue [16]–[23]. We have previously used image-guided fabrication techniques to create anatomically-correct tissue-engineered constructs [18], [19], [24]. These constructs may begin to restore joint conformity and promote more effective lubrication; however, fully effective lubrication may not be provided unless the surfaces of engineered tissue are boundary lubricated. Failure to provide boundary lubricated surfaces containing adsorbed lubricin within the knee can lead to tissue damage and deterioration in addition to apoptosis of superficial zone cells [12], [25], [26]. Consequently, in this study we aim to localize lubricin on engineered meniscal tissue.

Previous work has demonstrated the inability of meniscal constructs to effectively boundary lubricate initially, but culture of constructs *in vitro* and *in vivo* enhanced the frictional properties possibly by infiltration of extracellular matrix (ECM) constituents [7], [27]. We have recently shown that growth factor supplementation with insulin-like growth factor I (IGF-I) in alginate meniscal constructs induced the formation of a lubricin-rich surface layer [24]. We have also recently shown enhanced mechanical properties of meniscal constructs by use of high

density type I collagen gels which we have adopted in this study [28]. To effectively localize lubricin, ECM constituents with high binding affinities to lubricin must be localized at the construct surface, and type I collagen has not been shown to have a high affinity to lubricin [29]. Consequently, localization of other ECM components may be necessary to bind lubricin at the tissue surface. In this study we hypothesize that growth factor stimulus with IGF-I will facilitate the localization of candidate ECM components for lubricin binding (i.e. fibronectin and type II collagen) [29], and localized lubricin will enhance boundary lubrication.

Methods

Construct Fabrication

A total of 48 constructs (n=4 for biochemical content, histology/immunohistochemistry, and lubrication) were made in a similar fashion as previously described [28]. High density type I collagen gel was produced by isolating tendons from rat tails, solubilizing collagen in 0.1% acetic acid, and reconstituting at 30 mg/ml. Cells were obtained from the menisci of the stifle joint of 1-3 day old bovine calves and isolated overnight via collagenase digestion (0.3% collagenase, 100 U/mL penicillin, and 100 μg/mL streptomycin in Dulbecco's modified Eagle's medium (DMEM)). To create the cell seeded constructs, collagen was mixed with a basic working solution containing appropriate volumes of 1 N NaOH, 10x phosphate buffered saline (PBS), and 1x PBS to return the gel to physiologic pH and osmolarity [28], [30]. This solution was immediately mixed with a cell solution and the resulting mixture was injected between parallel glass plates spaced 1 mm apart and allowed to

gel for 30 minutes at 37˚C. The resulting collagen sheet gel was composed of 20 mg/ml collagen seeded at a density of 25 million cells/ml. Eight mm diameter biopsy punches were cut from the sheet and cultured. A control group was cultured in previously described media (Puetzer and Bonassar, 2013) (DMEM, 10% fetal bovine serum, 100 U/ml penicillin, 100 μg/ml streptomycin, 0.1 mM non-essential amino acids, 50 μg/ml ascorbate, and 0.4 mM L-proline). An IGF-I treatment group was cultured in the same media supplemented with 100 ng/ml recombinant human IGF-I (Life Technologies, Carlsbad CA) as previously described [24]. Constructs were cultured for 10 and 20 days with media collected and changed three times weekly. Construct contraction was analyzed during culture through photograph analysis with ImageJ (NIH, Bethesda MD).

Biochemical Analysis

After culture, constructs with and without IGF-I were analyzed for biochemical content. Constructs were weighed, lyophilized, and weighed again to obtain sample size. They were then digested overnight in a 1.25 mg/ml papain buffer at 60˚C. Constructs and collected media were analyzed biochemically for DNA content using Hoescht dye assay [31]. Constructs and media were also tested for GAG content using a modified DMMB assay [32].

Histology

Samples were fixed in 10% buffered formalin, embedded into paraffin blocks, and sectioned. Slide-mounted sections were cleared with xylene and dehydrated with steps of progressively stronger ethanol prior to staining. To detect the presence of a surface layer on the constructs sections were stained using Picrosirius red for 1 hour

and viewed under brightfield and polarized light for collagen localization and organization, respectively.

Immunohistochemistry

Immunohistochemistry was conducted in a similar manner to methods previously described [24]. Mounted sections of both constructs and native menisci were stained for localized lubricin, type-II collagen, fibronectin, and aggrecan. Slides were cleared and hydrated similarly to those for histology in xylene and ethanol. Antigen removal was facilitated by incubation in citric acid at 90˚C for 20 minutes (10 mM, pH 6.0). Slides were then washed twice for 5 minutes in TRIS buffered saline with 0.5% TWEEN-20 (pH 7.4), incubated for 30 minutes in 0.01% hyaluronidase, 30 minutes in 3% hydrogen peroxide, and 60 minutes in a blocking solution containing normal serum, bovine serum albumin, Triton X-100, and TWEEN-20. Between each step, slides were washed twice for 5 minutes in PBS. Primary antibodies were applied for 1 hour (Lubricin, Abcam product ab28484), (Collagen II, Abcam product ab34712), (Fibronectin, ICN/Cappel), (Aggrecan, Abcam product ab3778). A secondary antibody (Vector, Burlingame CA) was applied for 30 minutes followed by 30 minute incubation with an avidin-biotin complex (Vectastain ABC, Vector). Staining was then carried out with a peroxidase substrate (ImmPACT DAB, Vector) for up to 10 minutes.

Lubrication Analysis

Boundary-mode friction coefficients were measured using our custom-built tribometer (Figure 1B) as previously described [8], [10], [27]. Special care was taken to ensure boundary mode lubrication as described in the supplemental material.

Briefly, a sample was mounted to a biaxial load cell attached to a micrometer stage. The micrometer stage was used to apply a strain to the sample against a polished glass surface bathed in PBS with protease inhibitors (PBS+PI) (Figure 1C). A stationary contact area set-up (as opposed to a migratory contact area in which tissues are actively deformed, see supplemental section) was used in friction testing to eliminate effects of interstitial fluid pressurization on measured friction coefficient [33], [34]. After 50 minutes the tissue reached equilibrium under a prescribed strain, and the glass surface was reciprocated linearly at a prescribed speed (Figure S1). Preliminary data confirmed that testing between 30% and 50% strain with a sliding speed of 0.1 mm/s ensured boundary mode lubrication – no significant decreases of friction coefficient were evident from increasing speed to 0.3 mm/s. During sliding, arrays of both normal and shear forces were collected and the friction coefficient was determined as the average of the forward and reverse sliding direction friction coefficient values [35]. Friction coefficients were calculated as shear force divided by normal force.

To determine the efficacy of lubricin localization on boundary lubrication, each sample was tested three times for its boundary friction coefficient (Figure 7.1A) as previously described [27]. First, a sample was tested unaltered post culture after equilibrating in PBS+PI. Second, samples were tested after exposure to exogenous lubricin through 1 hour incubation in equine synovial fluid obtained from the carpus joints of skeletally mature horses and purified through centrifugation [8]. Third, each sample was tested after lubricin was removed from the surface. The lubricin removal was facilitated by incubation in 1.5M NaCl solution for 5 minutes as described

previously for both engineered and native tissues [27], [36]. After 1.5M NaCl incubation, the samples were returned to normal osmolarity by equilibrating for 1 hour in PBS+PI. The first friction measurement analyzed the natural lubricating ability, the second test determined whether exogenous lubricin could enhance lubrication, and the third test determined how a construct lubricated with an unlubricated surface (i.e. without lubricin).

Statistical Analysis

Tribology results were analyzed between groups using a two-way ANOVA with Student-Newman-Keuls post hoc. Within treatment groups a one-way ANOVA with repeated measures and one tailed Student-Newman-Keuls post hoc was used to test the hypotheses that exposure to lubricin reduces friction and removal of lubricin increases friction. For all tests, significance was recorded at $p < 0.05$. Values are presented as mean ± standard deviation.

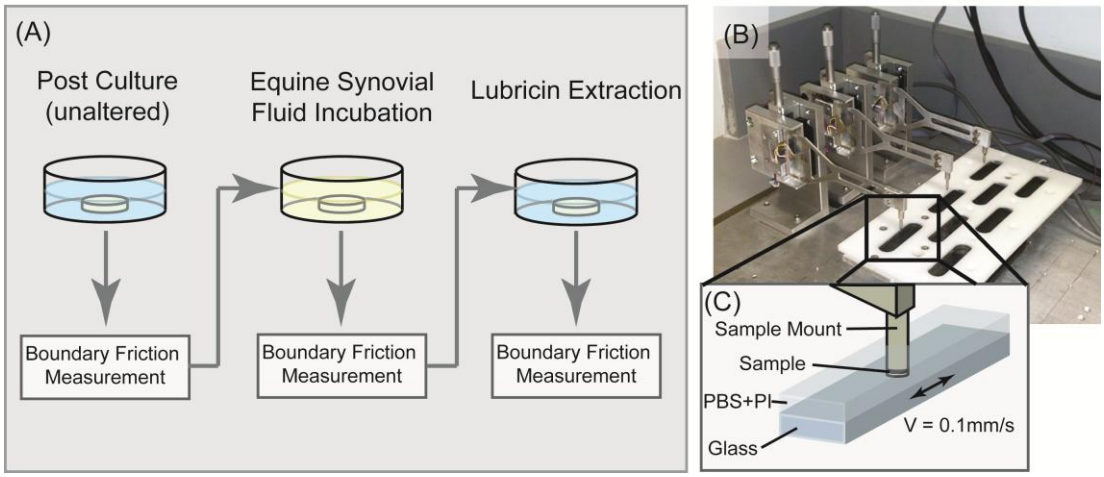

Figure 7.1 (A) Lubrication analysis method. Each sample was tested three times for its boundary friction coefficient: unaltered, after exposure to exogenous lubricin, and after lubricin was extracted from the surface. (B) Custom-built tribometer. (C) Samples are slid in PBS+PI against polished glass.

Results

Gross Appearance

The IGF-I treated constructs contracted more quickly than the control group; significant contraction was recorded after day 6 for the IGF-I group while controls exhibited significant contraction after day 8. The IGF-I group appeared to have fully contracted (75.3% ± 4.6% contraction by area, n=10) by day 10 while the control group did not appear to reach a contraction equilibrium by day 20 (83.7% ± 2.8% contraction by area, n=10).

Biochemical Content

Biochemical analysis for DNA content (Figure 7.2, left) revealed enhanced proliferation in the IGF-I treated constructs. At day 10, IGF-I constructs contained 55% more DNA content per construct ($p < 0.05$, $n = 4$). After 20 days of culture, IGF-I constructs contained 90% more DNA content than the 10 day IGF-I group ($p<0.05$), and 3-fold higher DNA content than control constructs ($p<0.05$). The 20 day control constructs contained slightly less DNA content than the 10 day control constructs ($p<0.05$). Analysis of the media showed significant amounts of DNA accumulated in the media by both groups over 20 days (14% more in IGF-I group).

Biochemical analysis for GAG content (Figure 7.2, right) demonstrated increased anabolic activity in the IGF-I treated constructs. At day 10, control constructs contained similar GAG content compared to IGF-I samples ($p>0.05$). By 20 days, control and IGF-I constructs contained more GAG content than the respective 10 day data, but IGF-I constructs now contained 2.5 times more GAG content than

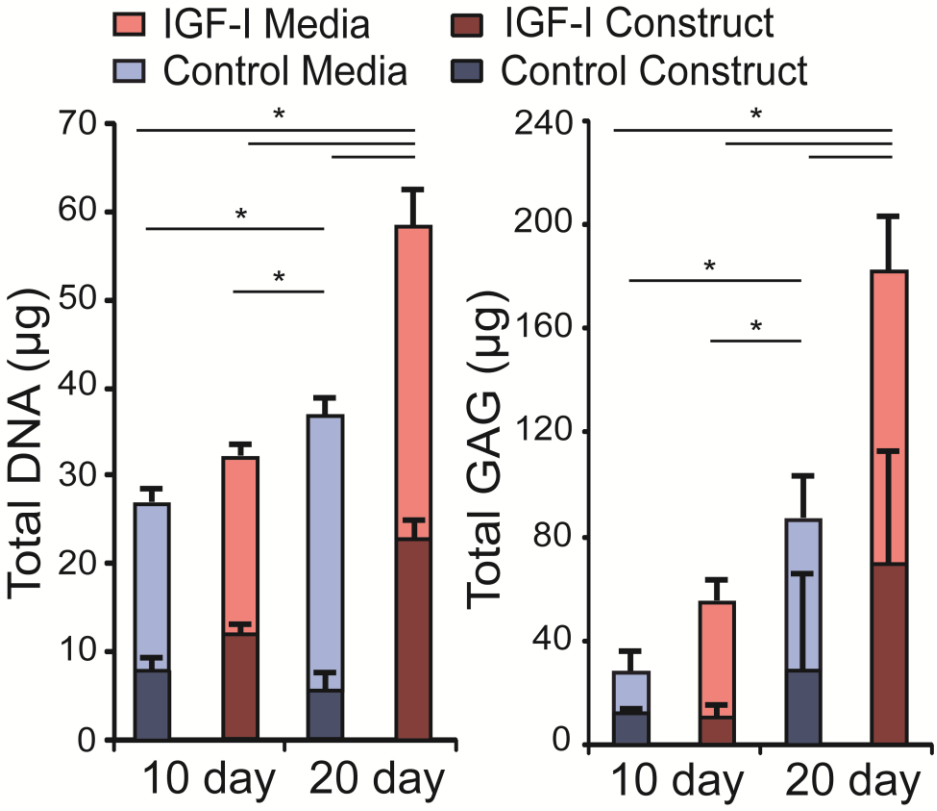

Figure 7.2 Total DNA and GAG content of both constructs and collected media for 10 and 20 day culture. Values are presented as mean ± standard deviation. (* denotes significance, $p<0.05$) (n=4)

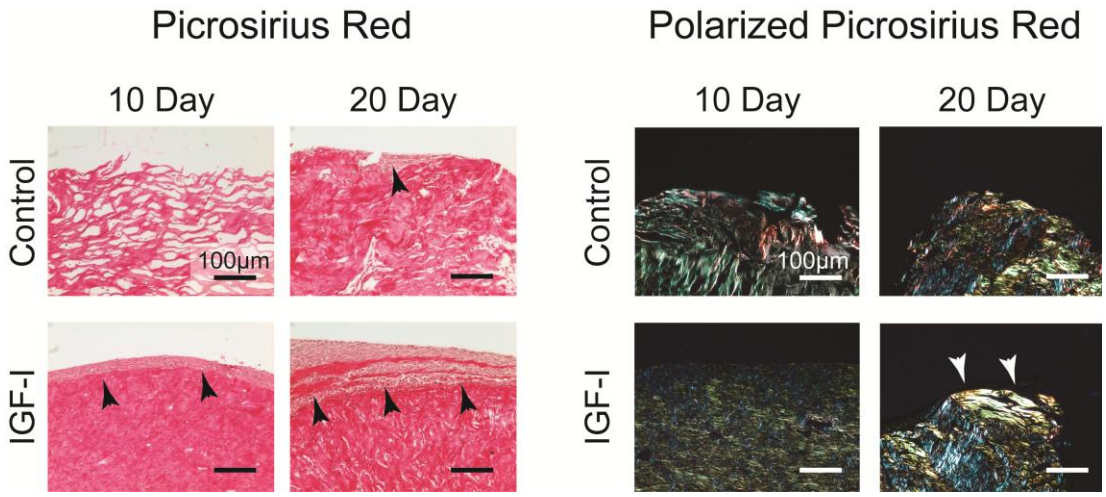

Figure 7.3 *Left* Picrosirius red staining of the construct surfaces demonstrating the formation of surface layers in the IGF-I treated constructs, viewed under brightfield at 200x. *Right* Picrosirius red staining of construct surfaces viewed with polarized light to show collagen organization. (bar = 100μm)

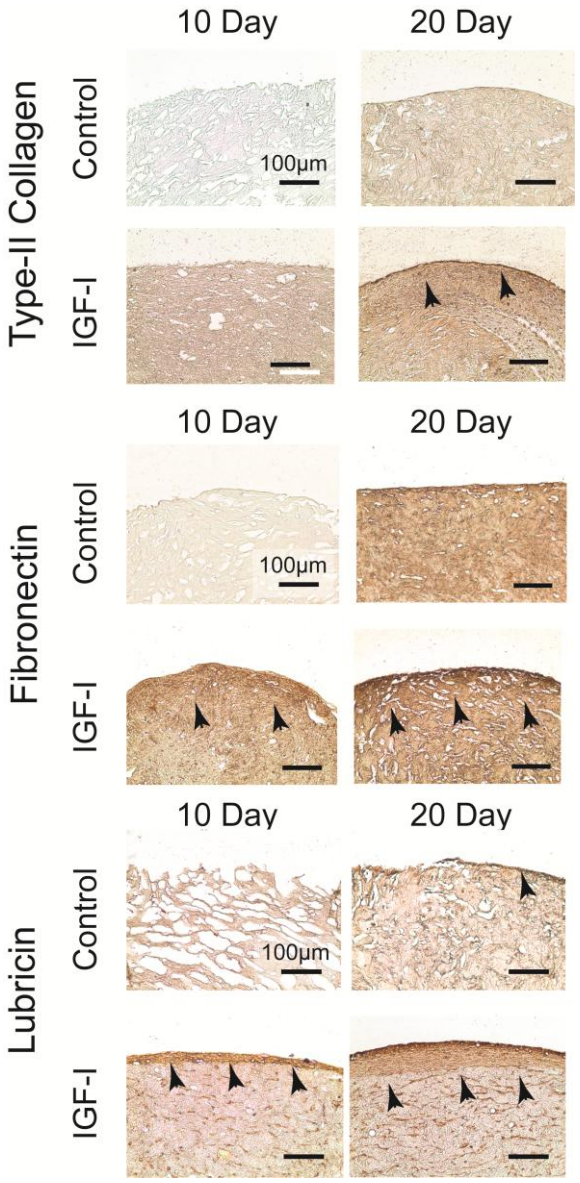

Figure 7.4 Immunohistochemistry staining of constructs. *Top* Type-II collagen localization within the constructs. *Middle* Fibronectin localizes near the surface of constructs most notably at 20 days with IGF-I treatment. *Bottom* Distinct lubricin localization in the IGF-I treated constructs. (bar = 100μm)

control constructs. Analysis of the media showed 2-fold higher GAG content accumulated in the media by IGF-I constructs over control constructs over 20 days.

Histology and Immunohistochemistry

IGF-I treated samples had well-defined surface zones containing localized fibronectin, type II collagen, and lubricin. Picrosirius red staining for collagen (Figure 7.3) revealed the formation of a distinct surface layer present in the IGF-I constructs at both 10 and 20 days. After 20 days this surface layer was more apparent and thicker. In the control samples, there was no evidence of a surface layer formed at 10 days, but by 20 days the initial development of a surface zone became apparent. Viewed under polarized light, the Picrosirius red staining also revealed substantial fiber formation near the surface in the IGF-I treated samples at 20 days (Figure 7.3, right).

IHC analysis of the tissue surface for lubricin-binding candidates revealed increased localization of type II collagen and fibronectin with IGF-I treatment and culture duration (Figure 7.4). After 10 days of culture the IGF-I treated constructs localized fibronectin near the surface and demonstrated increased collagen II presence throughout the tissue. After 20 days of culture, both groups demonstrated more pronounced staining for lubricin binding candidates. The IGF-I treated tissue had a distinct layer of type II collagen at the surface as well as a higher presence of fibronectin, while the control tissue had a layer of fibronectin, with little type II collagen.

A significant presence of adsorbed lubricin after 10 and 20 day culture times was revealed in the IGF-I treated samples by IHC for lubricin localization (Figure 7.4). No localized lubricin was detected in the control samples after 10 days of culture,

but after 20 days of culture thin, discontinuous areas along the surface of the constructs localized lubricin.

To evaluate the effect of lubricin extraction on engineered and native tissue we conducted subsequent IHC analysis (Figure 7.5). Distinct surface layers of localized lubricin present in both IGF-I treated gels and native meniscal tissues were no longer evident in samples that had been incubated in the hypertonic saline. To test the effects of lubricin removal on the bulk of the tissues, aggrecan IHC was conducted, and the staining revealed no loss of aggrecan in the bulk or at the tissue surface.

Lubrication Analysis

Both IGF-I treatment and increased culture duration enhanced lubrication properties (Figure 7.6). For native meniscus, exposure to synovial fluid lowered the friction coefficient by ~15% ($p<0.05$). After lubricin was removed from the native meniscus surface, the boundary friction coefficient was increased by 40% ($p<0.05$, $n=4$). At 10 days, both the control and IGF-I constructs' friction coefficients were significantly higher than those of native menisci ($p<0.05$). In the control group no significant changes were evident between surface treatments, but in the IGF-I group, the boundary friction coefficient trended higher (~50%) after lubricin was removed from the surface ($p=0.06$). After 20 days of culture, both the control and IGF-I groups had lower boundary friction coefficients compared to 10 day samples ($p<0.05$). After 20 days the IGF-I group had similar friction coefficients to native tissue, but the control group was still significantly higher ($p<0.05$). In the 20 day IGF-I group, the boundary friction coefficient was higher (~40%) after lubricin was removed from the surface ($p<0.05$).

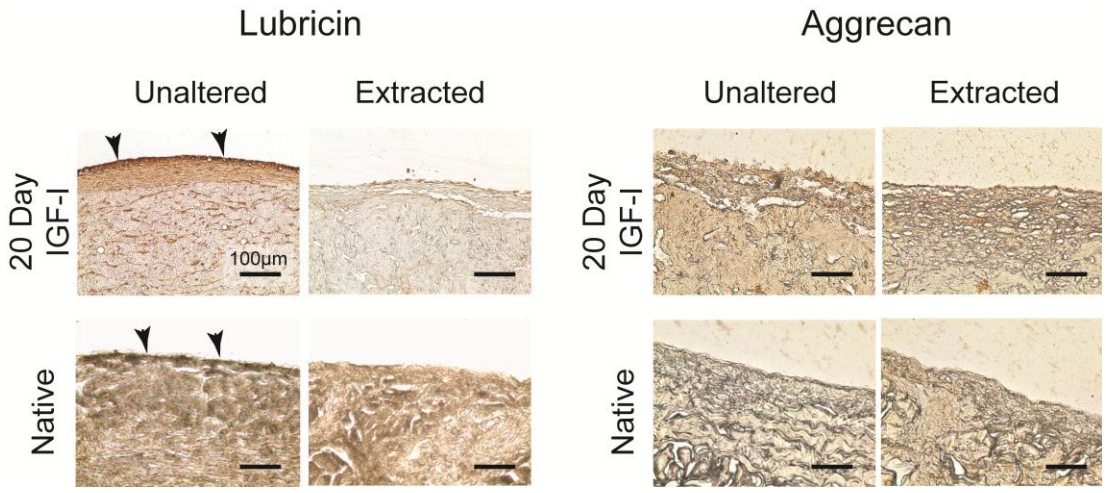

Figure 7.5 IHC staining before and after lubricin extraction protocol. *Left* Lubricin is removed from native and engineered tissue. *Right* Extraction has little effect on aggrecan localization. (bar = 100μm)

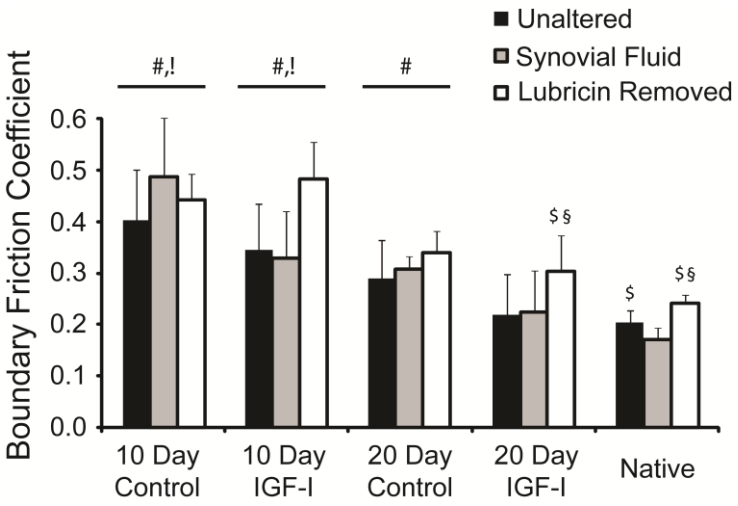

Figure 7.6 Boundary friction coefficients of constructs for different surface conditions: unaltered, incubated in synovial fluid, and lubricin removed from surface. Values are presented as mean ± standard deviation. (#, group is different from native; !, group is higher than respective 20 day; $, higher than synovial fluid; §, higher than unaltered; $p<0.05$ for all) (n=4)

Discussion

IGF-I supplementation during culture of meniscal constructs enhanced lubrication properties. 20 days of culture with 100 ng/ml IGF-I provided constructs with similar friction coefficients to native menisci and lower friction coefficients compared to the control group at 20 days. We also demonstrated that the growth factor supplemented constructs and native menisci were boundary lubricated by lubricin, a phenomenon that has not been explicitly shown for native meniscus previously. For IGF-I treated and native tissue, the removal of lubricin from the tissue surface increased the boundary friction coefficient by 40% to 50%. Culture duration also enhanced the frictional properties. Both the IGF-I and control constructs had overall lower friction coefficients at 20 days compared to the 10 day constructs.

Our results indicate that enhancing the localization of lubricin on the construct surface may be more important than enhancing lubricin synthesis. The groups with significantly elevated friction coefficients after lubricin extraction all had considerable lubricin localized at the tissue surface in an unaltered state, and exposure to exogenous lubricin did not significantly lower the friction coefficients. For the control constructs at both 10 and 20 days, exposure to synovial fluid did not alter the friction coefficients of the constructs, and the lubricin extraction procedure did not alter the friction coefficients either. These data reveal an inability of the constructs to effectively bind lubricin, as neither endogenous nor exogenous (in synovial fluid) lubricin altered friction coefficients in the control group.

In this study, growth factor treatment facilitated the localization of ECM constituents that are binding candidates for lubricin localization. Other studies have

shown increased type I and II collagen content after culture with IGF-I treatment in meniscal cell-seeded constructs [37], [38], but the role of IGF-I on fibronectin and lubricin synthesis in meniscal cells is not currently known. However, IGF-I has been shown to upregulate lubricin synthesis in articular chondrocytes [39], but have no effect on lubricin in articular cartilage explants [40]. Although the increased localization of lubricin in our study is likely attributed to the deposition of ECM components to which lubricin binds, lubricin expression may be altered by the IGF-I treatment.

Lubricin affinity to different extracellular matrix constituents is a topic of debate, but the data here confirm previous findings that type I collagen is comparatively a weaker binding candidate [29]. Preliminary reports of lubricin affinity to several ECM components including type I collagen, type II collagen, fibronectin, and hyaluronic acid found fibronectin to have the highest lubricin affinity. Hyaluronic acid and type II collagen had an intermediate affinity, and type I collagen had the lowest affinity [29]. Consequently, engineering orthopaedic tissues with a high density type I collagen gel, or any scaffold with a low affinity to lubricin, may require external stimulus to produce ECM components that are effective at localizing lubricin near the tissue surface. In this case we utilized chemical stimulus in the form of growth factor supplementation, but research in articular cartilage tissue engineering has been able to achieve similar results using mechanical stimulus [41], [42]. The results from our study revealed localization of fibronectin and type-II collagen near the construct surfaces with IGF-I treatment. From the 20 day culture, it may be unclear which binding candidate is responsible for lubricin localization - both candidates were

localized near the surface. However, the 10 day culture may indicate that fibronectin is more important for localization of lubricin near a construct surface. After 10 days of IGF-I treatment, we detected localized fibronectin and lubricin near the tissue surface but no distinct localization of type II collagen. These data may indicate the importance of fibronectin for lubricin localization to tissue surfaces.

In addition to enhancing boundary lubrication by localization of lubricin, structural changes within the tissues may enhance lubrication as well. Both control and IGF-I treated constructs demonstrated overall lower boundary friction coefficients at 20 days compared to the 10 day culture. By 20 days, both control and IGF-I supplemented samples had compacted more, contained more proteoglycan content, and showed more collagen fiber formation. It is likely that tissue maturation is essential to lowered boundary friction coefficients in addition to localizing boundary lubricants.

In this study, we have shown that growth factor treatment in meniscal tissue engineering may be crucial to generating functional tissue. We have demonstrated enhanced biochemical properties and the localization of proteins that are pivotal to boundary lubrication. By facilitating boundary mode lubrication, the efficacy of tissue replacement may be significantly enhanced. By reducing tissue wear and deterioration, tissue engineered menisci may prove an effective solution to replace damaged meniscal tissue.

REFERENCES

[1] S. Kawamura, K. Lotito, and S. A. Rodeo, “Biomechanics and healing response of the meniscus,” *Oper. Tech. Sports Med.*, vol. 11, no. 2, pp. 68–76, Apr. 2003.

[2] G. Peters and C. J. Wirth, “The current state of meniscal allograft transplantation and replacement,” *Knee*, vol. 10, no. 1, pp. 19–31, Mar. 2003.

[3] M. A. Sweigart and K. A. Athanasiou, “Toward tissue engineering of the knee meniscus.,” *Tissue Eng.*, vol. 7, no. 2, pp. 111–29, Apr. 2001.

[4] H. Roos, M. Laurén, T. Adalberth, E. M. Roos, K. Jonsson, and L. S. Lohmander, “Knee osteoarthritis after meniscectomy: prevalence of radiographic changes after twenty-one years, compared with matched controls.,” *Arthritis Rheum.*, vol. 41, no. 4, pp. 687–93, Apr. 1998.

[5] V. J. Baro, E. D. Bonnevie, X. Lai, C. Price, D. L. Burris, and L. Wang, “Functional characterization of normal and degraded bovine meniscus: rate-dependent indentation and friction studies.,” *Bone*, vol. 51, no. 2, pp. 232–40, Aug. 2012.

[6] E. D. Bonnevie, V. Baro, L. Wang, and D. L. Burris, “In-situ studies of cartilage microtribology: roles of speed and contact area.,” *Tribol. Lett.*, vol. 41, no. 1, pp. 83–95, Jan. 2011.

[7] N. K. Galley, J. P. Gleghorn, S. Rodeo, R. F. Warren, S. A. Maher, and L. J. Bonassar, “Frictional properties of the meniscus improve after scaffold-augmented repair of partial meniscectomy: a pilot study.,” *Clin. Orthop. Relat.*

Res., vol. 469, no. 10, pp. 2817–23, Oct. 2011.

[8] J. P. Gleghorn and L. J. Bonassar, "Lubrication mode analysis of articular cartilage using Stribeck surfaces.," *J. Biomech.*, vol. 41, no. 9, pp. 1910–8, Jan. 2008.

[9] B. L. Schumacher, T. A. Schmidt, M. S. Voegtline, A. C. Chen, and R. L. Sah, "Proteoglycan 4 (PRG4) synthesis and immunolocalization in bovine meniscus.," *J. Orthop. Res.*, vol. 23, no. 3, pp. 562–8, May 2005.

[10] J. P. Gleghorn, A. R. C. Jones, C. R. Flannery, and L. J. Bonassar, "Boundary mode lubrication of articular cartilage by recombinant human lubricin.," *J. Orthop. Res.*, vol. 27, no. 6, pp. 771–7, Jun. 2009.

[11] G. D. Jay, D. A. Harris, and C.-J. Cha, "Boundary lubrication by lubricin is mediated by O-linked β(1-3)Gal-GalNAc oligosaccharides," *Glycoconj. J.*, vol. 18, no. 10, pp. 807–815, Oct. 2001.

[12] K. A. Waller, L. X. Zhang, K. A. Elsaid, B. C. Fleming, M. L. Warman, and G. D. Jay, "Role of lubricin and boundary lubrication in the prevention of chondrocyte apoptosis.," *Proc. Natl. Acad. Sci. U. S. A.*, vol. 110, no. 15, pp. 5852–7, Apr. 2013.

[13] C. R. Flannery, C. E. Hughes, B. L. Schumacher, D. Tudor, M. B. Aydelotte, K. E. Kuettner, and B. Caterson, "Articular cartilage superficial zone protein (SZP) is homologous to megakaryocyte stimulating factor precursor and Is a multifunctional proteoglycan with potential growth-promoting, cytoprotective, and lubricating properties in cartilage metabolism.," *Biochem. Biophys. Res.*

Commun., vol. 254, no. 3, pp. 535–41, Jan. 1999.

[14] B. J. Cole, T. R. Carter, and S. A. Rodeo, "Allograft Meniscal Transplantation Background, Techniques, and Results," *J. Bone Jt. Surg.*, vol. 84, no. 7, pp. 1236–1250, Jul. 2002.

[15] P. Buma, N. N. Ramrattan, T. G. van Tienen, and R. P. H. Veth, "Tissue engineering of the meniscus," *Biomaterials*, vol. 25, no. 9, pp. 1523–1532, Apr. 2004.

[16] A. C. Aufderheide and K. A. Athanasiou, "Assessment of a bovine co-culture, scaffold-free method for growing meniscus-shaped constructs.," *Tissue Eng.*, vol. 13, no. 9, pp. 2195–205, Sep. 2007.

[17] E. Balint, C. J. Gatt, and M. G. Dunn, "Design and mechanical evaluation of a novel fiber-reinforced scaffold for meniscus replacement.," *J. Biomed. Mater. Res. A*, vol. 100, no. 1, pp. 195–202, Jan. 2012.

[18] J. J. Ballyns, J. P. Gleghorn, V. Niebrzydowski, J. J. Rawlinson, H. G. Potter, S. A. Maher, T. M. Wright, and L. J. Bonassar, "Image-guided tissue engineering of anatomically shaped implants via MRI and micro-CT using injection molding.," *Tissue Eng. Part A*, vol. 14, no. 7, pp. 1195–202, Jul. 2008.

[19] J. J. Ballyns and L. J. Bonassar, "Dynamic compressive loading of image-guided tissue engineered meniscal constructs.," *J. Biomech.*, vol. 44, no. 3, pp. 509–16, Feb. 2011.

[20] D. J. Huey and K. A. Athanasiou, "Tension-compression loading with chemical stimulation results in additive increases to functional properties of anatomic

meniscal constructs.," *PLoS One*, vol. 6, no. 11, p. e27857, Jan. 2011.

[21] D. J. Huey and K. A. Athanasiou, "Maturational growth of self-assembled, functional menisci as a result of TGF-β1 and enzymatic chondroitinase-ABC stimulation," *Biomaterials*, vol. 32, no. 8, pp. 2052–2058, Mar. 2011.

[22] S.-W. Kang, S.-M. Son, J.-S. Lee, E.-S. Lee, K.-Y. Lee, S.-G. Park, J.-H. Park, and B.-S. Kim, "Regeneration of whole meniscus using meniscal cells and polymer scaffolds in a rabbit total meniscectomy model.," *J. Biomed. Mater. Res. A*, vol. 78, no. 3, pp. 659–71, Sep. 2006.

[23] B. B. Mandal, S.-H. Park, E. S. Gil, and D. L. Kaplan, "Multilayered silk scaffolds for meniscus tissue engineering.," *Biomaterials*, vol. 32, no. 2, pp. 639–51, Jan. 2011.

[24] J. L. Puetzer, B. N. Brown, J. J. Ballyns, and L. J. Bonassar, "The effect of igf-I on anatomically shaped tissue-engineered menisci.," *Tissue Eng. Part A*, vol. 19, no. 11–12, pp. 1443–50, Jun. 2013.

[25] J. P. Gleghorn, S. B. Doty, R. F. Warren, T. M. Wright, S. A. Maher, and L. J. Bonassar, "Analysis of frictional behavior and changes in morphology resulting from cartilage articulation with porous polyurethane foams.," *J. Orthop. Res.*, vol. 28, no. 10, pp. 1292–9, Oct. 2010.

[26] G. D. Jay, J. R. Torres, D. K. Rhee, H. J. Helminen, M. M. Hytinnen, C.-J. Cha, K. Elsaid, K.-S. Kim, Y. Cui, and M. L. Warman, "Association between friction and wear in diarthrodial joints lacking lubricin.," *Arthritis Rheum.*, vol. 56, no. 11, pp. 3662–9, Nov. 2007.

[27] J. P. Gleghorn, A. R. C. Jones, C. R. Flannery, and L. J. Bonassar, “Boundary mode frictional properties of engineered cartilaginous tissues.,” *Eur. Cell. Mater.*, vol. 14, pp. 20–8; discussion 28–9, Jan. 2007.

[28] J. L. Puetzer and L. J. Bonassar, “High Density Type I Collagen Gels for Tissue Engineering of Whole Menisci.,” *Acta Biomater.*, vol. null, no. null, May 2013.

[29] G. Elsaid, KA, Chichester, CO, Jay, “Lubricin Purified from Bovine Synovial Fluid and Articular Cartilage Exhibit Similar Binding Affinities to Cartilage Matrix Proteins,” in *Transactions of the Orthopaedic Research Society*, 2001.

[30] V. L. Cross, Y. Zheng, N. Won Choi, S. S. Verbridge, B. A. Sutermaster, L. J. Bonassar, C. Fischbach, and A. D. Stroock, “Dense type I collagen matrices that support cellular remodeling and microfabrication for studies of tumor angiogenesis and vasculogenesis in vitro.,” *Biomaterials*, vol. 31, no. 33, pp. 8596–607, Nov. 2010.

[31] Y. J. Kim, R. L. Sah, J. Y. Doong, and A. J. Grodzinsky, “Fluorometric assay of DNA in cartilage explants using Hoechst 33258.,” *Anal. Biochem.*, vol. 174, no. 1, pp. 168–76, Oct. 1988.

[32] B. O. Enobakhare, D. L. Bader, and D. A. Lee, “Quantification of sulfated glycosaminoglycans in chondrocyte/alginate cultures, by use of 1,9-dimethylmethylene blue.,” *Anal. Biochem.*, vol. 243, no. 1, pp. 189–91, Dec. 1996.

[33] M. Caligaris and G. A. Ateshian, “Effects of sustained interstitial fluid pressurization under migrating contact area, and boundary lubrication by

synovial fluid, on cartilage friction.," *Osteoarthritis Cartilage*, vol. 16, no. 10, pp. 1220–7, Oct. 2008.

[34] R. Krishnan, M. Kopacz, and G. A. Ateshian, "Experimental verification of the role of interstitial fluid pressurization in cartilage lubrication.," *J. Orthop. Res.*, vol. 22, no. 3, pp. 565–70, May 2004.

[35] D. L. Burris and W. G. Sawyer, "Addressing Practical Challenges of Low Friction Coefficient Measurements," *Tribol. Lett.*, vol. 35, no. 1, pp. 17–23, Apr. 2009.

[36] A. R. C. Jones, J. P. Gleghorn, C. E. Hughes, L. J. Fitz, R. Zollner, S. D. Wainwright, B. Caterson, E. A. Morris, L. J. Bonassar, and C. R. Flannery, "Binding and localization of recombinant lubricin to articular cartilage surfaces.," *J. Orthop. Res.*, vol. 25, no. 3, pp. 283–92, Mar. 2007.

[37] C. A. Pangborn and K. A. Athanasiou, "Growth factors and fibrochondrocytes in scaffolds.," *J. Orthop. Res.*, vol. 23, no. 5, pp. 1184–90, Sep. 2005.

[38] K. Stewart, M. Pabbruwe, S. Dickinson, T. Sims, A. P. Hollander, and J. B. Chaudhuri, "The effect of growth factor treatment on meniscal chondrocyte proliferation and differentiation on polyglycolic acid scaffolds.," *Tissue Eng.*, vol. 13, no. 2, pp. 271–80, Feb. 2007.

[39] A. Khalafi, T. M. Schmid, C. Neu, and A. H. Reddi, "Increased accumulation of superficial zone protein (SZP) in articular cartilage in response to bone morphogenetic protein-7 and growth factors.," *J. Orthop. Res.*, vol. 25, no. 3, pp. 293–303, Mar. 2007.

[40] T. A. Schmidt, N. S. Gastelum, E. H. Han, G. E. Nugent-Derfus, B. L. Schumacher, and R. L. Sah, “Differential regulation of proteoglycan 4 metabolism in cartilage by IL-1alpha, IGF-I, and TGF-beta1.,” *Osteoarthritis Cartilage*, vol. 16, no. 1, pp. 90–7, Jan. 2008.

[41] S. Grad, M. Loparic, R. Peter, M. Stolz, U. Aebi, and M. Alini, “Sliding motion modulates stiffness and friction coefficient at the surface of tissue engineered cartilage.,” *Osteoarthritis Cartilage*, vol. 20, no. 4, pp. 288–95, Apr. 2012.

[42] S. Grad, C. R. Lee, K. Gorna, S. Gogolewski, M. A. Wimmer, and M. Alini, “Surface motion upregulates superficial zone protein and hyaluronan production in chondrocyte-seeded three-dimensional scaffolds.,” *Tissue Eng.*, vol. 11, no. 1–2, pp. 249–56, Jan. 2005.

CHAPTER 8

Mesenchymal Stem Cells Enhance Lubrication of Engineered Meniscus Through Lubricin Localization in Collagen Gels[7]

Abstract

This study evaluated the role of cell source in the boundary lubrication of engineered meniscus tissue. To accomplish this, both primary meniscal fibrochondrocytes (FCC) and bone marrow-derived mesenchymal stem cells (MSC) were obtained from neonatal bovine, seeded in high density collagen gels (20 mg/mL collagen with 25 x 10^6 total cells/mL) at various MSC:FCC ratios, and cultured for two weeks. After culture, the boundary friction coefficient, mechanical properties, surface roughness, and lubricin localization were all evaluated for engineered constructs. A strong correlation between MSC content and boundary friction coefficient was found ($R^2 = 0.948$). Aggregate modulus, permeability, and surface roughness revealed insignificant trends with MSC content; however, lubricin localization was highly correlated with increasing MSC content ($R^2 = 0.902$). Similarly, boundary friction coefficient had no significant trends with modulus, permeability, or roughness, but lubricin localization was significantly correlated with the boundary friction coefficient ($R^2 = 0.800$). Collectively, these data revealed a structure-function relationship in meniscus tissue engineering that is dictated by cell source. Specifically, the connection between MSC content, lubricin localization, and boundary friction coefficient reveal a method through which tuning the lubricating properties of engineered tissue is possible.

[7] This chapter to be published with co-authors: E.D. Bonnevie, M.C. McCorry, L.J. Bonassar

Introduction

The meniscus is an essential tissue within the knee joint, important for shock absorption, joint conformity, and lubrication [1]. Recently, meniscal surgeries numbered close 1 million per year in the United States [2] and this number is rising [3]. The common surgical practice to treat meniscal tears is either partial meniscectomy or full meniscectomy followed by allograft transplantation [4]. For allograft transplantation, the high prevalence of meniscal injuries results in a shortage of suitable allograft tissue, and even in cases where transplant tissue is available there is still the possibility of infection or host rejection. For these reasons, tissue engineering meniscus replacements has emerged as a promising solution.

The past decade has seen important advancements in meniscus tissue engineering, but there are still areas where engineered menisci perform inferior to native tissue. The use of aligned, fibrous scaffolds has emerged as a tool to recapitulate the load bearing properties of native meniscus in terms of both elastic moduli and degree of anisotropy (i.e., stiffer in the circumferential direction than the radial direction) [5]–[7]. Further, the emergence of 3D fabrication methods provides a tool to anatomically mimic healthy menisci to begin to restore joint conformity [8], [9]. While these advancements have brought meniscus tissue engineering closer to being clinically relevant, a comparatively under studied area has been lubrication.

Lubrication in meniscus tissue engineering is an important factor not only to ensure an engineered implant will be preserved *in vivo*, but also to ensure the contacting adjacent cartilage is left relatively unperturbed [10]. Native meniscus naturally provides low friction similar to that of native cartilage [11], [12], which is

dictated by both interstitial fluid pressurization [13] and boundary lubrication [14], [15]. The contribution of interstitial fluid pressurization is dependent on physical factors such as porosity, elastic modulus, permeability and tension-compression anisotropy [13]. The contribution of boundary lubrication is dictated by factors such as surface chemistry, roughness [16], and the adsorption of lubricating molecules, such as lubricin [14], [17]–[19]. In this study, we focus specifically on boundary lubrication, which is an important factor in cartilage homeostasis as increased boundary friction can result in cartilage degeneration [18] and chondrocyte apoptosis [20]. For meniscus tissue engineering, friction is an important factor as the boundary friction coefficients of possible scaffold materials are often over twice as high as native meniscus (polyurethane: μ~0.7 [10], alginate: μ~0.5 [19], collagen: μ~0.4 [15], native meniscus: μ~0.2 [15]).

In musculoskeletal tissue engineering in general, tuning the lubrication of implants has been studied based on a variety of factors. For cartilage tissue engineering, physical stimulation in the form of shear deformations attenuates lubricin production and localization, but this has not been studied for meniscus tissue engineering [21], [22]. Further, we have recently shown that growth factor stimulation can promote the localization of lubricin at the construct surface and consequently reduce boundary friction in meniscus tissue engineering [15]. Finally, for cartilage tissue engineering, cell source plays a role in lubricin content as selectively seeding superficial chondrocytes enhances lubricin content [23], but cell source has not been studied for lubrication in meniscus tissue engineering.

Within meniscus tissue engineering, primary meniscal fibrochondrocytes

(FCCs) [24], [25], mesenchymal stem cells (MSCs) [19], or co-culture of populations of the two [26]–[28] have been used to seed constructs. Use of FCCs may be limited due to either availability or expansion potential, and use of stem cells may be limited due to inclination towards hypertrophy after differentiation [27]. Consequently, co-culture has emerged as a method to balance these limitations [27], [28]. In this study we evaluate the role of cell source in meniscus tissue engineering regarding boundary lubrication and determine which physical and biochemical factors are most predictive of effective boundary lubrication.

Methods

Cell Isolation

Cell isolation was based on previously reported methods using tissue from neonatal bovine [28], [29]. Briefly, MSCs were extracted by incubating cubes from the trabecular bone of the femoral head in media supplemented with 300 U/mL heparin. This solution was centrifuged at 300 g followed by washing and plating of the pellet. After 48 hours of incubation, the unattached cell population was removed. Trilineage differentiation assays were performed to confirm multipotency of the remaining cell population for chondrogenic, ostegenic, and adipogenic differentiation as previously described and presented [28]. MSCs were expanded in 2D in low glucose Dulbecco's modified Eagle's medium (DMEM) supplemented with 10% fetal bovine serum (FBS), 100 U/mL penicillin, 100 U/mL streptomycin, 2mM L-glutamine, and 1 ng/mL basic fibroblast growth factor. MSCs were seeded at passage 4. FCCs were isolated from medial and lateral menisci overnight in 0.3% collagenase (Worthington Biochemical Corporation, Lakewood, NJ) in DMEM with 100 μg/mL penicillin and

100 μg/mL streptomycin. Following previously reported purification methods [28], cell-media mixtures were created at MSC:FCC ratios of 0:100, 25:75, 50:50, 75:25, and 100:0.

Construct Generation

As previously described, type I collagen gels were used as a construct material in this study [15], [25], [28]. Collagen type I was extracted from Sprague-Dawley rat tails (Pel-Freez Biologicals, Rogers, AZ) and reconstituted in 0.1% acetic acid at 30 mg/mL as previously described [15], [25], [28]. Briefly, 30 mg/mL collagen solution was mixed with a working solution of 1N NaOH, 10x phosphate-buffered saline (PBS), and 1x PBS to return the collagen solution to a neutral 7.0 pH and 300mOsm to initiate gelation. Cell-media suspensions were homogeneously mixed with the collagen solutions to form a collagen-cell-media solution at 20 mg/mL collagen seeded at a total density of 25 x 10^6 cells/mL. This solution was gelled between two glass plates to create 2 mm thick sheets, and then allowed to gel for 30 minutes at 37˚C. From each 2 mm thick gel, 8mm diameter samples were obtained using biopsy punches. Samples were cultured at 37°C and 5% CO_2 in media containing DMEM, 10% FBS, 100 μg/mL penicillin, 100 μg/mL streptomycin, 0.1 mM non-essential amino acids, 50 μg/mL ascorbate, and 0.4 mM L-proline. Culture media was refreshed every 3-4 days.

Boundary Friction Analysis

Boundary friction coefficients were measured on a custom-built tribometer as previsouly described in multiple publications [10], [15], [19], [30]. Briefly, samples were mounted onto a cylindrical post and attached to a biaxial, strain gauged load cell.

Samples were compressed to 30-50% axial strain against polished glass and allowed to equilibrate before sliding (20-30 minutes relaxation). Samples were then slid ±1 cm at 0.1 mm/s for 3 cycles. These conditions are known to produce boundary mode lubrication in both native [31] and engineered tissue [15], [19]. The friction coefficient was calculated as the shear force divided by the normal force and averaged for the forward and reverse sliding directions over the 3 cycles.

Histology

For histological analysis, samples were fixed in 10% buffered formalin, dehydrated in progressively stronger ethanol, embedded into paraffin blocks, sectioned, and mounted on slides. Immunohistochemistry was conducted as previously described [15] to analyze localization of lubricin (Abcam, Cambridge, MA, USA; Ab28484) at the construct surface as well as type II collagen (Abcam; Ab34710) and fibronectin (ICN/Cappel), which are extracellular matrix constituents that are known to have a high affinity to lubricin [32]. Briefly, antigen retrieval was conducted using citric acid at 90°C. Slides were then washed twice for 5 min in TRIS buffered saline with 0.5% TWEEN-20 (pH 7.4), incubated for 30 min in 0.01% hyaluronidase, 30 min in 3% hydrogen peroxide, and 60 min in a blocking solution containing normal serum, bovine serum albumin, Triton X-100, and TWEEN-20. Primary antibodies were applied overnight at 4°C. Secondary antibodies (Vectastain ABC, Vector) were applied for 30 minutes followed by 30 minutes in an avidin-biotin complex (Vectastain ABC, Vector). Staining was conducted with a peroxidase substrate (ImmPACT DAB, Vector). Images of stained sections were taken with a SPOT RT camera (Diagnostic Instruments, Steriling Heights, MI) attached to a Nikon Eclipse

TE2000-S microscope (Nikon Instruments, Melville, NY). Quantitative image analysis for lubricin localization was carried out on 3 stained slides for each construct group and conducted using ImageJ. Images at 200X that each contained the surface of the construct were thresholded and converted to binary images in ImageJ, and the percentage of pixels staining for lubricin were calculated for each image.

Mechanical Analysis

Three to Four samples per experimental group were trimmed to 4 mm diameter and mounted using an Enduratec ElectroForce 3200 System (Bose, Eden Prairie, MN) in a confined compression set up. Briefly, 10 steps of 5% strain were applied in stress relaxation. Data were fit to a poroelastic model using a custom MATLAB program to determine aggregate modulus and hydraulic permeability [33].

Surface Analysis

The surface roughness of both constructs and native meniscus were measured using a scanning white light interferometer (ADE Phase Shift MicroXAM Optical interferometric profiler). Four samples for each tissue engineered group and 9 of native meniscus were examined by analyzing the height distribution in a 209 μm x 179 μm window. The root mean squared roughness (S_q) was calculated for each sample and reported.

Statistics

Differences between construct groups were determined using a one-way ANOVA with Tukey post-hoc, and normality was determined with Kolmogorov-Smirnov test. Linear regression between measured parameters and either cell seeding ratio or boundary friction coefficient were conducted and significance was calculated

based on Pearson correlation coefficient. Significance was set at $p < 0.05$. Statistical analyses were performed using Sigma Plot version 11.0.

Results

Without *in vitro* culture, the boundary friction coefficient of a 20 mg/mL collagen gel was $\mu = 0.38 \pm 0.05$ (Figure 8.1 A). This value was 90% higher than the boundary friction coefficient of native meniscus tissue ($\mu = 0.20 \pm 0.02$; $p < 0.01$, $n = 4$). Collectively after 2 weeks of culture, all cell-seeded constructs had a lower boundary friction coefficient ($\mu = 0.25 \pm 0.10$) than uncultured collagen gel ($p < 0.05$) (Figure 8.1 B). Additionally after two weeks of culture, there was a significant correlation of decreasing boundary friction with increasing proportion of MSCs compared to FCCs ($R^2 = 0.948$, $p < 0.005$). The boundary friction coefficients of constructs containing 75% and 100% MSCs ($\mu = 0.16 \pm 0.05$ and $\mu = 0.15 \pm 0.05$, respectively) were 52% and 55% lower than the constructs containing 0% MSCs (i.e., 100% FCCs, $\mu = 0.33 \pm 0.10$) ($p < 0.05$ for both comparisons) and were not statistically different from native meniscus. To determine the dominant factors in the friction coefficient subsequent analyses were performed on mechanics, topology, and histology.

As previously described [28], confined compression analysis revealed a weak trend with increasing aggregate modulus with MSC content ($R^2 = 0.4$, $p > 0.1$) (Figure 8.2 A), and there was an even weaker relationship between hydraulic permeability and MSC content (Figure 8.2 B). Unlike friction coefficient, the aggregate modulus

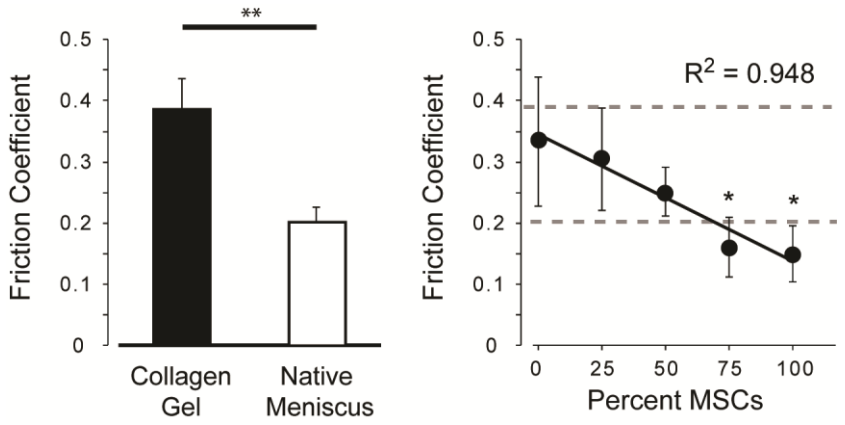

Figure 8.1(A) The boundary friction coefficient for a collagen gel was 90% higher than that of native meniscus (**$p < 0.001$, $n = 4$). (B) The friction coefficient of collagen gels cultured for 2 weeks was dependent on the percentage of seeded cells that were MSCs ($R^2 = 0.948$, $p<0.005$, $n = 4$). The friction coefficients of onstructs with 75% and 100% MSCs were significantly lower than those of 0% MSCs (*$p < 0.05$, $n = 4$). The dotted lines represent the average values for collagen gels and native menisci from panel A.

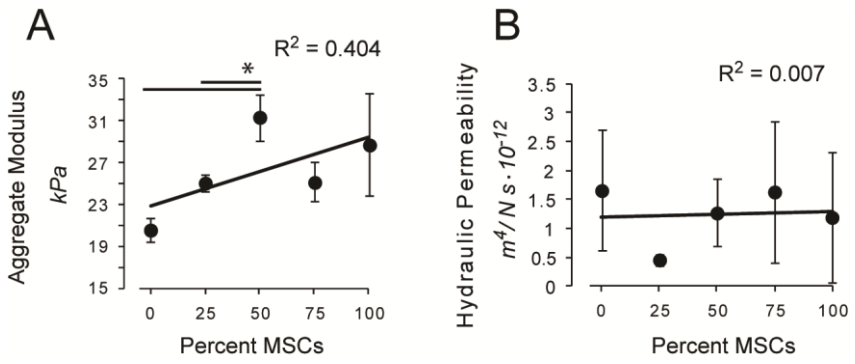

Figure 8.2 Confined compression analysis revealed a weak trend with (A) increasing aggregate modulus and percent MSCs and no trend with (B) hydraulic permeability and percent MSCs. For aggregate modulus, 50:50 co-culuture of FCCs and MSCs had higher moduli than FCC monoculture and 25:75 FCC to MSC constructs (*$p < 0.05$, n = 3-4).

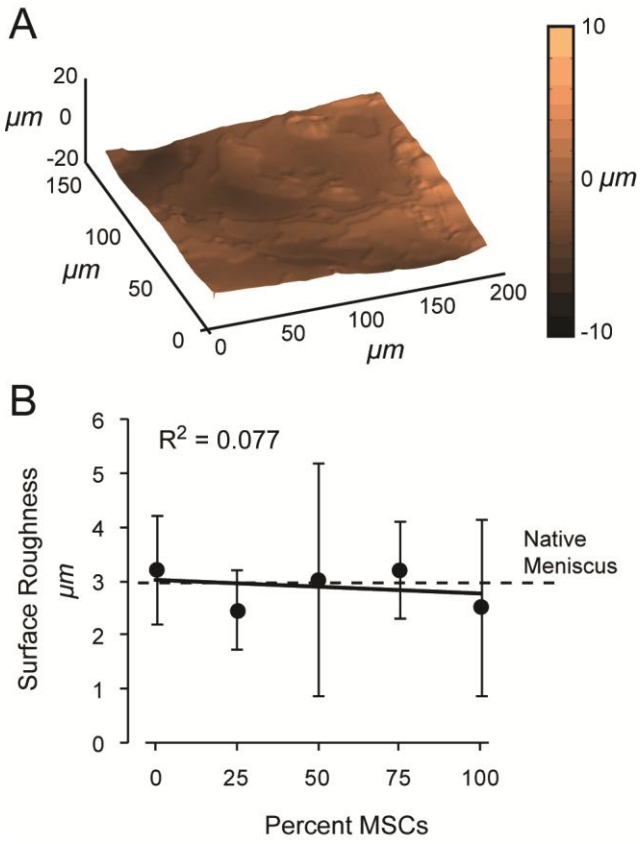

Figure 8.3 (A) A representative scanning white light profilometer scan of a construct reveals relatively smooth surfaces. (B) No trend of surface roughness with MSC content was found, but constructs had similar roughness values to native meniscus (n= 4 for constructs, n = 9 for native).

reached an optimal level from a co-culture group (50:50 MSC to FCC) that was significantly higher than FCCs alone and 25:75 MSC to FCC ($p < 0.05$).

Scanning white light profilometry revealed that all surfaces were relatively smooth based on RMS roughness ($S_q = 2.9\ \mu m \pm 1.3\ \mu m$ for all constructs, Figure 8.3). Scans of four constructs at 2 weeks from each group revealed no differences between each group and no trend with cell population ($R^2 = 0.077$). While no trend or differences were detected between construct groups, it is noteworthy that there were also no differences detected between the constructs and native meniscal surfaces ($p = 0.9$; $n = 4$ for constructs and $n = 9$ for native).

Immunohistochemical staining revealed that lubricin localized to the surfaces of constructs containing MSCs (Figure 8.4, top row). There was a significant trend of increasing lubricin localization with increasing MSC content revealed through analysis using ImageJ ($R^2 = 0.902$, $p = 0.013$, $n = 3$) (Figure 8.5). Further, staining for lubricin binding candidates, namely fibronectin (Figure 8.4, middle row) and type II collagen (Figure 8.4, bottom row)[32], revealed no visually striking trends with MSC content. However, there was positive staining evident for both molecules in all constructs.

To better understand the metrics that best predict boundary lubricating properties, linear regressions were performed between the measured parameters and boundary friction coefficient (Figure 8.6). Collectively, multiple linear regression of aggregate modulus, hydraulic permeability, and surface roughness only described 25% of the variation measured in friction coefficient (Figure 8.6 A-C). However, linear regression between lubricin staining and friction coefficient provided a significant

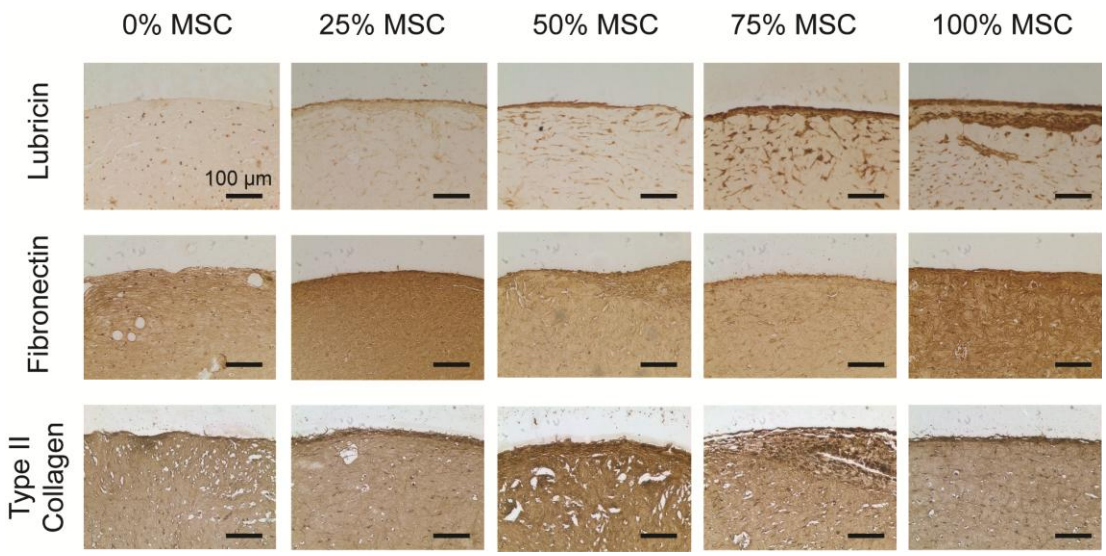

Figure 8.4 (Top row) Lubricin immunohistochemical staining revealed lubricin localized to construct surfaces as MSC content increased. (Middle and bottom rows) No visual trends with fibronectin content or type II collagen content were evident with MSC content.

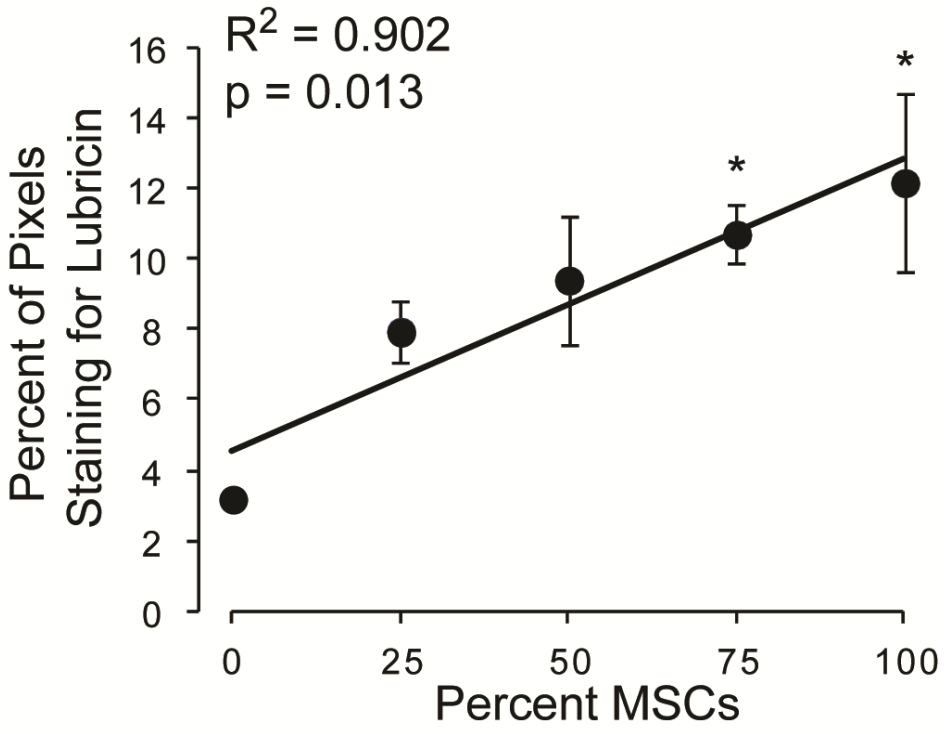

Figure 8.5 Lubricin localization to engineered tissue was highly correlated (R^2 = 0.902, p = 0.013) with MSC content, revealed through image analysis of immunohistochemistry stained tissue sections. Constructs with 75:25 MSC to FCC and 100% MSCs localized significantly more lubricin than 100% FCC constructs (*p < 0.05 vs 0% MSC, n = 3).

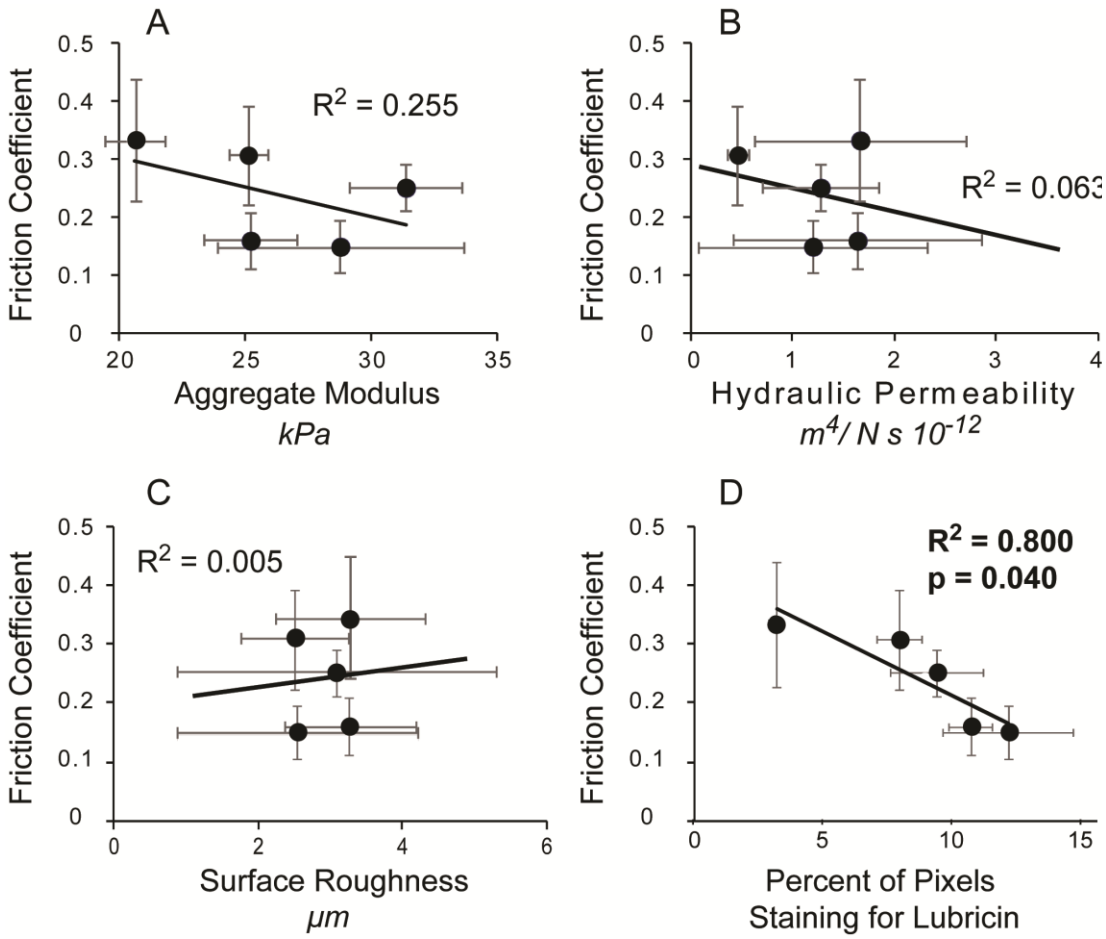

Figure 8.6 Structure-function relationships of engineered tissue for boundary lubrication. (A-C) Collectively, aggregate modulus, hydraulic permeability, surface roughness described 25% of the variation in boundary friction coefficient with aggregate modulus dominating the regression. (D) Lubricin staining at the tissue surface correlated strongly with the boundary friction coefficient (R^2 = 0.800, p = 0.04) revealing the dominant factor in altering boundary lubrication of engineered constructs.

correlation (R^2 = 0.800, p = 0.04, Figure 8.6 D), revealing it to be the dominant factor in predicting boundary lubricating ability.

Discussion

This study revealed a strong connection between the 3D culture of MSCs, localized lubricin, and low boundary friction coefficients in tissue engineered meniscus. These data suggest that the use of stem cells in meniscus tissue engineering can enhance the lubrication properties of implants given the proper scaffold choice. While tuning lubrication has not been studied in depth for meniscus tissue engineering, there is some previous evidence that using cell source as a tool enables control of tribological properties for engineered tissue [23]. However, most research has focused on articular cartilage. In articular cartilage tissue engineering, selectively seeding cells obtained from the superficial zone of cartilage increased the presence of localized lubricin in constructs [23]. Similarly, the use of articular or auricular chondrocytes both enhanced lubricin localization in engineered tissue compared to meniscus cells [34]. Additionally, chemical stimulation and mechanical stimulation have been used as tools to promote lubricin production or localization in constructs. In several articular cartilage models, dynamic shearing of constructs facilitated lubricin localization [22], [21], and in cartilage and meniscus supplementation of either IGF-1 or TGF-β facilitates lubricin production and localization [15], [35]. However, unlike these studies that have typically used culture with a single cell type with external stimulus, we have shown here that selectively introducing stem cells into 3D co-culture can enhance lubrication in a similar fashion to mechanical or chemical

stimulus.

In this study we also evaluated the connection between four different tissue engineering metrics and boundary friction to better understand the structure-function relationship of boundary lubrication. While surface roughness and permeability displayed very weak connections to boundary friction ($R^2 = 0.005$ and $R^2 = 0.063$, respectively), there was a trend, albeit a weak one, of decreasing friction with increasing aggregate modulus ($R^2 = 0.255$). In contrast to these metrics, the connection between lubricin localization and boundary friction was strong ($R^2 = 0.800$, $p < 0.05$). With regards to surface roughness, it is interesting to note that there was no connection between cell source and surface roughness. While often considered a dominant factor in boundary friction, recent evidence suggests that for hydrogels with roughness in the range of 1 to 10 μm, this metric may not be a good predictor of boundary friction [36]. Similarly to surface roughness, permeability was not a factor in determining boundary friction, nor was it a factor that scaled with cell source. However, the role of permeability may still have functional consequences in lubrication to be discussed later [13]. It is currently unclear whether the weak trend in aggregate modulus and boundary friction is due to a causal relationship. While increased modulus may decrease the real area of contact by inhibiting the flattening of asperities, this theory was not directly probed, nor was it possible to directly probe this in the absence of a boundary lubricant. Finally, the strong connection between lubricin localization and boundary friction is an expected result. The localization of lubricin has been connected to decreased friction on native articular cartilage and meniscus, as well as engineered cartilage and meniscus [15], [19], [37]. Lubricin is effective at

reducing the boundary friction coefficient due to its high degree of glycosylation and the hydrophilicity of its mucin-rich domain [37]. While this effect of decreased friction has implications for chondrocyte homeostasis [20], it has not been directly explored for meniscal fibrochondrocytes or cells within tissue engineered constructs, but it is likely to have protective effects. Further, as decreased boundary friction has been connected to decreased wear of articular cartilage [18], it is also likely that effectively lubricating an engineered construct may enhance the longevity of an implant in vivo.

While boundary friction was directly probed in this study due to its importance in soft tissue lubrication, it is necessary to note that the metrics that did not correlate with boundary friction may still have functional consequences on the lubrication of engineered menisci. Biphasic lubrication, which is a dominant factor in the extremely low friction values for articular cartilage (often $\mu < 0.01$) is also a dominant factor in the lubrication of meniscus tissue [11]–[13]. While modulus and permeability were not strong predictors of boundary friction, they are typically implicated in interstitial fluid pressurization which has been known for decades to greatly reduce the friction coefficient of soft tissue. Further, the surface roughness may also be a factor in determining the effects of fluid pressurization as increased surface roughness can inhibit the transition away from boundary lubrication towards a mixed mode of lubrication where interfacial fluid aids in reducing friction.

While synoviocytes are considered a primary cell type in the production of lubricin, it is well known that other cell types produce lubricin that can localize to tissue surfaces. Unlike articular cartilage where superficial zone cells are the primary

source of lubricin production, meniscus tissue displays localized lubricin throughout the tissue; lubricin in meniscus tissue is not only located on the tissue surface but also found between large fibers [14]. Similarly, we have previously found lubricin expression and localization of a heterogeneous population of meniscus cells after 3D culture in collagen gels, but significant lubricin localization was only noticed after growth factor supplementation [15]. Also, after extended culture of MSCs in alginate scaffolds there was not a significant amount of lubricin localized the construct surface; however, there was a non-negligible amount of lubricin found in analysis of the culture medium. This finding is consistent with the current study of increased lubricin localized to construct surfaces in MSC seeded gels likely dependent on the deposition of lubricin-binding molecules [32]. While only several studies have reported on lubricin expression from stem cells there is strong evidence that MSCs have a propensity to produce significant amounts of this protein. Studies indicate that MSCs in 3D culture produce significantly more lubricin than cells cultured in monolayer [38], and the results from this study indicate that the present study takes advantage of this fact through 3D culture in a collagen gel. Also of note, it is possible that increased lubricin synthesis may be attributed to cellular response to the hyperglycemic media environment which was recently connected to increases in proteoglycan synthesis in stem cell populations [39].

Although MSCs have previously been reported to produce lubricin, the results here highlight the importance of scaffold selection. As stated earlier in previous work using 3D culture of MSCs in alginate, significant lubricin concentrations were detected in the culture media [19]. However, despite the amounts of lubricin produced,

there was no evidence of localization of lubricin to the construct surface, and boundary friction was not reduced. Further, exposure of these constructs to exogenous lubricin in synovial fluid did not facilitate lubricin localization or reduction of boundary friction. However in this study, MSCs alone produced a surface layer of localized lubricin that was effective at boundary lubricating the engineered tissue. As we have previously seen, the type I collagen scaffold used in this study does not, by itself, facilitate the localization of lubricin to the tissue surface [15]. But, while immunohistochemical analysis revealed no distinct trends of type II collagen or fibronectin content with cell source, it is likely that these tissue components play a large role in the formation of a lubricin-rich surface layer [32]. These previous results combined with those from the present study suggest that collagen facilitates the deposition of extracellular matrix constituents that facilitate lubricin localization. And unlike the results for an alginate scaffold, once these components have been deposited in the tissue, they facilitate the localization of lubricin and the reduction of boundary friction.

This study presented a structure-function relationship for boundary friction in engineered meniscus tissue, and highlighted the potential of MSCs to tune the lubricating properties of engineered tissue, but there are several limitations to be addressed. Like many previous studies, the experiments detailed here utilized neonatal bovine cells [15], [19], [25], [28]. While clinically relevant cells come from mature autologous or allogenic sources, the propensity for lubricin production appears to be preserved between species and age [40]. Further, longer culture duration than two weeks was not studied here, but we have shown that longer term FCC cultures did not

produce lubricin localized to construct surfaces [15].

Collectively, the data in this study show: 1) tuning cell content within tissue engineered constructs can be used as a tool to achieve desired lubricating properties, 2) MSCs are a potent source of lubricin production, and 3) lubricin localization is the primary driver in tuning the boundary lubricating properties of engineered tissue.

REFERENCES

[1] S. Kawamura, K. Lotito, and S. A. Rodeo, “Biomechanics and healing response of the meniscus,” *Oper. Tech. Sports Med.*, vol. 11, no. 2, pp. 68–76, Apr. 2003.

[2] K. A. Cullen, M. J. Hall, and A. Golosinskiy, “Ambulatory surgery in the United States, 2006.,” *Natl. Health Stat. Report.*, no. 11, pp. 1–25, Jan. 2009.

[3] J. B. Thorlund, K. B. Hare, and L. S. Lohmander, “Large increase in arthroscopic meniscus surgery in the middle-aged and older population in Denmark from 2000 to 2011.,” *Acta Orthop.*, vol. 85, no. 3, pp. 287–92, Jun. 2014.

[4] T. Shybut and E. J. Strauss, “Surgical management of meniscal tears.,” *Bull. NYU Hosp. Jt. Dis.*, vol. 69, no. 1, pp. 56–62, Jan. 2011.

[5] B. M. Baker and R. L. Mauck, “The effect of nanofiber alignment on the maturation of engineered meniscus constructs.,” *Biomaterials*, vol. 28, no. 11, pp. 1967–77, Apr. 2007.

[6] J. L. Puetzer, E. Koo, and L. J. Bonassar, “Induction of fiber alignment and mechanical anisotropy in tissue engineered menisci with mechanical anchoring.,” *J. Biomech.*, vol. 48, no. 8, pp. 1436–43, Jun. 2015.

[7] D. J. Huey and K. A. Athanasiou, “Tension-compression loading with chemical stimulation results in additive increases to functional properties of anatomic meniscal constructs.,” *PLoS One*, vol. 6, no. 11, p. e27857, Jan. 2011.

[8] J. J. Ballyns, J. P. Gleghorn, V. Niebrzydowski, J. J. Rawlinson, H. G. Potter, S.

A. Maher, T. M. Wright, and L. J. Bonassar, “Image-guided tissue engineering of anatomically shaped implants via MRI and micro-CT using injection molding.,” *Tissue Eng. Part A*, vol. 14, no. 7, pp. 1195–202, Jul. 2008.

[9] C. H. Lee, S. A. Rodeo, L. A. Fortier, C. Lu, C. Erisken, and J. J. Mao, “Protein-releasing polymeric scaffolds induce fibrochondrocytic differentiation of endogenous cells for knee meniscus regeneration in sheep.,” *Sci. Transl. Med.*, vol. 6, no. 266, p. 266ra171, Dec. 2014.

[10] J. P. Gleghorn, S. B. Doty, R. F. Warren, T. M. Wright, S. A. Maher, and L. J. Bonassar, “Analysis of frictional behavior and changes in morphology resulting from cartilage articulation with porous polyurethane foams.,” *J. Orthop. Res.*, vol. 28, no. 10, pp. 1292–9, Oct. 2010.

[11] V. J. Baro, E. D. Bonnevie, X. Lai, C. Price, D. L. Burris, and L. Wang, “Functional characterization of normal and degraded bovine meniscus: rate-dependent indentation and friction studies.,” *Bone*, vol. 51, no. 2, pp. 232–40, Aug. 2012.

[12] E. D. Bonnevie, V. Baro, L. Wang, and D. L. Burris, “In-situ studies of cartilage microtribology: roles of speed and contact area.,” *Tribol. Lett.*, vol. 41, no. 1, pp. 83–95, Jan. 2011.

[13] G. A. Ateshian, “The role of interstitial fluid pressurization in articular cartilage lubrication.,” *J. Biomech.*, vol. 42, no. 9, pp. 1163–76, Jun. 2009.

[14] B. L. Schumacher, T. A. Schmidt, M. S. Voegtline, A. C. Chen, and R. L. Sah, “Proteoglycan 4 (PRG4) synthesis and immunolocalization in bovine

meniscus.," *J. Orthop. Res.*, vol. 23, no. 3, pp. 562–8, May 2005.

[15] E. D. Bonnevie, J. L. Puetzer, and L. J. Bonassar, "Enhanced boundary lubrication properties of engineered menisci by lubricin localization with insulin-like growth factor I treatment.," *J. Biomech.*, vol. 47, no. 9, pp. 2183–8, Jun. 2014.

[16] M. A. Accardi, S. D. McCullen, A. Callanan, S. Chung, P. M. Cann, M. M. Stevens, and D. Dini, "Effects of fiber orientation on the frictional properties and damage of regenerative articular cartilage surfaces.," *Tissue Eng. Part A*, vol. 19, no. 19–20, pp. 2300–10, Oct. 2013.

[17] G. D. Jay, "Characterization of a bovine synovial fluid lubricating factor. I. Chemical, Surface activity and lubricating properties," Jul. 2009.

[18] G. D. Jay, J. R. Torres, D. K. Rhee, H. J. Helminen, M. M. Hytinnen, C.-J. Cha, K. Elsaid, K.-S. Kim, Y. Cui, and M. L. Warman, "Association between friction and wear in diarthrodial joints lacking lubricin.," *Arthritis Rheum.*, vol. 56, no. 11, pp. 3662–9, Nov. 2007.

[19] J. P. Gleghorn, A. R. C. Jones, C. R. Flannery, and L. J. Bonassar, "Boundary mode frictional properties of engineered cartilaginous tissues.," *Eur. Cell. Mater.*, vol. 14, pp. 20–8; discussion 28–9, Jan. 2007.

[20] K. A. Waller, L. X. Zhang, K. A. Elsaid, B. C. Fleming, M. L. Warman, and G. D. Jay, "Role of lubricin and boundary lubrication in the prevention of chondrocyte apoptosis.," *Proc. Natl. Acad. Sci. U. S. A.*, vol. 110, no. 15, pp. 5852–7, Apr. 2013.

[21] S. Grad, C. R. Lee, K. Gorna, S. Gogolewski, M. A. Wimmer, and M. Alini, "Surface motion upregulates superficial zone protein and hyaluronan production in chondrocyte-seeded three-dimensional scaffolds.," *Tissue Eng.*, vol. 11, no. 1–2, pp. 249–56, Jan. 2005.

[22] S. Grad, M. Loparic, R. Peter, M. Stolz, U. Aebi, and M. Alini, "Sliding motion modulates stiffness and friction coefficient at the surface of tissue engineered cartilage.," *Osteoarthritis Cartilage*, vol. 20, no. 4, pp. 288–95, Apr. 2012.

[23] T. J. Klein, B. L. Schumacher, T. A. Schmidt, K. W. Li, M. S. Voegtline, K. Masuda, E. J.-M. A. Thonar, and R. L. Sah, "Tissue engineering of stratified articular cartilage from chondrocyte subpopulations," *Osteoarthr. Cartil.*, vol. 11, no. 8, pp. 595–602, Aug. 2003.

[24] B. M. Baker, A. S. Nathan, G. R. Huffman, and R. L. Mauck, "Tissue engineering with meniscus cells derived from surgical debris.," *Osteoarthritis Cartilage*, vol. 17, no. 3, pp. 336–45, Mar. 2009.

[25] J. L. Puetzer and L. J. Bonassar, "High Density Type I Collagen Gels for Tissue Engineering of Whole Menisci.," *Acta Biomater.*, vol. null, no. null, May 2013.

[26] W. M. Han, S.-J. Heo, T. P. Driscoll, J. F. Delucca, C. M. McLeod, L. J. Smith, R. L. Duncan, R. L. Mauck, and D. M. Elliott, "Microstructural heterogeneity directs micromechanics and mechanobiology in native and engineered fibrocartilage," *Nat. Mater.*, vol. advance on, Jan. 2016.

[27] X. Cui, A. Hasegawa, M. Lotz, and D. D'Lima, "Structured three-dimensional co-culture of mesenchymal stem cells with meniscus cells promotes meniscal

phenotype without hypertrophy," *Biotechnol. Bioeng.*, vol. 109, no. 9, pp. 2369–2380, Sep. 2012.

[28] M. C. McCorry, J. L. Puetzer, and L. J. Bonassar, "Characterization of mesenchymal stem cells and fibrochondrocytes in three-dimensional co-culture: analysis of cell shape, matrix production, and mechanical performance.," *Stem Cell Res. Ther.*, vol. 7, no. 1, p. 39, Jan. 2016.

[29] R. L. Mauck, X. Yuan, and R. S. Tuan, "Chondrogenic differentiation and functional maturation of bovine mesenchymal stem cells in long-term agarose culture," *Osteoarthr. Cartil.*, vol. 14, no. 2, pp. 179–189, Feb. 2006.

[30] E. D. Bonnevie, D. Galesso, C. Secchieri, I. Cohen, and L. J. Bonassar, "Elastoviscous Transitions of Articular Cartilage Reveal a Mechanism of Synergy between Lubricin and Hyaluronic Acid.," *PLoS One*, vol. 10, no. 11, p. e0143415, Jan. 2015.

[31] N. K. Galley, J. P. Gleghorn, S. Rodeo, R. F. Warren, S. A. Maher, and L. J. Bonassar, "Frictional properties of the meniscus improve after scaffold-augmented repair of partial meniscectomy: a pilot study.," *Clin. Orthop. Relat. Res.*, vol. 469, no. 10, pp. 2817–23, Oct. 2011.

[32] G. Elsaid, KA, Chichester, CO, Jay, "Lubricin Purified from Bovine Synovial Fluid and Articular Cartilage Exhibit Similar Binding Affinities to Cartilage Matrix Proteins," in *Transactions of the Orthopaedic Research Society*, 2001.

[33] V. L. Cross, Y. Zheng, N. Won Choi, S. S. Verbridge, B. A. Sutermaster, L. J. Bonassar, C. Fischbach, and A. D. Stroock, "Dense type I collagen matrices

that support cellular remodeling and microfabrication for studies of tumor angiogenesis and vasculogenesis in vitro.," *Biomaterials*, vol. 31, no. 33, pp. 8596–607, Nov. 2010.

[34] L. Zhang and M. Spector, "Comparison of three types of chondrocytes in collagen scaffolds for cartilage tissue engineering.," *Biomed. Mater.*, vol. 4, no. 4, p. 045012, Aug. 2009.

[35] T. A. Schmidt, N. S. Gastelum, E. H. Han, G. E. Nugent-Derfus, B. L. Schumacher, and R. L. Sah, "Differential regulation of proteoglycan 4 metabolism in cartilage by IL-1alpha, IGF-I, and TGF-beta1.," *Osteoarthritis Cartilage*, vol. 16, no. 1, pp. 90–7, Jan. 2008.

[36] S. Yashima, N. Takase, T. Kurokawa, and J. P. Gong, "Friction of hydrogels with controlled surface roughness on solid flat substrates.," *Soft Matter*, vol. 10, no. 18, pp. 3192–9, May 2014.

[37] G. D. Jay, D. A. Harris, and C.-J. Cha, "Boundary lubrication by lubricin is mediated by O-linked β(1-3)Gal-GalNAc oligosaccharides," *Glycoconj. J.*, vol. 18, no. 10, pp. 807–815, Oct. 2001.

[38] Y. Nakagawa, T. Muneta, K. Otabe, N. Ozeki, M. Mizuno, M. Udo, R. Saito, K. Yanagisawa, S. Ichinose, H. Koga, K. Tsuji, and I. Sekiya, "Cartilage Derived from Bone Marrow Mesenchymal Stem Cells Expresses Lubricin In Vitro and In Vivo.," *PLoS One*, vol. 11, no. 2, p. e0148777, Jan. 2016.

[39] D. J. Gorski, W. Xiao, J. Li, W. Luo, M. Lauer, J. Kisiday, A. Plaas, and J. Sandy, "Deletion of ADAMTS5 does not affect aggrecan or versican

degradation but promotes glucose uptake and proteoglycan synthesis in murine adipose derived stromal cells.," *Matrix Biol.*, vol. 47, pp. 66–84, Sep. 2015.

[40] A. R. C. Jones and C. R. Flannery, "Bioregulation of lubricin expression by growth factors and cytokines.," *Eur. Cell. Mater.*, vol. 13, pp. 40–5; discussion 45, Jan. 2007.

CHAPTER 9

Conclusions and Future Directions

Abstract

In this section, the previous 8 chapters will be tied together to offer a deeper perspective on the impact of the original research contained in this dissertation. The new understanding on the lubrication mechanisms of Chapter 2 provide a deeper understanding on the role of synovial fluid macromolecules on friction, and sheds light on possible issues within the clinical practice of HA injections. Additionally, the data from Chapter 2 will be applied to addressing future directions in tribosupplementation. The data in this dissertation also shed light on possible mechanisms of cartilage disease and damage progression by connecting the findings on lubrication changes in injury and disease (Chapters 3-5) and the findings concerning cellular responses to elevated friction (Chapter 6). Finally, the data on synovial fluid lubrication (Chapter 2), cellular responses to friction (Chapter 6), and lubrication in tissue engineering (Chapters 7-8) can be related to each other to provide perspectives on the role of lubrication in engineering cartilage substitutes.

Insights into Molecular Mechanisms of Lubrication

The work described in Chapter 2 presented a framework to systematically study the individual contributions of molecular lubricants of articular cartilage at a macroscopic level. We found that, as expected, lubricin facilitated boundary lubrication (i.e., it lubricated independent of sliding speed and at low Sommerfeld numbers). In contrast, hyaluronic acid was effective at reducing friction coefficients at elevated Sommerfeld numbers and displayed distinct dependence on sliding speed, behavior typical of a viscous lubricant. However, some of the most interesting data manifested in the combination of lubricin and hyaluronic acid together in the lubricating bath. While HA alone did not reduce friction at slow sliding speeds, when added into a lubricin bath, it reduced friction by 50% compared to lubricin alone. Further experimental evidenced suggested that lubricin helps to facilitate aggregation of HA near the articular surface promoting friction reduction.

This observation that lubricin facilitated both aggregation of and lubrication by hyaluronic acid is in agreement with recently proposed theories on biolubrication [1]. The recently proposed theory of viscous boundary lubrication was developed for the lubrication of adsorbed mucinous layers, where aggregation of mucins formed a viscous surface layer and shifted the operating conditions of sliding surfaces. Not only did the aggregation of hydrohpillic mucins lower the boundary friction coefficient, but they also facilitated a transition to low, viscous friction at lower sliding speeds compared to surfaces that had lowe concentrations of mucin. It was hypothesized that these adsorbed films lubricate through both boundary and viscous actions. Essentially, the increased viscosity of the surface layer compared to the viscosity of the un-bound

lubricating bath was hypothesized to be the key factor in shifting the system to low friction. A similar mechanism has been hypothesized for lubricin and chemically grafted HA with free lubricin lubricating mica surfaces [2]. But, we have shown in this dissertation that this lubricating mechanism is relevant for natural cartilage surfaces, that it is driven by lubricin localization, and that it is the major mechanism in the lubrication by synovial fluid.

Unlike previous studies, we found no indication that hyaluronic acid alone posses boundary lubricating ability. We did, however find friction reduction of cartilage at elevated sliding speed. Interestingly, in theory we would not have expected friction reduction due to viscous lubricants in our tribometer configuration. By sliding relatively flat cartilage against flat polished glass, the geometry is not conducive to forming viscous films as there is no clear mechanism of fluid entrainment. However, we found that cartilage does not behave similarly to typical bearing materials that are often both hard and isotropic. By visualizing the contact geometry of cartilage against glass on a confocal microscope (i.e., the configuration used in Chapter 6), we found that the compliance of the surface layer facilitated the formation of contact geometry reminiscent of a typical converging wedge (Figure 9.1). It is possible that the development of this altered contact geometry under friction is key to measuring viscous lubricant effects of lubricants on cartilage.

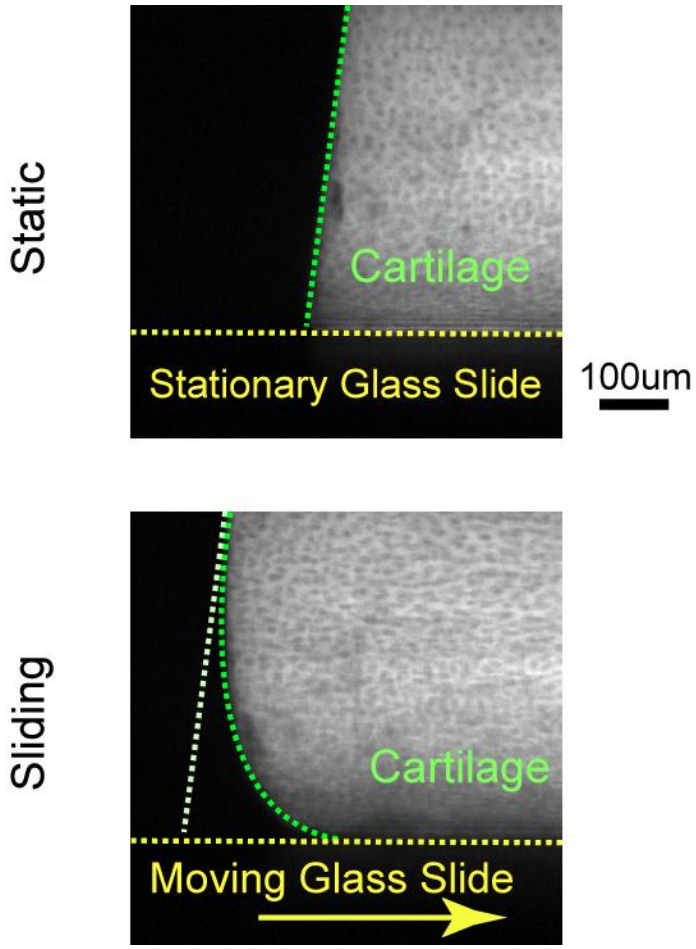

Figure 9.1 Changes in cartilage contact geometry under friction alter the assumed flat-on-flat configuration used in measuring cartilage boundary friction coefficients. Confocal tribometry of the leading edge of cartilage during friction testing revealed local deformations of actively sheared cartilage (bottom) compared to static cartilage (top) are conducive to forming a converging wedge.

Insights into Tribosupplementation

Although the practice of tribosupplementation has been applied for over 40 years [3], [4], the efficacy of tribosupplementation is still hotly contested [5], [6].Viscosupplementation in the form of hyaluronic acid injection provides pain relief over placebo (i.e., saline) injection; however, although the effect is significant it is considered small. But, it is important to note that saline injection alone also has analgesic effects. A meta-analysis of HA efficacy trials revealed a trend of increasing effectiveness with increasing molecular weight of HA. Connected to the data from Chapter 2 in this dissertation, there is mechanical insight into this effect. We found that HA did not, alone, possess boundary lubricating ability. Through presenting friction as a function of the Sommerfeld number (Figure 2.2) we presented the dominant lubricating effect of HA as a viscosity driven mechanism. Consequently, we showed that lubricants with higher viscosities were able to promote lower friction compared to lower viscosity lubricants. As viscosity scales with the molecular weight of HA [7], it is expected that if the dominating aspect of HA's intraarticular effect is mechanical, then higher molecular weight or chemically modified HAs that possess enhanced rheological properties should prove more effective. To begin to test this theory, several clinically-approved HA lubricant formulations were tested in our tribometer for their efficacy in lubricating cartilage (Appendix A). Expectedly, friction scaled with the inverse of viscosity, solidifying HA's role in viscous lubrication.

However, while HA alone did not possess any discernible boundary lubricating ability, when lubricin was added HA possessed enhanced lubricating ability (Figure 2.3). Lubricating cartilage with no lubricin in the bath, HA did not reduce friction at

low sliding speeds. However, with lubricin added into the bath at 20 μg/mL, HA was able to decrease friction 50% compared to lubricin alone at slow sliding speeds. The mechanism responsible for this effect is likely an association between the two lubricants causing a viscous surface layer consistent with the theory of viscous boundary lubrication [1]. We also showed that this phenomenon was facilitated by lubricin, which is known to bind to the cartilage surface [8]. This lubricin-initiated mechanism can also shed light on the contested efficacy of HA in tribosupplementation. Viscosupplementation is typically only utilized in symptomatic OA, and in many of these cases it is likely that there is extensive cartilage damage within the joint. Considering that lubricin levels can drop significantly with degeneration and inflammation [9], [10], it is possible that efficacy of HA injections is dependent on the current disease state of a joint. This may be a key, not yet studied, factor in dictating injection effectiveness since HA's lubricating ability was found to be dependent on the presence of lubricin. One study that indirectly studied this question was an anterior cruciate ligament transaction rodent model of OA [5]. In the study, either PBS, lubricin, HA, or HA+lubricin was injected into the joint space. Considering lubricin levels can drop 90% after ACL rupture in humans [9], it is possible a similar process can occur leading to lubricin-deficient joints in the rodent model. The study found no change in OARSI score between saline and HA injection. However, significant decreases in OARSI score were detected in lubricin and HA+lubricin injection compared to HA and saline. Further, it appeared (although not determined significant due to low statistical power) HA when added to the lubricin injection was effective at reducing OARSI score. Therefore, as could be expected

from the lubrication data in Chapter 2 of this dissertation, HA effectiveness in both lubrication and treatment can be dependent on the presence of lubricin to promote viscous boundary lubrication.

Future Directions in Tribosupplementation

As previously discussed, the presence of lubricin is a key factor in the lubrication of cartilage. It is also a key factor in facilitating lubrication by HA. Recent studies using rodent models have presented chondroprotection through lubricin injection, but as discussed prior this treatment has not yet been studied in humans. It is likely to be an effective treatment in humans based on the lubricating properties of lubricin, however the scale-up of lubricin production or purification may pose obstacles. Recombinant lubricin production can be hindered due to the degree of glycosylation of the protein [11], preventing it from be produced recombinantly in prokaryotic cells such as E. coli. Further, the high affinity of lubricin to other molecules in synovial fluid such as fibronectin [12] pose a challenge in cost-efficient purification methods for clinical use. With these aspects in mind, production of a synthetic lubricant that is able to replace lubricin in the lubricin-HA synergy lubrication mechanism may prove effective. Recall that the lubrication synergy was theorized to be dependent on lubricin binding to the surface and facilitating HA association. We showed that this effect could be replicated by using another viscous lubricant, dextran, substituted for HA (Figure 2.3). We did not, however, present evidence for the alternative experiment: a non-lubricin lubricant that can bind to the articular surface and facilitate HA association and lubrication. Recent progress has

been made in producing a synthetic lubricin-mimetic that can bind to and boundary lubricate the articular cartilage surface [13]. This lubricin-mimetic presents a cost-effective alternative to lubricin supplementation, and preliminary experimental evidence suggests that a similar lubrication mechanism can occur between this mimetic lubricin and HA to promote low friction in a manner similar to that natural synovial fluid (Appendix B). In summary, the utilization of a boundary lubricant (i.e., lubricin or a lubricin mimetic) is likely key to the efficacy of tribosupplementation in diseased joints and the addition of a viscous lubricant such as HA can be more effective when there is a molecule present at the cartilage surface to facilitate its association.

Role of Friction in Disease and Degeneration

Cartilage friction has classically been studied for two main reasons: to understand the lubricating mechanisms that facilitate some of the lowest friction coefficients measured in nature and to understand the role of friction in the "wear and tear" disease of osteoarthritis. The evidence provided in this dissertation indicate that "wear and tear" may not be the most applicable words to describe the progression of OA. There have been dozens of studies that have analyzed the mechanical effects of repeatedly applied friction to the articular surface of cartilage. In one instance, cartilage was slid repeatedly in PBS for 24 hours against a polished surface under normal loads three times higher than those studied in Chapter 6, and not enough of the cartilage surface had eroded to measure the biochemical content lost to the lubricating bath using standard assays [14]. However, in 30 cycles of sliding under lower load

conditions, the chondrocytes presented severe dysfunction. Within the superficial zone when cartilage was lubricated by PBS, more than 90% of the cells had died within 2 hours of sliding. Further, deeper in the tissue a large fraction of the cells underwent mitochondrial depolarization and 24 hours later were capsase-positive. It is evident from this study, that biological repercussions can precede mechanical wearing of cartilage due to applied friction.

Connected to disease and degeneration, it is possible that friction-mediated biological effects can appear more acutely. We demonstrated in Chapters 4 and 5 that the intrinsic lubricating ability of cartilage is hindered both following trauma and through inflammation. In the inflammation model, we noted that biochemical content of cartilage was altered and the tissue become softer and more permeable. Further, recent evidence suggests similar biochemical changes can result in significantly decreased shear moduli [15]. With both increased friction and decreased shear modulus, the frictional shear strains will be amplified by both of these changes. Thus, already damaged cartilage is predisposed to the friction-mediated effects seen from high friction in Chapter 6.

Friction in Tissue Engineering

There has been significant progress on tuning the lubricating properties on engineered tissue in the last decade of research through both mechanical and chemical stimulation and selectively seeding lubricin-producing cells [16]–[19]. Additionally, this dissertation provides two more cases of enhancing lubrication in tissue engineering, however for meniscus tissue unlike most previous studies that have

focused on articular cartilage. In most cases, the goal for enhancing lubrication within tissue engineering is to ensure either an implant will not wear away, or it will not cause wear of the contacting cartilage surface it will articulate against. However, evidence presented in this dissertation suggests that promoting effective lubrication is necessary but not sufficient to ensure success. We have recently reported on a large animal *in vivo* model of cartilage defect repair using engineered tissue and autologous chondrocytes [20]. At 53 weeks after implantation, we found no differences in the boundary friction coefficient of engineered tissue compared to control. We also found for matrix-assisted autologous chondrocyte implantation (MACI®) compressive properties approaching those of native cartilage. However, the aspect that remained well below native values was the shear modulus of the engineered tissue. With a significantly decreased shear modulus, it is expected that frictional stresses can result in large frictional strains. It is not known what biological effects high friction has on engineered tissue yet, but from the data in this dissertation it arises as an important question.

Future Directions

The conclusions drawn from this dissertation highlight areas of further exploration. Several important questions to be addressed are:

1) What role does a mimetic-lubricin play in localizing HA to the articular surface? Pointed tribological studies combined with imaging similar to those conducted in Chapter 2 can resolve the question regarding mechanism and effectiveness in reducing friction. Additionally, analyzing the biological responses of

cartilage lubricated by a mimetic-lubricin and HA complex can provide an *in vitro* basis to before conducting animal trials using this lubricant formulation.

2) Does enhanced lubrication in engineered tissue protect the seeded cells? By conducting similar experiments to those in Chapter 6, the role of lubrication in the biological response of friction in tissue engineering can be elucidated. A major question remains to whether more compliant pericellular matrices in engineered tissue can be protective to the cells by limiting strain transfer. For this study, further characterization of both local tissue strain and transfer to cellular strain can be conducted to answer key questions in mechanotransduction within tissue engineering.

3) Is damaged or degraded tissue predisposed to cell death and apoptosis due to changes in friction and local moduli? Once again similar experiments to those in Chapter 6 can be employed on either impacted tissue or cytokine-exposed tissue to determine how function changes to the tissue can alter the biological responses to high friction.

4) Can non-synovial fluid lubricants preserve chondrocyte homeostasis? We have shown hyper-viscous formulations of HA to lubricate cartilage at a similar level to that of synovial fluid; however, there is no indication that they have boundary lubricating abilities. Studies on the role of friction versus boundary lubrication can shed light on the ability of different lubricant formulations to both lubricate cartilage and protect the chondrocytes.

5) How does local compliance of the cartilage superficial zone effect lubrication? As described in Figure 9.1, the compliant superficial zone of cartilage is conducive to altering contact geometry while measuring friction coefficients. An open

question remains as to the role of this altered geometry in measuring friction reductions by viscous lubricants at the cartilage surface. Specifically, pointed confocal tribometry can shed light on whether contact compliance of cartilage facilitates viscous molecule (i.e., hyaluronic acid) entrainment and lubrication.

REFERENCES

[1] G. E. Yakubov, J. McColl, J. H. H. Bongaerts, and J. J. Ramsden, “Viscous boundary lubrication of hydrophobic surfaces by mucin.,” *Langmuir*, vol. 25, no. 4, pp. 2313–21, Feb. 2009.

[2] S. Das, X. Banquy, B. Zappone, G. W. Greene, G. D. Jay, and J. N. Israelachvili, “Synergistic interactions between grafted hyaluronic acid and lubricin provide enhanced wear protection and lubrication.,” *Biomacromolecules*, vol. 14, no. 5, pp. 1669–77, May 2013.

[3] N. W. Rydell, J. Butler, and E. A. Balazs, “Hyaluronic acid in synovial fluid. VI. Effect of intra-articular injection of hyaluronic acid on the clinical symptoms of arthritis in track horses.,” *Acta vet.*, vol. 11, pp. 139–155, 1970.

[4] E. A. Balazs and J. L. Denlinger, “Viscosupplementation: a new concept in the treatment of osteoarthritis.,” *J. Rheumatol. Suppl.*, vol. 39, pp. 3–9, Aug. 1993.

[5] E. Teeple, K. A. Elsaid, G. D. Jay, L. Zhang, G. J. Badger, M. Akelman, T. F. Bliss, and B. C. Fleming, “Effects of supplemental intra-articular lubricin and hyaluronic acid on the progression of posttraumatic arthritis in the anterior cruciate ligament-deficient rat knee.,” *Am. J. Sports Med.*, vol. 39, no. 1, pp. 164–72, Jan. 2011.

[6] G. H. Lo, M. LaValley, T. McAlindon, and D. T. Felson, “Intra-articular Hyaluronic Acid in Treatment of Knee Osteoarthritis,” *JAMA*, vol. 290, no. 23, p. 3115, Dec. 2003.

[7] S. Hokputsa, K. Jumel, C. Alexander, and S. E. Harding, “Hydrodynamic characterisation of chemically degraded hyaluronic acid,” *Carbohydr. Polym.*, vol. 52, no. 2, pp. 111–117, 2003.

[8] A. R. C. Jones, J. P. Gleghorn, C. E. Hughes, L. J. Fitz, R. Zollner, S. D. Wainwright, B. Caterson, E. A. Morris, L. J. Bonassar, and C. R. Flannery, “Binding and localization of recombinant lubricin to articular cartilage surfaces.,” *J. Orthop. Res.*, vol. 25, no. 3, pp. 283–92, Mar. 2007.

[9] K. A. Elsaid, B. C. Fleming, H. L. Oksendahl, J. T. Machan, P. D. Fadale, M. J. Hulstyn, R. Shalvoy, and G. D. Jay, “Decreased lubricin concentrations and markers of joint inflammation in the synovial fluid of patients with anterior cruciate ligament injury.,” *Arthritis Rheum.*, vol. 58, no. 6, pp. 1707–15, Jun. 2008.

[10] M. K. Kosinska, T. E. Ludwig, G. Liebisch, R. Zhang, H.-C. Siebert, J. Wilhelm, U. Kaesser, R. B. Dettmeyer, H. Klein, B. Ishaque, M. Rickert, G. Schmitz, T. A. Schmidt, and J. Steinmeyer, “Articular Joint Lubricants during Osteoarthritis and Rheumatoid Arthritis Display Altered Levels and Molecular Species,” *PLoS One*, vol. 10, no. 5, p. e0125192, May 2015.

[11] G. D. Jay, D. A. Harris, and C.-J. Cha, “Boundary lubrication by lubricin is mediated by O-linked β(1-3)Gal-GalNAc oligosaccharides,” *Glycoconj. J.*, vol. 18, no. 10, pp. 807–815, Oct. 2001.

[12] G. Elsaid, KA, Chichester, CO, Jay, “Lubricin Purified from Bovine Synovial

Fluid and Articular Cartilage Exhibit Similar Binding Affinities to Cartilage Matrix Proteins," in *Transactions of the Orthopaedic Research Society*, 2001.

[13] K. Samaroo, "Biomimetic Boundary Lubricants Of Articular Cartilage," 2015.

[14] S. R. Oungoulian, S. Chang, O. Bortz, K. E. Hehir, K. Zhu, C. E. Willis, C. T. Hung, and G. A. Ateshian, "Articular Cartilage Wear Characterization With a Particle Sizing and Counting Analyzer," *J. Biomech. Eng.*, vol. 135, no. 2, p. 024501, Feb. 2013.

[15] D. J. Griffin, J. Vicari, M. R. Buckley, J. L. Silverberg, I. Cohen, and L. J. Bonassar, "Effects of enzymatic treatments on the depth-dependent viscoelastic shear properties of articular cartilage," *J. Orthop. Res.*, vol. 32, no. 12, pp. 1652–1657, Dec. 2014.

[16] T. J. Klein, B. L. Schumacher, T. A. Schmidt, K. W. Li, M. S. Voegtline, K. Masuda, E. J.-M. A. Thonar, and R. L. Sah, "Tissue engineering of stratified articular cartilage from chondrocyte subpopulations," *Osteoarthr. Cartil.*, vol. 11, no. 8, pp. 595–602, Aug. 2003.

[17] S. Grad, M. Loparic, R. Peter, M. Stolz, U. Aebi, and M. Alini, "Sliding motion modulates stiffness and friction coefficient at the surface of tissue engineered cartilage.," *Osteoarthritis Cartilage*, vol. 20, no. 4, pp. 288–95, Apr. 2012.

[18] S. Grad, C. R. Lee, K. Gorna, S. Gogolewski, M. A. Wimmer, and M. Alini, "Surface motion upregulates superficial zone protein and hyaluronan production in chondrocyte-seeded three-dimensional scaffolds.," *Tissue Eng.*,

vol. 11, no. 1–2, pp. 249–56, Jan. 2005.

[19] S. M. McNary, K. A. Athanasiou, and A. H. Reddi, “Engineering lubrication in articular cartilage.,” *Tissue Eng. Part B. Rev.*, vol. 18, no. 2, pp. 88–100, Apr. 2012.

[20] D. J. Griffin, E. D. Bonnevie, D. J. Lachowsky, J. C. A. Hart, H. D. Sparks, N. Moran, G. Matthews, A. J. Nixon, I. Cohen, and L. J. Bonassar, “Mechanical characterization of matrix-induced autologous chondrocyte implantation (MACI®) grafts in an equine model at 53 weeks,” *J. Biomech.*, vol. 48, no. 10, pp. 1944–1949, 2015.

APPENDIX A

The Lubricating Ability of Commercially Available Hyaluronic Acids

Abstract

In this appendix, 6 clinically-available hyaluronic acid viscosupplements were compared in terms of *in vitro* lubrication of cartilage. Further, rheological characterizations were conducted to better understand which mechanical parameters of a viscous cartilage lubricant best predict friction coefficient. As expected dynamic viscosity best predicted the variation in friction coefficient between different lubricant formulations ($p = 0.045$). However, this parameter only described ~65% of the variation in friction coefficient, so future efforts should be aimed at elucidating other factors of viscous lubricants that affect cartilage friction.

Introduction

As stated earlier, viscosupplementation has been used clinically for over 40 years [1], [2]. Working on the theory that the addition of a viscous fluid to the joint cavity can enhance lubrication and energy dissipation between cartilage surfaces [2], very viscous formulations of hyaluronic acid have been developed. Modified HAs have been developed via chemical cross-linking and amidation that have greatly increased rheological properties (i.e., viscosity, storage modulus, etc.) [3], [4]. More viscous formulations of HA have also shown more clinical success in reducing pain scores compare to PBS and unmodified HA [3]. With this evidence that increased viscosity may be connected to decreased pain, we study here an alternative question: is increased viscosity connected to decreased friction for commercial HA products?

Methods

Six clinically-approved HA injections were tested for friction of cartilage against glass. The formulations used were Synvisc, Euflexxa, Monovisc, Hyalgan, Hymovis, and Supartz. And tested in a manner previously described [5] for four cartilage samples obtained from the patellofemoral groove of neonatal bovine. In addition to testing frictional properties of these solutions, we tested the rheological properties as well in a similar manner to previously described [5]. Rheological factors presented were: complex viscosity from oscillatory shear, dynamic viscosity, storage modulus, and phase angle for oscillatory shear.

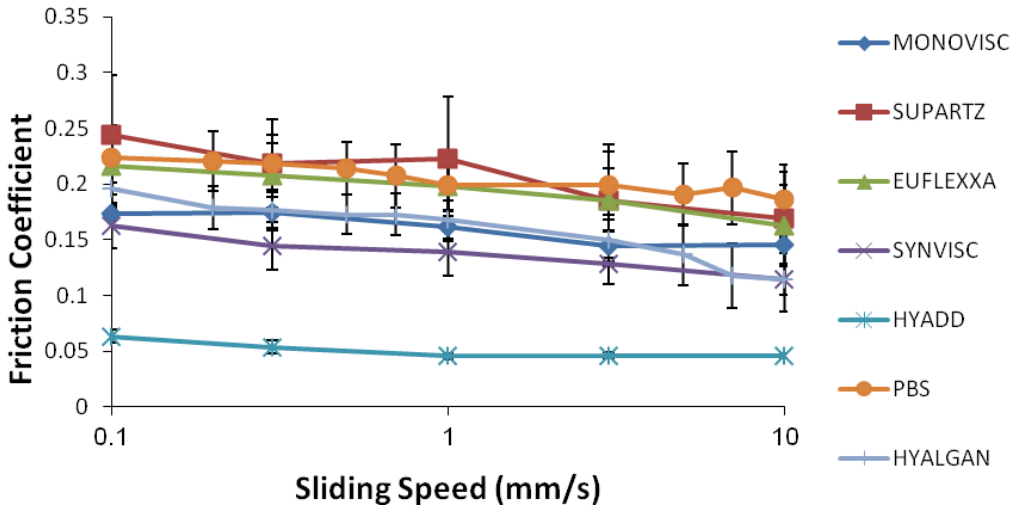

Figure A.1 Friction coefficient as a function of sliding speed for 6 different HA formulations and PBS against cartilage. (n = 4-5)

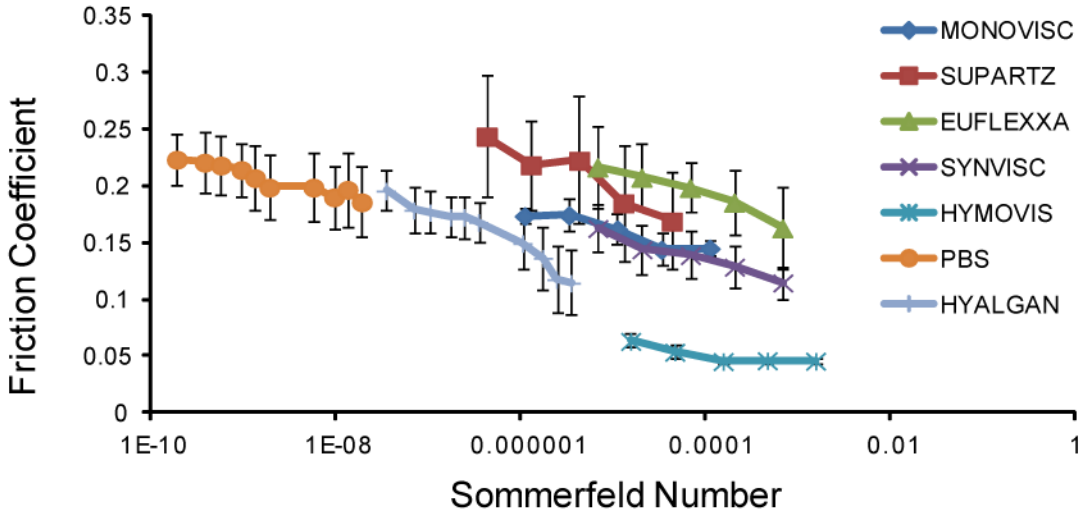

Figure A.2 Friction coefficient as a function of Sommerfeld number for 6 different HA formulations and PBS against cartilage. The Sommerfeld number is equal to: *sliding speed * viscosity * contact width / normal load*. (n = 4)

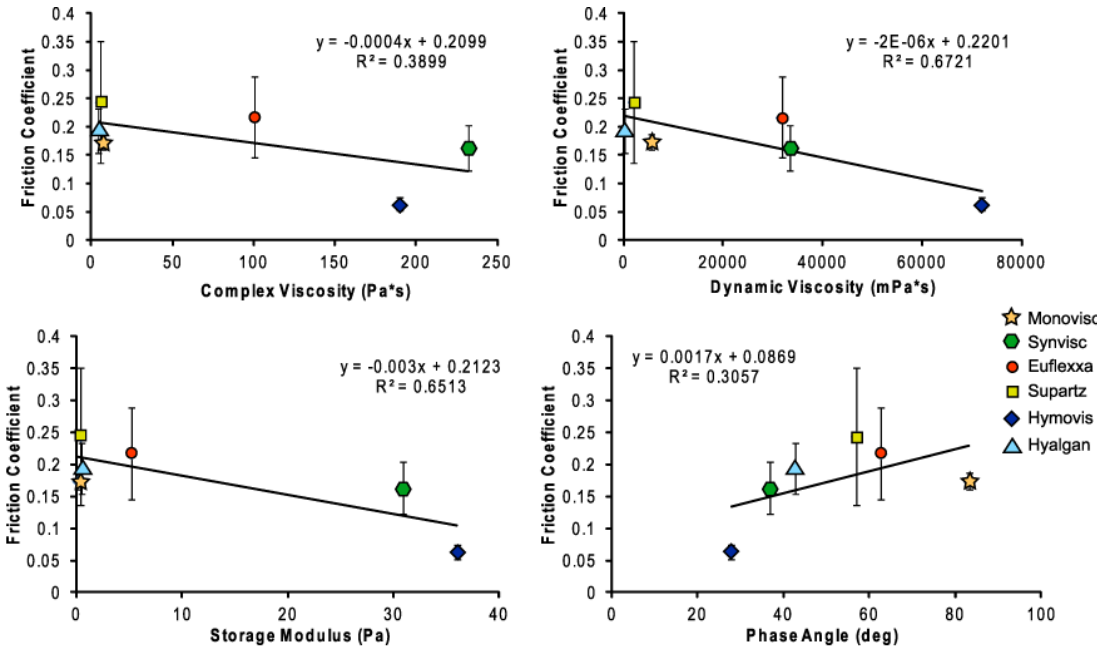

Figure A.3 Friction coefficient at 1mm/s for cartilage lubricated by 6 different commercial HA formulations as a function of rheological parameters. Dynamic viscosity best predicted lubricating ability ($p = 0.045$). ($n = 4$ for each)

Results

Friction coefficients of all lubrication as a function of sliding speed alone are presented in Figure A.1. However, friction coefficients as a function of sliding speed, dynamic viscosity, normal load, and contact width (encompassed in the Sommerfeld Number) revealed speed and viscosity dependence of decreasing friction with increasing speed and viscosity as expected (Figure A.2). However, all formulations did not fall on a single curve as would be expected for Newtonian fluids with minimal boundary lubricating ability. We then compared friction coefficients at slow speed (i.e. 1 mm/s sliding speed) for all lubricants against the measured rheological parameters. The best fit of friction coefficient with these parameters were evident in both dynamic viscosity ($R^2 = 0.6721$, $p = 0.045$) and storage modulus ($R^2 = 0.6513$, $p = 0.052$) (Figure A.3).

Discussion

While dynamic viscosity has been confirmed to be a predictor of friction coefficient of cartilage lubricated by HA formulations, there are likely other factors that play substantial roles. Future efforts in cartilage lubrication may be aimed at determining what those parameters are. Better understanding the parameters that best predict low cartilage friction by viscous lubricants can inform future efforts to engineer more effective cartilage therapies.

REFERENCES

[1] N. W. Rydell, J. Butler, and E. A. Balazs, “Hyaluronic acid in synovial fluid. VI. Effect of intra-articular injection of hyaluronic acid on the clinical symptoms of arthritis in track horses.,” *Acta vet.*, vol. 11, pp. 139–155, 1970.

[2] E. A. Balazs and J. L. Denlinger, “Viscosupplementation: a new concept in the treatment of osteoarthritis.,” *J. Rheumatol. Suppl.*, vol. 39, pp. 3–9, Aug. 1993.

[3] M. E. Adams, M. H. Atkinson, A. J. Lussier, J. I. Schulz, K. A. Siminovitch, J. P. Wade, and M. Zummer, “The role of viscosupplementation with hylan G-F 20 (Synvisc) in the treatment of osteoarthritis of the knee: a Canadian multicenter trial comparing hylan G-F 20 alone, hylan G-F 20 with non-steroidal anti-inflammatory drugs (NSAIDs) and NSAIDs alone.,” *Osteoarthritis Cartilage*, vol. 3, no. 4, pp. 213–25, Dec. 1995.

[4] I. Finelli, E. Chiessi, D. Galesso, D. Renier, and G. Paradossi, “Gel-like structure of a hexadecyl derivative of hyaluronic acid for the treatment of osteoarthritis.,” *Macromol. Biosci.*, vol. 9, no. 7, pp. 646–53, Jul. 2009.

[5] E. D. Bonnevie, D. Galesso, C. Secchieri, I. Cohen, and L. J. Bonassar, “Elastoviscous Transitions of Articular Cartilage Reveal a Mechanism of Synergy between Lubricin and Hyaluronic Acid.,” *PLoS One*, vol. 10, no. 11, p. e0143415, Jan. 2015.

APPENDIX B

Synergy Between Hyaluronic Acid and a Synthetic Boundary Lubricant

Abstract

We have recently revealed a mechanism of lubricating synergy between two molecules in synovial fluid. The viscous lubricant, hyaluronic acid, and the boundary lubricant, lubricin, work together to form a viscous complex at the cartilage surface that provides synovial fluid with its ability to minimize cartilage friction. In this study, we experimentally test whether a synthetic lubricin-mimetic lubricant that binds to the cartilage surface can facilitate lubrication in a similar manner to the natural mechanism of synovial fluid. We show preliminarily, that the mimetic lubricant and HA together lubricate much more effectively than either lubricant on their own, and reach similar lubrication levels to that of synovial fluid.

Introduction

Osteoarthritis (OA) is the leading cause of severe disability in the United States [1], and its prevalence is expected to increase in the coming decades as the population ages. The economic burden of this disease can reach as much as 2.5% gross national product of industrialized countries resulting in costs reaching almost $100 billion annually [2]. OA involves the mechanical failure of the body's load bearing and lubricating tissue found in joints, articular cartilage. Conventional treatment for advanced OA involves the injection of viscous lubricants, with the naturally occurring polysaccharide hyaluronic acid (HA) being injected as standard practice [3]. This treatment has shown some efficacy in the clinic, but results appear to be individually dependent and may rely on more factors at play within the joint [4].

One specific example of another factor at play in the joint capsule is the presence of lubricin, a naturally occurring glycoprotein [5], [6]. We have recently shown that optimal lubrication by synovial fluid, the lubricating liquid within the body's joints, occurs when both lubricin and HA are present [7]. Lubricant synergy is initiated by lubricin, which is known to bind to the tissue's surface [8]. Lubricin, known for its boundary lubricating ability, has also emerged as a potential treatment to mitigate the progression of osteoarthritis and has emerged as an effective treatment in animal models [9], but this treatment is yet to be tested in human trials and approved within the United States. Further, lubricin production and purification is a costly and time consuming process, and consequently, our group has recently disclosed a synthetic substitute to lubricin treatment that is both cheaper and easier to manufacture [10]–[12]. This synthetic lubricant has proven effective in mitigating the onset of

cartilage in a rat model of OA.

In vitro cartilage friction has been linked to in vivo effectiveness of injectible lubricants, and in this disclosure we present a method for reducing cartilage friction using a synthetic boundary lubricant in combination with a viscous lubricant [13]. Unlike lubricin, the synthetic polymer lacks a chemical domain or terminus that causes aggregation of the molecule. Consequently, friction coefficients of the synthetic lubricant saturate after binding of the lubricant to the cartilage surface. Specifically, introducing more synthetic polymer to a lubricant solution after long enough exposure does not have an additive effect to lubrication on its own. The data in this appendix show, however, that when HA is introduced into a lubricant solution with the synthetic polymer, levels of lubrication are reached that greatly exceed the individual contributions of the molecules to lubrication. The friction coefficients reach lower values than lubricin and HA together and are close to the levels of healthy synovial fluid.

Methods

The lubricin mimetic was synthesized in a manner previously described [10]. Briefly, the polymer is a poly-acrylic acid (PAA) back bone with poly-ethylene glycol (PEG) side chains used at a concentration of 3 mg/mL. The polymer contains a thiol terminus that can bind to the cartilage surface. The hyaluronic acid used in this study was a 630 kDa recombinant HA at 10 mg/mL. Cartilage from the patellofemoral groove of neonatal bovine was used in the friction measurements of cartilage sliding against glass.

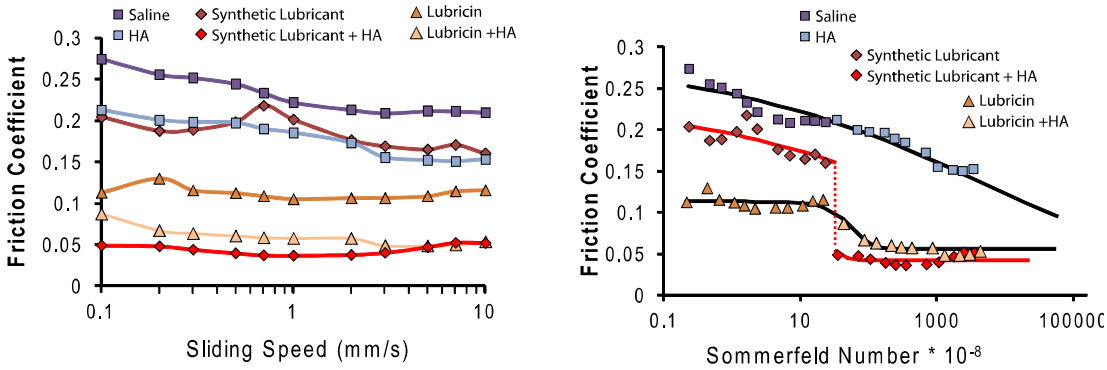

Figure B.1 (Left) Friction coefficient vs sliding speed for different lubricants. The synthetic lubricant (3mg/mL) in combination with HA (10mg/mL) provided the lowest friction coefficients. (Right) When presented as a function of the Sommerfeld number (sliding speed * lubricant viscosity * contact width / normal load) a friction transition occurred with the addition of HA to the synthetic lubricant that greatly enhanced lubrication by either HA or the synthetic lubricant and surpassed lubricin in combination with HA.

Results

Friction coefficient for 6 different lubricating baths (saline, HA, lubricin, synthetic lubricant, HA + lubricin, and HA + synthetic lubricant) versus sliding speed revealed stronger dependence on lubricant composition that sliding speed. However, this same data normalized to viscosity, contact geometry, and normal load using the Sommerfeld number provided mechanistic insight. Although the synthetic lubricant alone did not lubricate to levels of lubricin alone, the synthetic lubricant with HA did replicate lubrication of lubricin with HA.

Discussion

Although the results presented here are preliminary in nature, they provide insight into effective treatments for arthritis. By having a synthetic lubricant that binds to the articular surface and maintains intrinsic boundary lubricating ability, it is able to replicate the synergy between lubricin and HA. Future studies should be aimed at increasing the experimental sample sizes, measuring the affinity of the synthetic lubricant to HA, and testing the combination treatment in an animal model to determine whether *in vitro* lubricating ability can predict damage mitigation *in vivo*.

REFERENCES

[1] L. Murphy, T. A. Schwartz, C. G. Helmick, J. B. Renner, G. Tudor, G. Koch, A. Dragomir, W. D. Kalsbeek, G. Luta, and J. M. Jordan, "Lifetime risk of symptomatic knee osteoarthritis.," *Arthritis Rheum.*, vol. 59, no. 9, pp. 1207–13, Sep. 2008.

[2] R. Bitton, "The economic burden of osteoarthritis.," *Am. J. Manag. Care*, vol. 15, no. 8 Suppl, pp. S230–5, Sep. 2009.

[3] E. A. Balazs and J. L. Denlinger, "Viscosupplementation: a new concept in the treatment of osteoarthritis.," *J. Rheumatol. Suppl.*, vol. 39, pp. 3–9, Aug. 1993.

[4] G. H. Lo, M. LaValley, T. McAlindon, and D. T. Felson, "Intra-articular Hyaluronic Acid in Treatment of Knee Osteoarthritis," *JAMA*, vol. 290, no. 23, p. 3115, Dec. 2003.

[5] J. P. Gleghorn, A. R. C. Jones, C. R. Flannery, and L. J. Bonassar, "Boundary mode lubrication of articular cartilage by recombinant human lubricin.," *J. Orthop. Res.*, vol. 27, no. 6, pp. 771–7, Jun. 2009.

[6] G. D. Jay, J. R. Torres, D. K. Rhee, H. J. Helminen, M. M. Hytinnen, C.-J. Cha, K. Elsaid, K.-S. Kim, Y. Cui, and M. L. Warman, "Association between friction and wear in diarthrodial joints lacking lubricin.," *Arthritis Rheum.*, vol. 56, no. 11, pp. 3662–9, Nov. 2007.

[7] E. D. Bonnevie, D. Galesso, C. Secchieri, I. Cohen, and L. J. Bonassar, "Elastoviscous Transitions of Articular Cartilage Reveal a Mechanism of Synergy between Lubricin and Hyaluronic Acid.," *PLoS One*, vol. 10, no. 11, p. e0143415, Jan. 2015.

[8] A. R. C. Jones, J. P. Gleghorn, C. E. Hughes, L. J. Fitz, R. Zollner, S. D. Wainwright, B. Caterson, E. A. Morris, L. J. Bonassar, and C. R. Flannery, "Binding and localization of recombinant lubricin to articular cartilage surfaces.," *J. Orthop. Res.*, vol. 25, no. 3, pp. 283–92, Mar. 2007.

[9] C. R. Flannery, R. Zollner, C. Corcoran, A. R. Jones, A. Root, M. A. Rivera-Bermúdez, T. Blanchet, J. P. Gleghorn, L. J. Bonassar, A. M. Bendele, E. A. Morris, and S. S. Glasson, "Prevention of cartilage degeneration in a rat model of osteoarthritis by intraarticular treatment with recombinant lubricin.," *Arthritis Rheum.*, vol. 60, no. 3, pp. 840–7, Mar. 2009.

[10] M.-C. Tan, "Synthesis, Characterization And Evaluation Of Poly(Acrylic Acid)-Graft-Poly(Ethylene Glycol)'S As Boundary Lubricants For Treatment Of Osteoarthritis," Cornell University, 2015.

[11] D. Putnam, M. Tan, K. J. Samaroo, and L. J. Bonassar, "Biomimetic boundary lubricants for articular cartilage," 2013.

[12] K. Samaroo, "Biomimetic Boundary Lubricants Of Articular Cartilage," 2015.

[13] E. Teeple, K. A. Elsaid, G. D. Jay, L. Zhang, G. J. Badger, M. Akelman, T. F. Bliss, and B. C. Fleming, "Effects of supplemental intra-articular lubricin and hyaluronic acid on the progression of posttraumatic arthritis in the anterior cruciate ligament-deficient rat knee.," *Am. J. Sports Med.*, vol. 39, no. 1, pp. 164–72, Jan. 2011.